Cardiac sympathetic neural signalling in hypertension

Julia A. Shanks

Thesis submitted for the Degree of
DOCTOR OF PHILOSOPHY
in the University of Oxford

Lady Margaret Hall
Oxford University
October 2013

Abstract

The work presented in this thesis examines the role of cardiac sympathetic signalling in the development and maintenance of hypertension in the spontaneously hypertensive rat (SHR); and the role the norepinephrine re-uptake transporter (NET) plays in the sympathetic phenotype during hypertension.

Chapter One: reviews (i) cardiac impairment observed in hypertension, (ii) the mechanisms underlying sympathetic neurotransmission and signal termination, (iii) the structure, function, mechanism of action, and role of the norepinephrine (NE) re-uptake transporter in a number of diseases related to sympathetic dysfunction including hypertension.

Chapter Two: comprises a detailed rational for the approach taken to; (i) record NET rate in single isolated cells from major sympathetic ganglia using a novel fluorescent assay (NTUA); (ii) measure norepinephrine release from isolated sympathetic cells using a method of carbon fibre based amperometry; (iii) measure autonomic function on living tissue *in-vivo* and *in-vitro* using organ bath and whole animal preparations; (iv) quantification of protein expression and protein levels within single cells and isolated ganglia.

Chapter Three: examined the cardiac autonomic phenotype of the young pre-hypertensive SHR. Baseline haemodynamics were comparable between the SHR and age matched WKY controls, apart from *in-vivo* heart rate which the SHR displayed a small, but significant tachycardia. Release of sympathetic neurotransmitter NE, and the co-transmitter NPY were also elevated in the young SHR compared to WKY even though the SHR showed no elevation in arterial blood pressure at this age. Tyrosine hydroxylase levels were unaltered. ^{3}H-NE release studies also revealed there may be a dysfunction in NET in the SHR at this age, as DMI treatment normalised the difference in ^{3}H-NE overflow between the SHR and WKY.

Chapter Four: described an investigation in to the activity of the NE re-uptake transporter between older, SHR with established hypertension and age matched normotensive WKY. A novel fluorescent assay of the monoamine transporter family was used to monitor NET activity within isolated sympathetic cells from three ganglia associated with hypertension. Direct evidence for the first time is reported that NET activity was lower in cardiac stellate neurons of the SHR compared to the WKY, but not in the other ganglia tested (superior cervical ganglion (SCG) – vascular innervation of head and neck, and celiac/superior mesenteric ganglia (CG/SMG)– renal and abdominal organs). The data support the notion that NET is regulated in a site-specific fashion, which may account for the sympathetic heterogeneity of NE spillover reported in humans.

Chapter Five: examined differences in NET activity and expression levels between four-week-old pre-hypertensive SHR and age matched WKY. The NTUA assay revealed a significantly lower rate of NET activity within stellate neurons of the young SHR compared to WKY, with no difference in NET protein expression. No difference again was seen in the other ganglia. The SCG was the only ganglia in which NET significantly decreased with age, indicating the NET dysregulation within the vasculature may develop at a later stage of hypertension than observed in cardiac ganglia.

Chapter Six: examined the ability to modulate NET activity in WKY and SHR stellate neurons in response to a number of pharmacological agents that stimulate cGMP (BNP, SNP, 8-Br-cGMP) and inhibition of PKC. These were agents previously implicated in NET modulation in other cell types. All activators of cGMP reduced NET rate to a similar degree in the WKY. No change in NET rate was observed in the SHR, indicating that NET modulation either intrinsically, and/or receptor membrane insertion, was faulty in the SHR. PKC inhibition increased NET rate in both groups.

Chapter Seven: is a concluding discussion summarising the main findings from this thesis, placing them in to physiological context, and discusses avenues of further research.

Acknowledgements

There are many people that I would like to acknowledge for their consistent, unfaltering assistance, and support throughout my doctoral studies. First, I would like to thank **Professor David Paterson** for providing me with the opportunity to complete this DPhil project and work within his highly inspirational and talented group. The support, supervision and mentoring I have received from David has been exceptional and beyond expectations. Even at the busiest time David always has time for his students. A truly awe inspiring person to work alongside. This leads me on to acknowledge the huge gratitude I have towards all members of the Paterson group. Specifically, **Dr Dan Li**, for the tutoring, guidance, infinite patience and always being there, one of the most inspirational people I have ever met. **Dr Neil Herring** a phenomenal mentor, cardiologist, scientist, tutor, all round incredibly talented and kind person who always has the time. **Dr Gil Bub and Dr Rebecca Burton**, two of the most talented and grounded people I have ever met, it has been an honour to work with and know both of you. **Dr Gouliang Hao, Chieh Ju-Lu, Dr Manish Kalla and Hege Ekeberg Larsen**, for continuing support within the group. I would also like to acknowledge the help I have received from the dissertation students I have mentored over the years, **Rebecca Ryan, Saras Mane and Antony Kalin,** it has been a pleasure to work with all three. I would also like to recognise the co-supervision of **Derek Terrar**, I could not feel in safer hands. Finally, I would like to thank the British Heart Foundation for providing me with the funding to carry out this work.

There are many additional people I would like to acknowledge at the start of this thesis for their infinite support, caring and wisdom for the last five years, without whom I would not have been able to complete this thesis as half the person I am today.

First, my amazing group of friends from Yorkshire. I have not been around as much the last few years but you have all been there throughout. To the people who have seen me through my GCSE's and beyond and always believed in me, **Katy, Vicki, Alice, Sarah, Susie, Laura** this is for you.

Secondly, for believing in me when I decided to take a masters course in Oxford and stay in science, while everyone departed to 'the real world' **Karen**, **Chloe, Laura, Amit, James and Ian**.

Thirdly, the girls that made my first two years in Oxford unforgettable! Truly meeting friends for life, **Rachel, Sara, Annette, Ella.** I would likely not still be in Oxford if it had not been for your generosity in taking me in and kindness in all aspects of life.

Friends from LMH through the ages, to many to mention but you know who you are. Pretty much any person I have ever met there has made a lasting impression on me and has enriched my life.

Special thanks goes out to a few. **Gabrille Mearns**. Starting our Oxford journey together and continuing to Phd's, thank you for the sanity throughout.

Ruth, Emma, and Simon, the only remaining MSc living to tell the tale. A privileged five years of knowing you.

Megan Edwards. What can I say? Inspirational, compassionate, inspiring, a truly good friend and an amazing friendship that will last a lifetime. Without you I would have crumbled.

Helen Batchelor one of the strongest most beautiful people I know. Work colleague, housemate, yoga buddy and above all friend.

Finally I would like to acknowledge the support of my family over the last 5 years, and throughout my entire further education. My grandmother **Dr Ann Shanks** for supporting me throughout my masters. My mother **Gina Shanks** for forever supporting me and never restricting any of my life choices. My sister **Helen** who it is unlikely I would have completed this DPhil without. I would also like to acknowledge my father a man of science and the world that would never settle for the mundane. To the man who never saw me receive my A-levels I wonder what he would think of this now. This thesis is dedicated to my family and my father.

Statement of contribution to this thesis

The majority of the planning, design and undertaking of the experimental work in this thesis, as well as analysis and interpretation of results were done by me alone. However, I would like to acknowledge the extent of help provided by others.

Chapter 3: A proportion (30%) of the ^{3}H-NE experiments and atrial contraction studies were carried out by undergraduate dissertation student Soti Manou-Statopoulou. Assistance and supervision was provided by Dr. Neil Herring for all *in vivo* experiments. Western blot was carried out by Cheih-Ju Lu (DPhil student). Amperometry experiments were carried out in collaboration with Dr. Guoliang Hao.

Chapters 4 & 5: A proportion (<5%) of the NET experiments were carried out by undergraduate students Rebecca Ryan and Sara Mane, under my supervision, all data were analysed by myself.

Publications associated with this thesis

Original contributions

1. **Shanks J,** Manou-Stathopoulou S, Lu CJ, Li D, Paterson DJ, Herring N. Cardiac sympathetic dysfunction in the pre-hypertensive spontaneously hypertensive rat. *American Journal of Physiology. Heart and Circulatory Physiology*. 2013.
2. **Shanks J,** Mane S, Ryan R, Paterson DJ. Ganglion-specific impairment of the norepinephrine transporter in the hypertensive rat. *Hypertension*. 2013;61:187-193
3. Herring N, Cranley J, Lokale MN, Li D, **Shanks J,** Alston EN, Girard BM, Carter E, Parsons RL, Habecker BA, Paterson DJ. The cardiac sympathetic co-transmitter galanin reduces acetylcholine release and vagal bradycardia: Implications for neural control of cardiac excitability. *Journal of Molecular and Cellular Cardiology*. 2012;52:667-676

Reviews

1. **Shanks J,** and Herring N. Invited review EB2012: Peripheral cardiac sympathetic hyperactivity in cardio vascular disease role of neuropeptides. *American Journal of Physiology. Regulatory, Integrative and Comparative Physiology.* 2013.

Presentation to professional societies

Experimental biology, San Diego, 2012 (abstracts in FASEB)

1. Shanks JA, Manou-Stathopoulou S, Lu CJ, Li D, Paterson DJ, Herring N. Peripheral cardiac sympathetic dysfunction in the pre-hypertensive spontaneously hypertensive rat. *Experimental Biology*, 2012

2. Shanks JA, Mane S, Ryan R, Paterson DJ. Impaired cardiac norepinephrine transport in the hypertensive rat [abstract]. *Experimental Biology*. 2012.

IUPS, Birmingham 2013

1. Shanks JA, Manou-Stathopoulou S, Lu CJ, Li D, Paterson DJ, Herring N. Peripheral cardiac sympathetic dysfunction in the pre-hypertensive spontaneously hypertensive rat. *IUPS, 2013.*

2. Shanks JA, Mane S, Ryan R, Li D, Paterson DJ. Site specific impairment of the norepinephrine transport in the hypertensive rat [abstract]. *IUPS, 2013.*

Abbreviations and terms

^{3}H-NE	Radio labeled (tritiated) NE
8-Br-cGMP	8 bromo-cyclic-GMP
Ach	Acetylcholine
BNP	Brain natriuretic peptide
Ca^{2+}	Calcium
CG	Celiac ganglia
DAT	Dopamine re-uptake transporter
DMI	Desipramine
NE	Norepinephrine (noradrenaline)
NET	Norepinephrine re-uptake transporter
NTUA	Neurotransmitter transporter uptake assay
RSC	Renal sympathetic chain
SCG	Superior cervical ganglia
SD	Sprague-Dawley rat
SERT	Serotonin re-uptake transporter
SHR	Spontaneously hypertensive rat
SMG	Superior mesenteric ganglia
SNP	Sodium nitroprusside
WKY	Wistar kyoto

Contents

CHAPTER 1:
INTRODUCTION

PREFACE

In this thesis, I have set out to examine the underlying causes of the sympathetic hyperactivity that is observed in hypertension of the SHR, and at what developmental stage these sympathetic irregularities arise. Recent studies have identified elevated depolarisation induced intracellular calcium transients in the SHR stellate ganglion compared to age matched normotensive WKY at both 16 weeks of age, where the SHR display established hypertension, and 4 weeks of age before hypertension has developed[1]. This is coupled to increased heart rate and cardiac norepinephrine spill over observed in both human hypertensive and animal models[2, 3]. The role for altered norepinephrine re-uptake by the norepinephrine re-uptake transporter (NET) has previously been implicated in the study of hypertension but with conflicting results.

This thesis focused on the idea that cardiac sympathetic dysregulation may occur at an early age of the SHR, as is observed with the enhanced calcium transients in sympathetic neurons. To do this I studied the SHR at a young age prior to the development of hypertension. To ascertain if there was a role for NET dysfunction in hypertension, I investigated the direct action of the transporter within single cells from different sympathetic ganglia.

The following general introduction reviews the relationship between autonomic dysfunction in cardiovascular diseases, leading onto the focus of cardiac sympathetic hyperactivity observed in hypertension. It then briefly reviews the processes involved in sympathetic neurotransmission and factors that regulate them before focusing on the neuronal norepinephrine re-uptake transport (NET). Specifically, its discovery, physiological importance, structure, function, molecular modulation, and the putative role for NET transport dysfunction in disease.

1.1. CARDIAC IMPAIRMENT IN HYPERTENSION

1.1.1 THE IMPORTANCE OF AUTONOMIC BALANCE IN CARDIOVASCULAR DISEASE

High cardiac sympathetic drive promotes myocyte calcium influx, increases the inotropic state of the heart and increases myocardial oxygen demand. This can exacerbate the harmful effects of pre-existing cardiac ischaemia and precipitate life-threatening ventricular arrhythmias[4, 5]. This is particularly prevalent when there is an abnormal cardiac structural phenotype to support re-entrant pathways, such as an ischaemic or dilated cardiomyopathy, hypertrophic cardiomyopathy, or arryhthmogenic right ventricular cardiomyopathy. High sympathetic drive to the heart can also precipitate arrhythmia when there is an abnormal cardiac electrophysiological substrate such as the long QT, or Brugada's syndrome. Excessive adrenergic activity is unsurprisingly a negative prognostic indicator post myocardial infarction[6, 7] and during congestive cardiac failure[8, 9]. Moreover it has also been implicated in both the aetiology and progression of hypertension[10]. Increased

Figure 1.1:

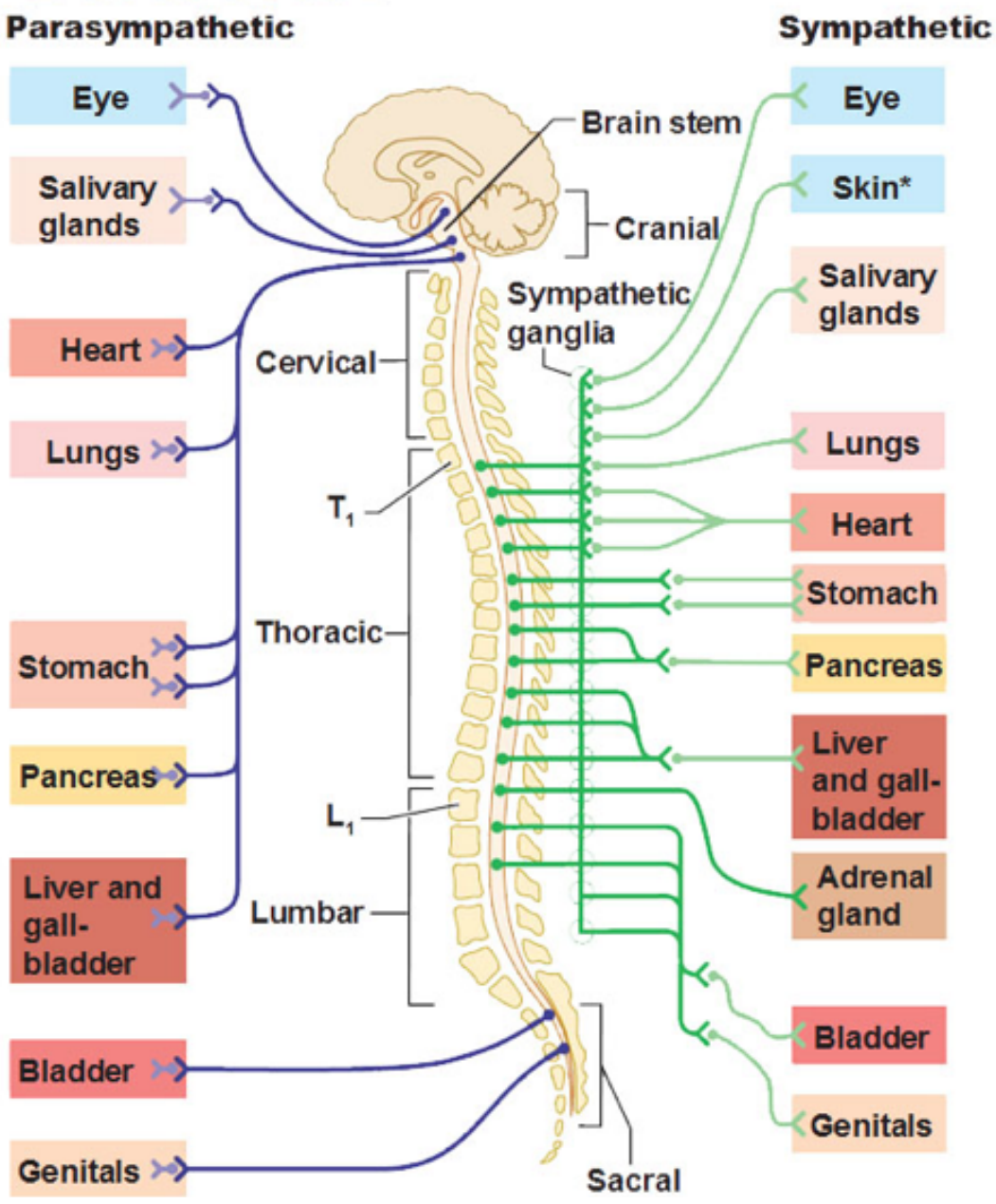

Figure 1.1: Differences in sympathetic and parasympathetic divisions of the autonomic nervous system. Preganglionic neurons emerge from different regions of the CNS: sympathetic, from the thoracolumbar region. Parasympathetic, from the craniosacral region. Different locations of ganglia: sympathetic, close to the spinal cord in the sympathetic chain. Parasympathetic, close to the target organ. Lengths of postganglionic fibres: sympathetic, long. Parasympathetic, short. Postganglionic branching: sympathetic, lots so multiple organs can be stimulated at once. Parasympathetic, very little branching. (image: Antranik.org. The Autonomic Nervous System. http://antranik.org/the-autonomic-nervous-system/. 28.04.2013, 12.13pm.)

sympathetic activity to the heart is correlated with hypertensive left ventricular remodelling and hypertrophy[11], an independent predictor of morbidity and mortality[12].

Under normal conditions the cardiac vagus acts to reduce the inotropic and chronotropic action on the heart, preventing intracellular calcium overload and slowing heart rate. It can directly raise the threshold for induction of ventricular fibrillation[13]. Conditionals that promote high vagal tone (e.g. exercise training[14]), gene transfer of nNOS[15, 16] protect against mortality[17] whilst impaired vagal function has been demonstrated in both congestive cardiac failure[7] and hypertensive patients[18]. However, the cardiac vagus is notoriously difficult to target pharmacologically and as a consequence, therapy has been directed at the sympatho-adrenal axis and renin-angiotensin pathways. Although randomized controlled trials have demonstrated that beta-blockers and ACE inhibitors are highly beneficial in the context of myocardial infarction, congestive heart failure and hypertension (eg. ISIS1[19], CIBIS II [20], CONSENSUS [21], SAVE [22]) a significant mortality nevertheless remains.

1.1.2 SITES OF AUTONOMIC DYSFUNCTION IN CARDIOVASCULAR DISEASE

There is a wealth of data supporting the notion that the autonomic dysfunction associated with cardiovascular disease can arise at many distinct anatomical sites. For example the success of renal sympathetic nerve denervation in reducing muscle sympathetic nerve activity, plasma catecholamines and arterial blood pressure in patients with drug refractory hypertension supports the notion that renal afferents contribute, at least in part, to the generation of the hypertension in these patients [23,

[24]. Evidence from preclinical animal models and human subjects also supports carotid body hypersensitivity as a mechanism by which central sympathetic drive is promoted in heart failure and hypertension[25, 26]. There has therefore been a resurgence in interest in carotid body denervation as a therapeutic strategy in these conditions[26], as well as implantable carotid sinus stimulators to activate the high pressure arterial baroreflex and reduce sympathetic drive and increase vagal tone in hypertension[27].

Afferent signalling can also arise from the heart itself. Whilst the vagi relay sensory information to the nodose ganglion of the brainstem, mechanical and chemical information regarding the myocardium is relayed via neurons of the upper thoracic and lower cervical dorsal root ganglia, and also within sensory neurons of the intrinsic cardiac plexi. This opens the possibility of afferent modulation of efferent signalling not just at the level of the brainstem, but also at the levels of the intrinsic cardiac plexi[28], and via spinal sympatho-sympathetic reflexes. This reflex pathway has been demonstrated to maintain sympathetic drive in response to both myocardial ischaemia[29] and hypertension[30].

Centrally, afferent inputs converge on the nucleus tractus solitarius (NTS) in the medulla. This information is then relayed to the caudal ventrolateral medulla (CVLM), which provides a GABA-ergic inhibition of the rostral VLM. The NTS also relays information via inhibitory GABA-ergic inter-neurons communicating with preganglionic vagal neurons of the nucleus ambiguous, and dorsal motor nuclei of the vagus. Whilst these brainstem nuclei are key integrating sites and determinants of efferent sympathetic outflow in both hypertension and heart failure[31-33], evidence

also suggests that a significant component of the sympathetic hyperactivity observed in the genetic model of essential hypertension, the spontaneously hypertensive rat (SHR), originates at the level of the efferent post-ganglionic neuron[1, 34-37].

Parasympathetic

Vagal preganglionic efferent fibres are long and do not synapse until they reach the end organ. In the case of the heart, preganglionic fibres synapse at the sinoatrial node. Preganglionic efferents release neurotransmitter acetylcholine (Ach), which binds to nicotinic receptor on postganglionic neurons. Nicotinic Ach receptors (AchRs) are ligand gated ion channels in the plasma membrane; opening of the ion channel allows the movement of positive ions predominantly Na^+ in and K^+ out. The net flow of positively charged ions is inward, depolarising the postganglionic cell (figure 1.1).

Sympathetic

Preganglionic sympathetic fibres are shorter than those of vagal efferents. These fibres enter the paravertebral ganglia, or sympathetic chain, which runs either side of the spinal cord, and synapse with the cell bodies of postganglionic sympathetic fibres. Preganglionic sympathetic fibres like vagal efferents also release Ach, which activates postganglionic nicotinic receptors. Postganglionic sympathetic fibres exit the paravertebral chain, travelling to the target organ and releasing NE. However, some preganglionic sympathetic fibres do not synapse in the paravertebral ganglia, but in the prevertebral ganglia that is located in the abdomen (celiac, superior mesenteric and inferior mesenteric ganglia) (figures 1.1 & 1.2).

1.1.3 CARDIAC-AUTONOMIC SIGNALLING IN HYPERTENSION

The classical view of cardiovascular control by the autonomic nervous system is that brainstem autonomic outflow merely responds to changes in afferent feedback from peripheral arterial, cardiopulmonary and renal baro- and chemoreceptors[23, 24, 26, 38]. The sympathetic and parasympathetic efferent output therefore act to oppose changes in circulatory disturbance, and maintain adequate arterial blood pressure and perfusion of organ systems. It is becoming increasingly apparent that this system is not "hard-wired" and integration and plasticity exists at many neuroanatomical sites in the cardiac-vascular-renal neural axis. Recently, the identification that a significant component of the sympathetic hyperactivity associated with hypertension arises at the level of the post-ganglionic neuron has opened up a new field of research.

1.1.4 PERIPHERAL SYMPATHETIC HYPERACTIVITY AS AN EARLY HALLMARK FOR HYPERTENSION

Hypertension is a multi-organ disease and can involve the kidney, vasculature, and the autonomic nervous system. Increased sympathetic activity and reduced vagal tone are now well established as major contributing factors to the pathophysiology of human hypertension[39-44], and that observed in the SHR[1, 34, 37, 38, 45]. Hypertension is associated with increased muscle sympathetic nerve activity[40, 41], and increased levels of plasma NE spillover[43, 46]. A progressive impairment of autonomic regulation is also observed in individuals who are not clinically hypertensive as blood pressure increases[47]. Increased muscle sympathetic nerve activity in response to mental stress has also been documented within normotensive offspring from families with a

history of hypertension[48]. This suggests that sympathetic activation may be an early marker of hypertension in those who are genetically predisposed to the disease.

Noradrenaline was identified as the principle transmitter of the sympathetic nervous system by Euler in the 1950's. The internationally accepted terminology for the neuronal noradrenaline re-uptake transporter classified as uptake-1 is NET (norepinephrine re-uptake transporter), utilising the American word for noradrenaline, norepinephrine. Norepinephrine is also an internationally accepted term for noradrenaline. To eliminate confusion in this thesis I will use the terms norepinephrine and norepinephrine re-uptake transport (NET) throughout when refereeing to noradrenaline mediated sympathetic neurotransmission. Norepinephrine (NE) is one of the principle neurotransmitters of the central and peripheral nervous systems, mediating diverse range of physiological and behavioural processes. The importance of NE signalling was established in 1970 when Euler, Katz and Axelrod were awarded the Noble prize for physiology or medicine, honoured for their independent study of the mechanisms of nerve impulses.

Centrally NE has been identified in control of feeding behaviour, sleep wake cycle, cognition, mood, and depression. Within the autonomic nervous system NE is the principle neurotransmitter of the sympathetic branch essential in the regulation of heart rate[49], vascular diameter[50], and release of adrenaline from the adrenal medulla.

1.2 SYMPATHETIC NEUROTRANSMISSION

Neurotransmitter release is triggered by Ca^{2+} entry into the postganglionic nerve terminal via membrane bound N-type Ca^{2+} channels[51]. The key features of cell depolarisation induced neurotransmitter release are, the regulation of Ca^{2+} channels that allow for Ca^{2+} entry into the nerve terminal, and the Ca^{2+} sensors within the fusion machinery that regulate exocytosis.

1.2.1 CELL DEPOLARISATION AND INITIATION OF ACTION POTENTIAL.

In order for neurotransmitter release to occur the membrane potential is raised above the threshold potential for voltage gated Ca^{2+} channels (L-type -30mV—10mV[52]), allowing Ca^{2+} entry into the cell via L-type Ca^{2+} channels. The resultant increase in intracellular Ca^{2+} initiates presynaptic vesicle binding and neurotransmitter release.

Autonomic preganglionic neurons release Ach binding to nicotinic acetylcholine receptors on the postganglionic cell. Nicotinic receptors are ligand gated ion channels, binding of the agonist stabilises the open state of the channel allowing for the movement of charged ions across the plasma membrane, predominantly, Na^{+} in and K^{+} out, resulting a net flow of positive charge into the cell. In turn, elevating the cell membrane potential above the threshold required for the opening of voltage gated Ca^{2+} channels. This produces the intracellular Ca^{2+} transient observed in response to cell depolarisation[1]. Within sympathetic nerve terminals 80% of the intracellular Ca^{2+} transients observed are initiated by Ca^{2+} entry through voltage gated Ca^{2+} channels[53].

A very short latency occurs between Ca^{2+} entry into the presynaptic terminal and neurotransmitter release. This indicates two things, that Ca^{2+} channels are spatially located close to the active site[54, 55] and, that a number of vesicles are primed at the membrane ready in a late stage of exocytotic release. Ca^{2+} channels have been shown to bind to syntaxin, a known protein of the fusion machinery[56, 57]. Injection of peptides that inhibit the Ca^{2+} channel/syntaxin interaction inhibit transmitter release[58]. In addition, nerve terminal poison with botulinum toxin (that cleaves syntaxin) display an altered spatial organisation of extracellular membrane bound Ca^{2+} channels[59], contributing to the theory that Ca^{2+} channels locate close to the site of neurotransmitter release.

1.2.2 Mechanisms behind neurotransmitter release

The now well-established principle that neurotransmitters mediate the transfer of information form one nerve cell to another, or from nerve cell to effector by the process of synaptic transmission was first postulated in the early 1900's. The work of Thomas Elliot in 1905 described how adrenaline and other catecholamines would elicit a response that was comparable to sympathetic nerve stimulation in a range of tissues. He concluded that it might be the catecholamines that are transmitted in response to sympathetic nerve stimulation from the postganglionic neuron to the postsynaptic effector site[60, 61]. Although in hindsight Elliot's work outlined the principles of sympathetic neurotransmission it was mainly over looked by his peers at the time. It was Loewi during his time at the University of Graz in Austria that cemented the idea of diffusible neurotransmitters. Loewi performed a series of experiments in which he suspended two frog hearts, upon stimulating the vagus or

sympathetic nerves in one heart a corresponding change in heart rate was identified in the adjacent heart, indicating some sort of chemical messenger must be diffusing between the hearts. Loewi originally suggested the sympathetic neurotransmitter to be adrenaline; Euler later identified it as norepinephrine.

Sympathetic and central neurons as well as adrenal chromaffin cells (ACCs) store and release catecholamines from dense core vesicles (DCV). Dense core vesicles' contain a chromogranin matrix that allows for storage of a very high concentration of catecholamines[62]. Norepinephrine containing vesicles also contain dopamine-β-hydroxylase in soluble and membrane bound forms as well as neuropeptides and co-transmitters such as ATP and neuropeptide Y (NPY). Constant intravesicular NE concentration is thought to be of 0.5-0.9mM[63, 64].

Two types of vesicle release have been characterised. First, full fusion, in which there is a full release of the entire vesicle quantum of NE, detected in amperometry as a spike with rapid rise time and exponential decay. Secondly a phenomenon that is described as 'kiss and run' first described by Katz and del Castillo in 1955. Commonly seen within ACCs, partial exocytosis is thought to reflect leakage of NA through a transiently open fusion pore[63, 65]. Partial fusion often precedes full fusion, this is observed as a 'footspike' on an amperometry trace[63-65].

Vesicle fusion to the plasma membrane is controlled by a number of proteins referred to as the SNARE complex. The Nobel Prize for Physiology or Medicine 2013 was awarded to jointly to James E. Rothman, Randy W. Schekman and Thomas C. Südhof *"for their discoveries of machinery regulating vesicle traffic",* including their identification of the vesicle release complex.

In the early 1990's synaptobrevin[66, 67], syntaxin-1 and SNAP-25[68, 69], were identified as targets of botulinum and tetanus toxins. These neurotoxins enter presynaptic terminals and act as highly specific proteases, blocking membrane fusion without changing the morphology of the terminal structure[70]. The classification of the protein targets of botulinum and tetanus toxins identified these proteins as essential in neurotransmission, later classifying them as components of the SNARE complex responsible for vesicle membrane fusion. SM (Sec1/Munc18-like) proteins have also been identified as essential in vesicle exocytosis in most mammalian cells. SM proteins are highly conserved cytosolic proteins that are thought to wrap around the SNARE complex stabilising it[71]. The amino terminus of syntaxin contains a conserved sequence that bind to the SM proteins, localising the proteins to SNARE[71, 72]. The SNARE and SM proteins are controlled by the cell depolarisation induced increase in intracellular Ca^{2+} via synaptotagmin and complexin[70, 73]. Primed vesicles fuse very quickly in response to cytoplasmic Ca^{2+} elevations. The SNARE complex acts to bridge the gap between the neurotransmitter vesicle membrane and neuronal presynaptic membrane. Zippering of the SNARE complexes is thought to create the fusion pore, although it has also been suggested that full zipping may only stress the membrane, and that SM proteins may be involved in the fusion pore[70]. With the opening of the fusion pore norepinephrine moves from the vesicle into the synaptic cleft.

1.2.3 Auto-inhibition and regulation of neurotransmitter release by alpha$_2$-adrenrecoptors.

The ability of neurotransmitters to regulate their own release through presynaptic auto- inhibitory receptors was established in the 1970's. Brown and Gillespie

reported that phenoxybenzamine, a α_2-adrenorepctor (α_2-AR) blocking agent, enhanced the overflow of NE elicited by nerve stimulation in the perfused cat spleen[74]. Additionally ^{3}H-NE release in the presence of phenoxybenzamine was also increased[75]. Alpha$_2$-adrenoreceptors are now known to play a critical role in regulating Ca^{2+} dependent NE release from sympathetic nerve terminal by a negative feedback mechanism. Alpha$_2$-adrenoreceptors are G_i coupled G-protein-coupled-receptors. They inhibit the activity of adenylyl cyclase, leading to a reduction in the formation of cAMP and in turn reduced activation of PKA. Protein kinase A catalyses Ca^{2+} induced Ca^{2+} release in response to cell depolarisation. Therefore, inhibition of this process results in reduced intracellular Ca^{2+} transients and neurotransmitter release. Activation of α_2-adrenergic receptors by NE within rat postganglionic sympathetic neurons inhibits NE release[76]. A dysregulation in this auto-inhibition pathway has been linked to some models of hypertension[77].

1.2.4 Termination of sympathetic signal by neurotransmitter re-uptake into the postganglionic sympathetic neuron.

The concentration at which NE is present in the synapse following release is regulated by, both the amount and frequency of NE being released, as well as, the kinetics by which NE is removed from the synaptic cleft and metabolised. The majority of released NE (>90%) is taken up into the sympathetic nerve terminal by the norepinephrine re-uptake transporter (NET) (uptake-1), with less than 5% being metabolized within the extracellular space[78]. Re-uptake of NE from the synaptic cleft is essential for both termination of the sympathetic response and for the replenishment of intracellular NE stores. $NET^{-/-}$ mice show reduced norepinephrine

release, a reduced rate of NE re-uptake and an increase in NE synthesis, indicating NE re-uptake to be one of the primary determinants of NE storage levels within the cell[79].

Fine control of the sympathetic nervous system is managed by the two NE re-uptake transporters, neuronal (NET) and non-neuronal solute carrier family 6 (neurotransmitter noradrenaline) transporter 2 (SLC6A2). NE if not recycled into a new synaptic vesicle can be metabolized both intracellularly and extracellularly by the enzymes monoamine oxidase-A (MAO-A)[80] or catechol-O-methyl transferase (COMT)[81]. The increased concentration of cardiac NE release observed within hypertension may in part be due to impairment of the NET.

1.3 THE NEURONAL NOREPINEPHRINE RE-UPTAKE TRANSPORTER

The role of the norepinephrine re-uptake transporter (NET) as the principle mechanism for sympathetic signal termination from postganglionic sympathetic neurons was first established by Whitby, Axelrod and Weil-Malherbein in 1961[82]. Prior to this it was believed that the rapid reduction in NE action following release was due to enzymatic break down in a similar way to acetlycholinesterase. Whitby and Axelrod *et.al.* Investigated the effect of tissue accumulation and storage of ^{3}H-NE in a number of sympathetically innervated tissues of the cat[82]. They identified that ^{3}H-NE was rapidly taken up in to tissue where it remained unchanged. Where as, Herrting in 1961 observed that ^{3}H-NE uptake into the heart was virtually eliminated in animals in which sympathetic innervation had been destroyed by

surgical removal of the SCG, linking the sequestration of NE to the sympathetic nerve terminal. Whilst testing cardiac ^{3}H-NE accumulation with known sympatholytics imipramine (tricyclic antidepressant[83]), and amphetamine (vesicular monoamine transporter ($VMAT_2$) substrate[84]) a significant reduction in tissue accumulation, alongside elevation in plasma levels of ^{3}H-NE was observed. Axelrod and Herrting suggested that re-uptake of NE by the same terminals that released it may terminate its action.

1.3.1 Structure and function

The norepinephrine re-uptake transporter is Na^+/Cl^--dependent transporter of the monoamine transporter family[85, 86]. The predominantly intracellular direction of the transporter is maintained by a number of factors including an inward Na^+ gradient, an outward K^+ gradient (maintained by the Na^+/K^+ ATPase) and the resting membrane potential which holds the inside of the cell negative[85, 87]. Functional studies indicate a binding order to the carrier of Na^+/Cl^- then substrate[85, 87, 88] with Na^+ and Cl^- both acting as co-substrates also transported into the cell. K^+ does not participate directly in the transport process, but has roles in maintaining appropriate ionic gradients and membrane potential[88]. Norepinephrine transport by NET is electrogenic with a net gain of positive charge[87].

Cloned human norepinephrine re-uptake transporter (hNET) cDNA has a 1857 base pair open reading frame predicting a protein of 617 amino acids with a mass of approximately 69kDa[89]. Human NET consists of 14 exons and 13 introns spanning 45kb, localized to chromosome 16q12.2[90, 91]. Functional studies have identified the COOH terminus as essential in determining substrate affinity, whereas, the amino-

Figure 1.2:

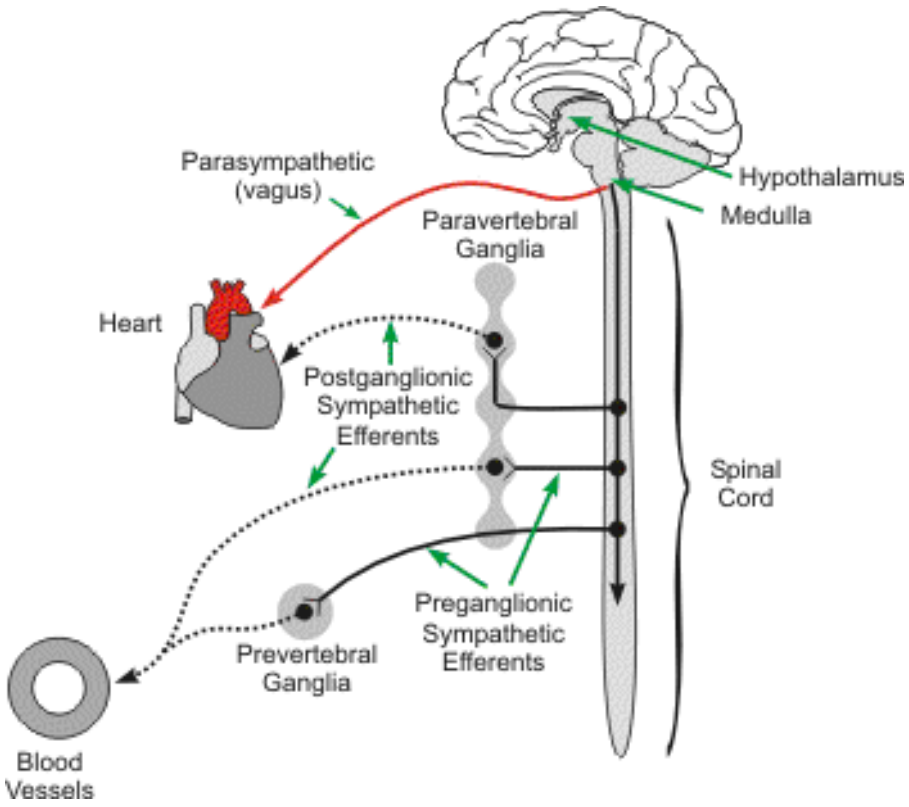

Figure 1.2: Sympathetic autonomic preganglionic and post-ganglionic efferents; site of ganglia.

Figure 1.3:

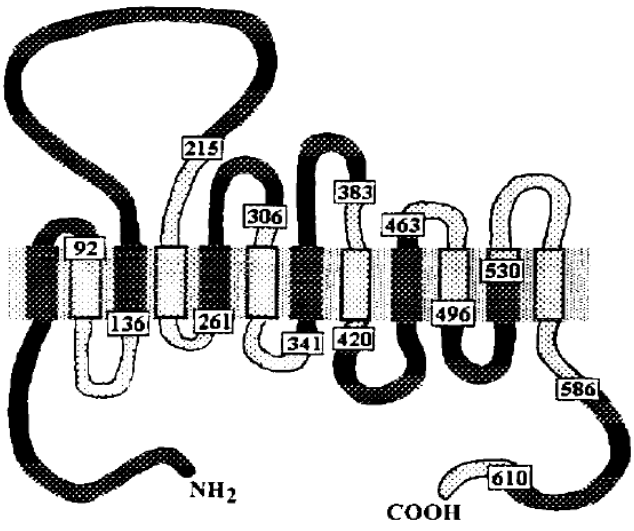

Figure 1.3: Transmembrane topology of hNET protein. Different exons are represented by black or dotted segments with labels showing amino acid number at the exon junctions (Porzgen, *et.al.* 1995).

terminal through the first 5 transmembrane domains is involved in uptake and ion dependence[92, 93]. Transmembrane domains 6-8 are predicted to be involved in tricyclic antidepressant binding[92]. A 4 kb region of the promoter flanking sequence confers hNET cell-selective expression, and is regulated by a combination of positive cis-acting elements[94] (figure 1.3). Major sequence and structural homology exists between all the monoamine transporters[86].

KINETICS OF NOREPINEPHRINE RE-UPTAKE TRANSPORTER

Studies by Schwartz and colleagues (2003) using ASP^+ and GFP-hNET, in HEK293 cell lines have been able to differentiate between the binding and transport kinetics of NET. Previous studies were unable to distinguish between these two processes, or provide adequate temporal or spatial kinetic resolution. Schwartz identified that while transport depended on both extracellular Na^+ and Cl^-, binding itself was independent of Na^+ and in fact increased in low Cl^-[95]. They also demonstrated a high inefficiency between the binding of the substrate to the carrier and the subsequent transport of that substrate into the cell. Binding rates were shown to exceed transport rates by approximately 100 fold, although these results may be different *in vivo* [95].

The K_m of ^{3}H-NE uptake is inversely related to the external Na^+ concentration[96], whereas an increase in cellular Na^+ concentration has been shown to favour outward transport of NE via NET[97]. Increasing intracellular Na^+ diminishes all three asymmetries previously described, resulting in a preference for outward transport of

NE. Release of NE during ischaemia is hypothesized to be due to carrier mediated outward transport [98].

3.3.2 Molecular Modulation

Extensive study of the NET protein gene sequence has revealed several regulatory domains and consensus sites for protein kinases and phosphatases[99, 100]. Initial studies demonstrated that neurons change the level of NET protein expression to adapt to changes in neurotransmission. Phosphorylation of NET is a major pathway for regulating cell surface expression and therefore NET activity. In general phosphorylation of the NET protein has been associated with an intracellular inactive sequestration of NET from the surface membrane, where as dephosphorylation promotes transporter incorporation in the cell membrane, increasing the transport capacity of NET. The extracellular loop between transmembrane domains 3 and 4 contains three potential N-glycosylation sites, N-linked carbohydrate additions to NET regulate transporter plasma membrane expression. There is a greater probability of glycosylated NET proteins being expressed on the plasma membrane, with poorly of un-glycosylated proteins being retained in the cytoplasm[101, 102].

Protein kinase C (PKC)

Protein kinase C (PKC) regulation of transporter expression is uniform among monoamine transporters, a number of phosphorylation sites for PKC within the NET gene sequence have been identified, specifically threonine 258 and serine 259.

Phosphorylation by PKC facilitates NET receptor internalisation, reducing the number of transporters at the cell membrane, and transport capacity[103-106].

Insulin

An insulin-regulated action on NET activity within cardiac tissue has been of great clinical interest and extensively studied[107, 108]. However, insulin's actions on NET to date appear to be dependent upon the cell line in which it is studied. Rat sympathetic ganglia express both insulin receptors and insulin-like growth factor (IGF-1) receptors[109, 110]. Effect of acute insulin treatment decreases NE uptake within PC12 cells expressing NET[111]. Insulin is known to decrease NET mRNA expression within the locus coeruleus of the rat[112]. Within PC12 cells the insulin induced decrease in uptake is caused by a decrease in V_{max} and surface membrane transport receptor number[111]. Whereas, PC12 cell treatment with IGF-1 shows an increase in uptake, distinguishing different effects of insulin regulation due to down steam processes of the insulin and IGF receptors. Exposure of SK-N-SH cells to insulin enhances NET activity via down stream processes involving PI3 kinase, p38 MAPK and PP2A (protein phosphatase 2A)[113, 114]. In contrast to the proposed inhibitory effect of insulin on NET, insulin stimulates increase in uptake are independent of changes in the cell surface expression of the transporter, and therefore may involve a conformational change in the transporter that effects its catalytic activity[114]. Impaired insulin regulation of NET may provide an important contribution to the well-documented sympathetic hyperactivity in obesity related hypertension[115].

Cell depolarisation and calcium dependence.

Potassium-induced depolarisation of PC12 cells increases NE uptake in a Ca^{2+} dependent manner[116]. Regulation of transporter function by interaction of components of the vesicle release SNARE complex (predominantly syntaxin-1A) and NET have also been observed[117, 118], revealing a Ca^{2+} dependent NET regulation via a PKC dependent pathway. Syntaxin-1A regulation of NET results in both, an increase in surface trafficking of NET, and also a direct interaction that acts to limit NET catalytic function[117, 118]. It seems the role for Ca^{2+} in the SNARE complex mediated modulation of NET is predominantly due to the need for cell depolarisation and Ca^{2+} entry for vesicle release. Anti-oligo nucleotide syntaxin 1A and botulinum toxin treatment both block the direct interaction of syntaxin 1A with NET and decrease NE uptake rate[117, 118]. The role for Ca^{2+} in the syntaxin 1A/NET interaction therefore appears to facilitate the movement of transporters to the site of release. Interestingly PKC induced NET regulation is abolished when the syntaxin 1A interaction is blocked, suggesting that it is the pool of NET transporter in the membrane that are most sensitive to kinase interaction not the cytoplasmic pool[117, 118].

Neuronal nitric oxide synthase

*E*merging evidence has shown that dysregulation of nNOS in SHR stellate neurons are coupled to downstream proteins that target protein kinases and intracellular Ca^{2+} handling. Abnormally high intracellular Ca^{2+} transients in cardiac sympathetic neurons from the pre-hypertensive SHR[1] are associated with decreased expression of nNOS , beta-1 subunit of soluble guanylate cycles (GC), and cGMP. Gene transfer of Ad-PRS-nNOS-mCherry can rescue the impaired Ca^{2+} transient in these neurons

and neurotransmission[36]. Studies to date on the potential role for cGMP and NO on NET modulation have been inconclusive. Apparsundaram showed the NO donor SNAP had no effect on NE uptake in SK-N-SH cells[119], whereas others, reported that SNAP depressed desipramine sensitive NE uptake in both PC12 cells and cultured SCG neurons[120]. As expected, SNAP increased intracellular cGMP levels, but 8-Br-cGMP had no affect on NE re-uptake suggesting a non-cGMP dependent modulation that might result from of S-nitrosylation of a regulatory site on the plasmalemmal NE transporter[120, 121]. Since the SNAP response was attenuated by 1mM cysteine, this raises the possibility that NO may regulate NET by modulating nitrosylation of regulatory sites. Indeed Kaye et al 2000 demonstrated SNAP mediated nitrosylation of the cysteine residue in NET[121].

B-type natriuretic peptide.

B-type natriuretic peptide (BNP) mediated activation of particulate guanylyl cyclase (GC) leads to an increase in intracellular cGMP, and a resultant increase in NET activity in hypothalamic brain slices in wistar rats, which is consistent with a role for cGMP[122]. This data when viewed with the observed negative result on desipramine sensitive NE uptake with 8-Br-cGMP combined with the presence of an appropriate motif in GC for S-nitrosylation[123], adds to the complexity of interpreting the NO/BNP results. One key factor which influences the interpretation of all these data are that the investigations have not been performed on cardiac sympathetic neurons, instead 'analogues' of sympathetic ganglia (eg PC12 cells) have been studied. Given the heterogeneity of response in the sympathetic nervous system in terms of neurotransmission[46], no firm conclusions nor mechanistic understanding can

therefore be drawn to support the idea that NET dysregulation underpins enhanced cardiac sympathetic activity in hypertension.

1.3.3 Implications for NET dysregulation in cardiovascular diseases

The fundamental nature of NE signalling in a wide range of physiological processes means that NE regulation is essential. Disruption of the noradrenergic system has been implicated in a number of conditions; including, depression[124-128], essential hypertension[46, 3, 129], cardiac failure[130], pre-eclampsia[131], and orthostatic intolerance[132-134].

Hypertension

As mentioned the hypertensive phenotype in clinical patients and the SHR model is known to partially arise due to sympathetic hyperactivity[37, 129, 135, 136]. However, the exact mechanisms by which this occurs have not yet been fully elucidated. Dysregulation in the rate at which NET clears synaptic NE may facilitate the increased sympathetic drive observed in hypertensive models. Norepinephrine re-uptake transporter knock out mice show elevated mean arterial pressure and heart rate compared to controls[137].

The SHR rat was developed by selectively breeding male and female wistar rats that expressed elevated blood pressure[138]. The blood pressure within the SHR showed a steady rise with age ranging from 136±13.4mmHg at 5 weeks of age to 188±17.5mmHg at 15 weeks of age. Blood pressure of the SHR rats was significantly higher than the control at 10 weeks of age[138]. The neural phenotype of the SHR in its hypertensive state has been extensively studied; Increased intracellular Ca^{2+}

transients from sympathetic neurons, and increased cardiac NE release contribute to the sympathetic hyperactivity observed in the SHR.

Previous studies into the role of NET in hypertension have often produced inconclusive or conflicting results. Patient studies by the Esler group have demonstrated a reduction in NET activity within lean but not obese related hypertensive utilising radiotracer methodologies, linked to no change in NET gene sequence[46 3, 129]. Whereas, both a reduction in uptake capacity[139], and no change in re-uptake between strain (SHR or WKY) or age (4-14 weeks) have been observed within atrial tissue of rat models [77, 140].

Orthostatic intolerance.

Orthostatic intolerance (OI), is characterised by the symptoms, light-headedness, fatigue, and postural tachycardia without orthostatic hypotension[132, 133], and predominantly effects women aged 20-50. OI is currently the only syndrome directly linked to a single nucleotide polymorphism within the hNET gene. Bradbury and Eggleston (1925) linked the symptoms of OI to a potential failure of the autonomic nervous system. Many studies had focused on the role of abnormal NE release in OI until NE overflow studies and analysis of the NET gene sequence in affected individuals identified a dysfunction of NET[132-134]. A missense mutation at position 237 exon 10 (G237C) results in an alanine to proline substitution (Ala457Pro) within a highly conserved region of transmembrane domain 9[132, 134]. When expressed in CHO cells the mutated protein shows a greater than 98% reduction in NET activity compared to the wild type[133], thought to be due to reduced NET-1 surface expression [141].

The differences in these results may be due to experimental numbers, and methods of study, indicating the importance of using the appropriate model system to draw conclusions.

The main aims of this thesis were:

1. To establish if the cardiac sympathetic hyperactivity observed in the adult SHR was present in the younger pre-hypertensive rat using novel fluorescence imaging technique with *in vitro* autonomic phenotyping.

2. To investigate NET rate in isolated sympathetic neurons of both young pre-hypertensive and older hypertensive SHR.

3. To establish how the dynamic action of NET may be modulated within single neuronal cells by a number of known sympathetic modulators.

CHAPTER 2:
GENERAL METHODS

The methods employed in this thesis were used to study end organ neuronal sympathetic signalling in the development of hypertension in the spontaneously hypertensive rat (SHR) and its aged matched normotensive control (WKY). All treatment of animals conformed to the Guide for the Care and Use of Laboratory Animals, Home Office UK; Animals (scientific Procedures) Act 1986 (PPL: 30/2360; PIL: 30/8431).

2.1. ANIMALS

Male SHR or WKY rats aged, pre-hypertensive 4 to 5 weeks (90g-120g), and hypertensive 16 to 17 weeks (340g-365g) were rendered unconscious using general anaesthesia (3% isoflurane and 97% oxygen), then humanly killed by the approved home office schedule 1 method of overdoes by pentobarbital followed by exsanguination. The young SHR were classified pre-hypertensive as they had normal blood pressure levels within the same range as age matched WKY.

2.2. ISOLATION AND PREPARATION OF SYMPATHETIC POST-GANGLIONIC NEURONS

Studying sympathetic nerve function in single cells isolated from nerve ganglia provide for a unique method of ascertaining physiological roles for nerve function under different conditions.

2.2.1. DISSECTION OF SYMPATHETIC GANGLIA

Cells were isolated from three major sympathetic ganglia previously implicated in neurogenic hypertension. The stellate ganglion, providing innervation to the heart[142], the superior cervical ganglion that predominantly innervates the head

Figure 2.1:

A

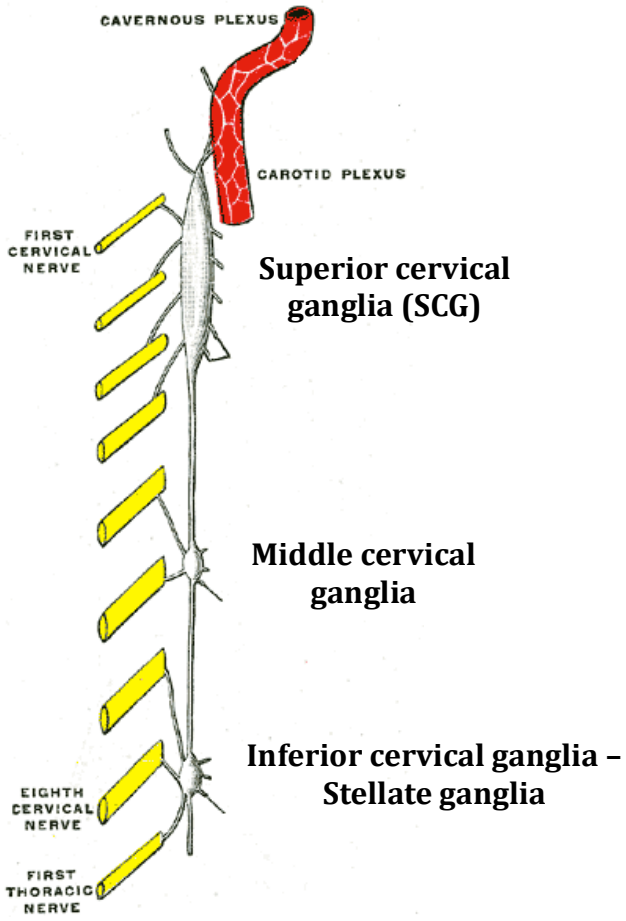

Figure 2.1.A: Schematic representation of the autonomic sympathetic chain anterior region, providing nerve innervations to the face, neck and upper thorax. The superior cervical ganglia is the largest and upper most ganglia innervating the face and neck (Bowers, *et.al.* 1979). The inferior cervical ganglia (Stellate ganglia) is located adjacent to C7, provides sympathetic innervation predominantly to the heart, in addition to the lower neck and arm (Pardini, *et.al.* 1990).

(Gray's subject no. 216 978)

B

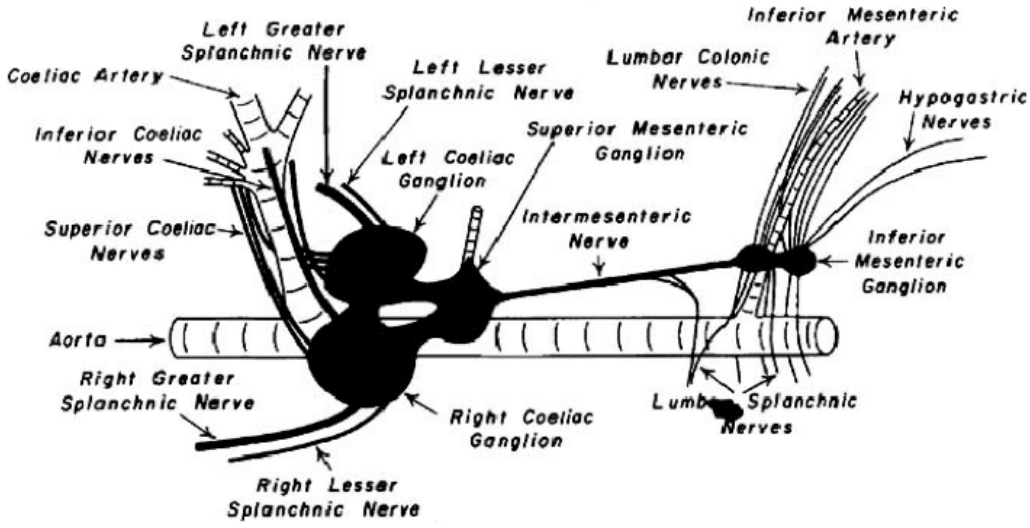

Figure 2.1.B: Schematic representation of the sympathetic innervation of the renal and mesenteric plexus. The morphology of the celiac ganglia and superior mesenteric ganglia meant it was often difficult to determine them as separate entities therefore for the purpose of the study the coeliac ganglia and superior cervical ganglia were dissected and cells isolated from it as one population.

(Physiology of prevertebral ganglia in mammals with special reference to inferior mesenteric ganglion. *J. H. Szurszewski, B. F. King*)

and neck region[143], and the celiac ganglion, superior mesenteric ganglion and sympathetic chain that innervate the kidneys, and other abdominal organs [143, 144] (figure 2.1.A&B).

Within all experiments sympathetic ganglia were dissected from both the left and right sides to increase cell yield. Due to the morphology of renal sympathetic innervation [145] the celiac ganglia and superior mesenteric ganglia could not always be identified as separate structures therefore these ganglia were dissected in unison and combined for all experiments (figure 2.1.B).

Sympathetic ganglia were identified by location and physical appearance using a dissection microscope to improve magnification. Dissected ganglia were carefully removed and placed in Leibovitz'z L-15 medium on ice.

2.1.3. Preparation of isolated sympathetic post-ganglionic neurons.

Neurons were dissociated mechanically by a method previously described by Orike, et.al, 2001[146]. In brief, dissected ganglia were cleaned of all connective tissue and desheathed. Cleaned ganglia were cut into small fragments before being placed in a 10ml falcon tube containing collagenase type 4 (1mg/ml in Ca^{2+} and Mg^{+2}-free phosphate-buffered saline (PBS); Worthington) for 18min - 42min depending on the type of ganglia and age of the animal, at 37^{o}C in a shaking water bath. The collagenase was then removed and replaced with trypsin TRL3 (1.25mg/ml in PBS; Worthington) for 22min - 42min, 37^{o}C. Following trypsin incubation ganglia were washed for 2 x 5min washes in an L-15 based blocking medium, followed by 2 x 5min washes in L-15 based plating medium to stop the action of the digestion enzymes.

Ganglia were then titrated into a single-cell suspension with a narrow opening fire polished Pasteur pipette 4-5 times. After titration the solution was left to rest for four minutes to allow any large tissue fragments to settle to the base of tube whilst leaving the single cells in suspension. The top 0.5ml of solution was then removed and placed in a plastic petri dish (2.5mm diameter). 0.5ml of fresh L-15 based plating medium was added to the falcon tube and this process was repeated 5-6 times.

The plastic petri dish containing the cell suspension was incubated at 37^{o}C, 5% CO_2, for 1.5-2 hours to allow any fibroblast contamination to settle out of solution on to the bottom of the plate. The cell suspension solution was then added to wells containing Poly-D lysine and laminin coated cover slips (5mm), placed at 37^{o}C 5% CO_2 for 1-2 days before use.

2.1.4 Preparation of solutions.

The mediums used for the isolation and culture of the isolated postganglionic sympathetic neurons were based on those previously described by He and Bass, 2003[147].

L-15 blocking medium is composed of an L-15 incomplete medium (Leibovitz's L-15 medium, 96.8% (v/v); D- (+)-Glucose solution (45%), 0.6% (w/v); 200mM L-glutamine, 2mM; Penicillin (10,000 units/ml), 100 units/ml; Streptomycin (10,000 µg/ml), 100 µg/ml.) at 90% (v/v), plus foetal bovine serum, 10% (v/v).

The L-15 plating medium used contains, L-15 incomplete medium, 90% (v/v); $NaHCO^3$, 24mM; Glucose, 38mM; Penicillin (10,000 units/ml), 50 units/ml;

Streptomycin (10,000 µg/ml), 50 µg/ml; Nerve growth factor, 25ng/ml; Foetal bovine serum, 10% (v/v).

Poly-D-Lysine was prepared in a 1mg/ml stock solution in borate buffer (Borax, 4.75mg/ml; Boric acid, 3.1mg/ml; double-distilled H_2O, 100% (v/v)). Glass coverslips were coated in 0.1mg/ml poly-D-lysine diluted in borate buffer over night at 4^oC, followed by 6 x 5 min washes in double distilled water. Cover slips were allowed to dry and kept at room temperature for one month.

On the day of use poly-D-lysine coated cover slips were incubated in 30µl laminin diluted in 720µl Leibovitz's L-15 medium, 37^oC, for 3-4hours. Laminin was completely removed before replacing with medium containing the single cell suspension.

2.1.6 Drugs and reagents.

Phosphate buffered saline (PBS), Leibovitz's L-15 medium, D- (+)-Glucose (45%), L-glutamine (200mM), foetal bovine serum, borax, boric acid and poly-D-lysine were all purchased from Sigma. Penicillin 10,000 units/ml; Streptomycin 10,000 µg/ml, nerve growth factor (NGF), and laminin were purchased from Invitrogen. Collagenase type 4 and trypsin TRL3 were purchased from Worthington.

2.3. Dynamic study of norepinephrine re-uptake transporter function.

As mentioned previously in chapter one sympathetic nervous system activity[39-41], and enhanced cardiac norepinephrine release[3, 37, 77], are well established as contributing factors to the pathophysiology of hypertension. One factor that may contribute to this is impaired NE re-uptake through the norepinephrine re-uptake

transporter (NET), although evidence to support this is currently inconclusive and methods used for study indirect[3, 43, 77, 139, 148].

In order to directly assess NET function ideally it needs to be studied at the level of a single nerve terminal or within tissue of high sympathetic innervation. The ability to specifically stain sympathetic nerves can help identify the nervous composition of a tissue. Although, techniques to effectively label sympathetic neurons have been established for decades, current processes involve fixation of the tissue preventing dynamic processes from being monitored within the same sample after nerve labelling.

Early methods of identifying sympathetically innervated tissue involved the use of triturated NE (^{3}H-NE) analogues, measuring relative degrees of ^{3}H-NE accumulation within homogenated tissue samples[82, 149]. While the development of scintiscans and Positron Emission Topography (PET) has allowed for ^{3}H-NE detection within intact tissue at a high spatial resolution (approximately 1mm), it still does not allow visualisation at the single nerve terminal[150]. High spatial resolution and visualisation of sympathetic innervation within intact tissue and nerve culture can be achieved with immunohistochemistry using fluorescent-tagged antibodies [151, 152]. However, this also requires tissue fixation therefore the same preparations can no longer be used to monitor dynamic processes. Formaldehyde-glutaraldehyde induced catecholamine fluorescence (FAGLU), an early method utilising the characteristic for hot formaldehyde vapour to form fluorophores with catecholamines in freeze dried tissue[153] has been shown to allow high spatial resolution of nerve terminals within sympathetically innervated tissue[154]. However, again this requires tissue to be fixed.

Previous methods of measuring NET activity within sympathetic tissue have been indirect. Direct visualisation of sympathetic nerves, and then having the ability to then monitor dynamic processes within that tissue has not previously been possible. Therefore before studies of NET have always relied on deducing the effect of transporter activity across a whole organ or tissue populations[77, 148]. Pre-administration of triturated NE (^{3}H-NE) is a common technique that allows for NET function to be inferred by measuring either the tissue accumulation or plasma run off of the ^{3}H-NE[98, 155]. The advantage of this technique is that it is highly versatile; although it gives some idea on the function of the transporter it does not provide any kinetics of uptake. 4-(4-(dimethylamion)styrl)-N-methyl-pyridnium (ASP^{+}) a fluorescent analogue of 1-methyl-4-phenylpyridinium (a neurotoxic metabolite and known substrate of monoamine transporters) has been used to investigate monoamine transporter activity in both single cell experiments and multiwell platforms[95, 156], however preliminary experiments (Unpublished data- R. Amos and K. Brain) were unable to use ASP^{+} to label mature sympathetic nerve terminals in intact tissue.

Current techniques used to measure NET activity have been insufficient in helping us gain further understanding into the dynamic function of NET within individual neuronal cells. Methods developed in this thesis have utilized a novel commercially available assay (Molecular devices: Sunnyvale, CA) to allow dynamic monitoring of NET function in single cells for the first time. The assay has previously been validated to monitor NET transport rates in cell culture systems[157] (figure 2.2.B) and intact tissue samples[158].

Figure 2.2:

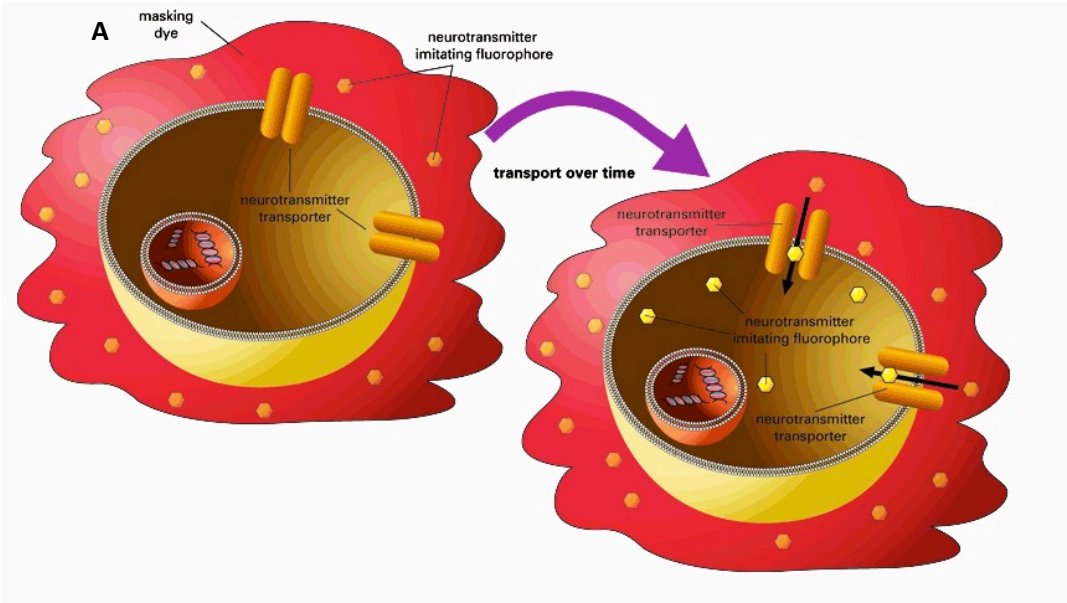

Figure 2.2.A: The neurotransmitter transporter uptake assay (NTUA) is a fluorescent substrate of the monoamine transporters. The assay is composed of two compounds, an extracellular masking dye and the monoamine transporter substrate which fluorescence is exposed upon uptake into the cell. (Molecular Devices, Sunnyvale, CA).

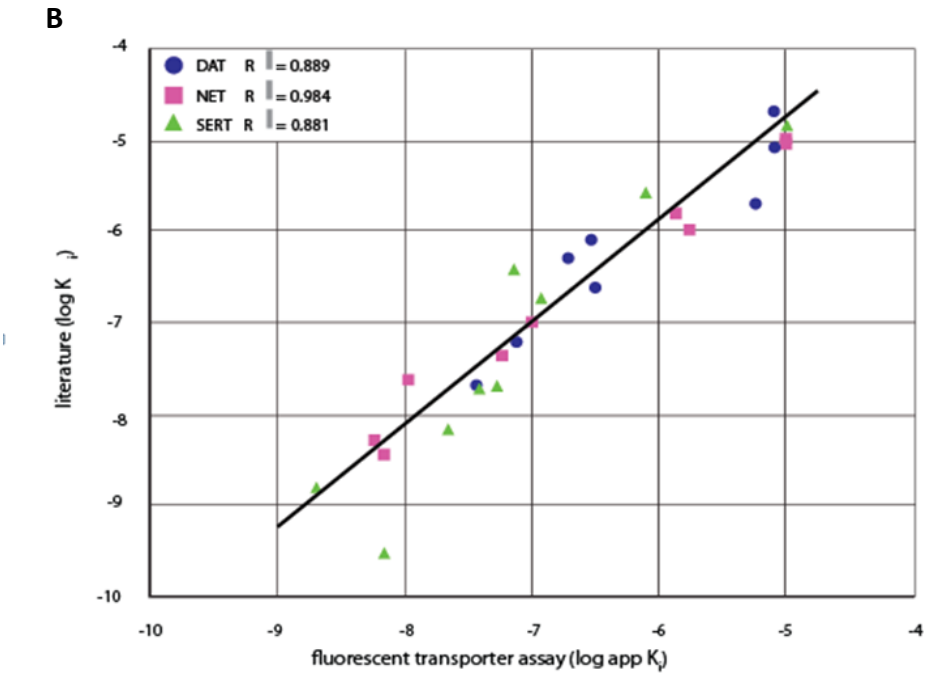

Figure 2.2.B: IC_{50} correlation NTUA uptake for NET, SERT, and DAT treated with eight known monoamine transporter inhibitors. Results obtained with NET were compared with the known Ki values of the monoamine inhibitors for the three transporters. The correlation coefficients R^2 for each transporter presented in the graph, R^2 value for all 24 values was 0.91. *(Molecular Devices, Sunnyvale, CA; Customer result)*

2.3.1. Using a fluorescent substrate to monitor norepinephrine re-uptake transporter activity.

The dynamic kinetics of NET action was measured in neuronal cells isolated from rat sympathetic ganglia. The commercially available Neurotransmitter Transporter Uptake Assay (NTUA) contains two compounds, a fluorescent substrate of NET and a masking dye that hides extracellular fluorescence (figure 2.2.A). Throughout this thesis NTUA refers to the intracellular fluorescence signal that arises on exposure to this kit, although the component leading to this signal cannot be entirely confirmed.

2.3.2. Assay preparation.

The NTUA kit was purchased from MDS analytical technologies (catalogue R8173; Wokingham, Berkshire, UK) and diluted with Tyrode solution (10ml per unit) to make a stock solution. This was divided into 1ml aliquots that were then stored at -20^{o}C for subsequent use. All drugs only underwent one freeze-thaw cycle.

2.3.3 Protocol

Prior to the start of experiments cells were pre-incubated in a low 1:100 concentration of the assay in L-15 based cell plating medium for 20 minutes, 37^{o}C, 5% CO_2 95% O_2. Coverslips were then transferred to a temperature controlled (37^{o}C) gravity fed perfusion chamber (volume: 500µl) on the stage of a Nikon Eclipse TE200-U microscope. Cells expressing the transporter were selected for study based on physical appearance and expression of a basal level of NTUA fluorescence under phase contrast (excitation wavelength 440nm, emissions band 535±35nm) using a 10x air objective, changing to a 60x oil objective for recording (figure 2.3). Rate of

intracellular fluorescence increase over time was measured by selecting a region of interest (ROI) around the isolated cell. Images were acquired every 2 seconds using a photometrics CoolSNAP HQ^2 camera, excitation wavelength 440nm, emissions band 535±35nm.

A control period of 5 minutes perfusion (3ml/min) in Tyrode solution to allow the cells to equilibrate within the system, was followed by a 5 minute perfusion with Tyrode + NTUA (1:10) assay (concentration consistent with previous studies[158]) so that the assay was at a constant concentration within the extracellular solution of the dish. The perfusion system was then stopped (to prevent any cell drift, and preserve the volume of NTUA already in the chamber, reducing assay wastage), and cells held stationary in the NTUA containing buffer at 37±0.5^{o}C for 10 minutes, where the rate of increase in fluorescence within the cell was recorded (figure 2.3.C). Any cell in which there was either spatial or depth (due to loss of objective focus) drift during the 10 minute hold were excluded from analysis as change in fluorescence over time could not be accurately tracked (figure 2.4.).

2.3.4. Confirmation of NTUA specificity to the norepinephrine re-uptake transporter.

To confirm the specificity of the NTUA assay to NET the NET inhibitor desipramine[82] (DMI 1µM) was added to the perfusing Tyrode solution and rate of fluorescence increase in the presence of NTUA (1:10) and DMI measured. Desipramine is a tricyclic antidepressant[82] and inhibitor of all major monoamine re-uptake transporters (norepinephrine, dopamine and serotonin). Although the NTUA assay has affinity for other monoamine transporter, there is no compelling data supporting

Figure 2.3:

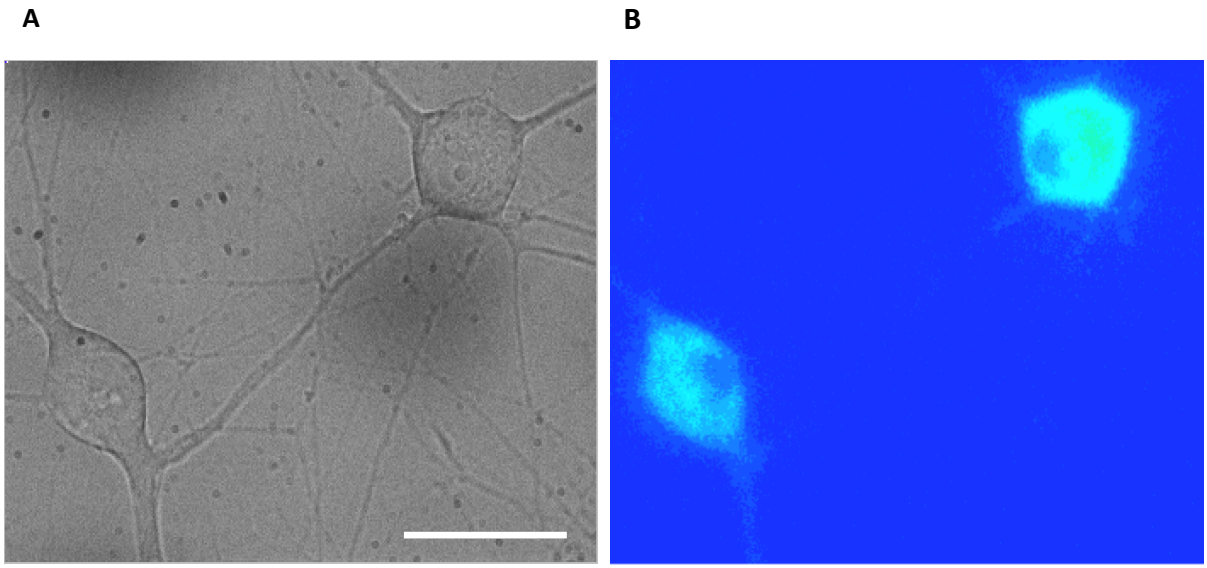

Figure 2.3: A, Bright field image of isolated sympathetic neuronal cells plated on poly-D-lysine coated coverslips as imaged under Nikon Eclipse TE200-U microscope. **B,** Sympathetic neurons after 20 minute NTUA (1:100) preload. Scale bar: 50µm.

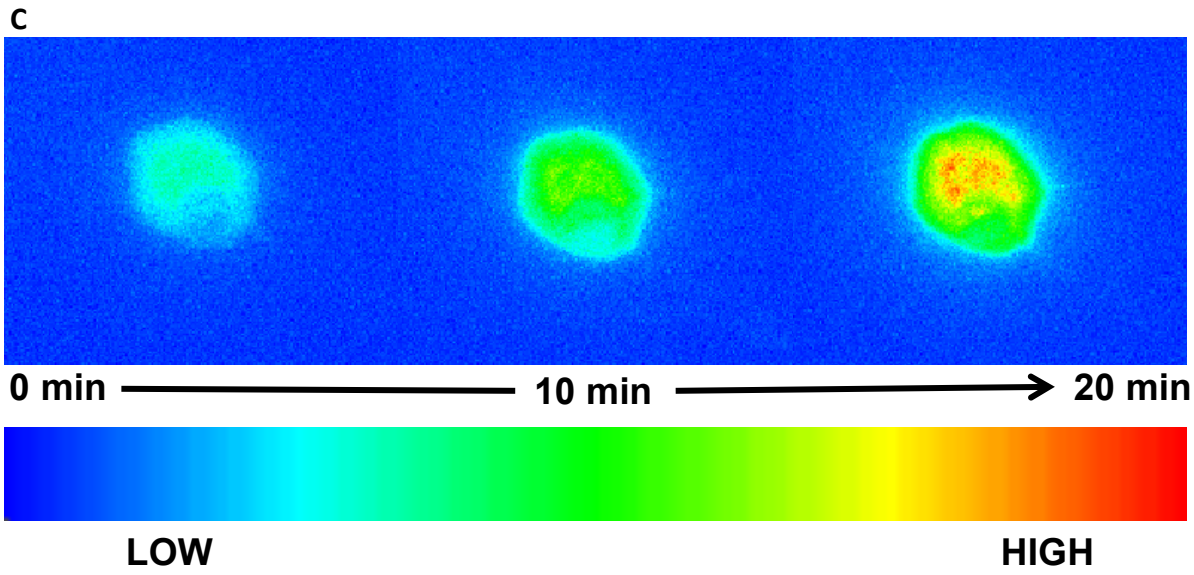

Figure 2.3:C, Rate of intracellular fluorescence increases over time from low to high during 10 minute NTUA (1:10) incubation.

Figure 2.4:

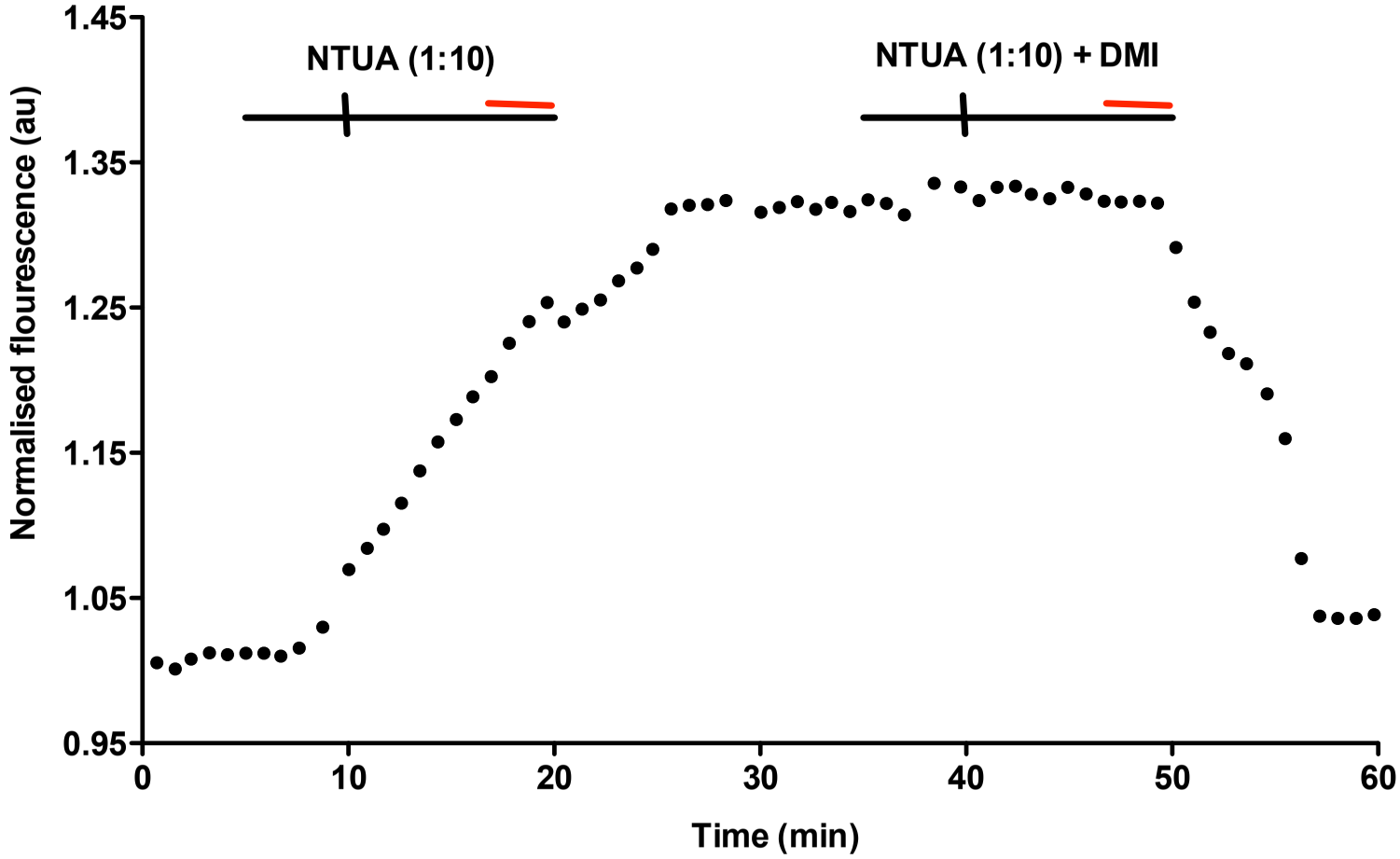

Figure 2.4: Representative raw data trace measuring NET activity using NTUA assay. Black horizontal bar indicates period in which NTUA (1:10) is added to perfusing Tyrode solution. Black vertical bar indicates when perfusion was stopped, cell held stationary and rate of intracellular fluorescence increase over time due to NTUA (1:10) measured (S1). Fluorescence increases linearly over time due to exposure to NTUA, this increase is completely inhibited by NET blocker Desipramine (1µM)(S2). Red horizontal bar indicators 2.5 minute period in which field stimulation (10Hz, 20V, 1ms) was initiated in stellate ganglia experiments.

significant expression of other transporters in the ganglia studied[159]. Moreover, DMI is a potent inhibitor of NET with a Ki of 4 nmol/L compared with the serotonin transporter (Ki = 61 nmol/L: Sigma data sheet product code D3900). Therefore any cellular fluorescence increase that occurred that could be blocked by DMI was concluded to be due to NTUA uptake through the NET transporter.

Within all experiments after the first NTUA (1:10) hold (designated S1 throughout) at 20 minutes the perfusing Tyrode was changed to one that contained DMI (1µM). At 35 minutes cells were re-perfused with a Tyrode solution containing NTUA (1:10) + DMI (1µM) and the hold protocol repeated from 40-50min (S2) (figure 2.4). Any cell in which the increase in fluorescence was not blocked by DMI was excluded from analysis (<5%), as any previous rate of uptake of the assay could not be confirmed to be NET specific (figure 2.5.A).

Results were presented as increase in fluorescence over time, normalised to the starting intracellular fluorescence of the cell at the start of each hold, allowing for comparison of changes in rate that was independent of the initial fluorescence (figure 2.6).

2.3.5. Effect of time on NTUA induced increase in cellular fluorescence.

Many fluorescent substrates and dyes used in microscopy protocols are known to be susceptible to photobleaching affecting the integrity of results over time[160, 161]. The NTUA assay has previously been shown to not be susceptible to photobleaching over long protocols, but only bleaches when high intensity light is focused onto a small area of tissue during FRAP (Fluorescent Recovery After Photo bleaching)

Figure 2.5:

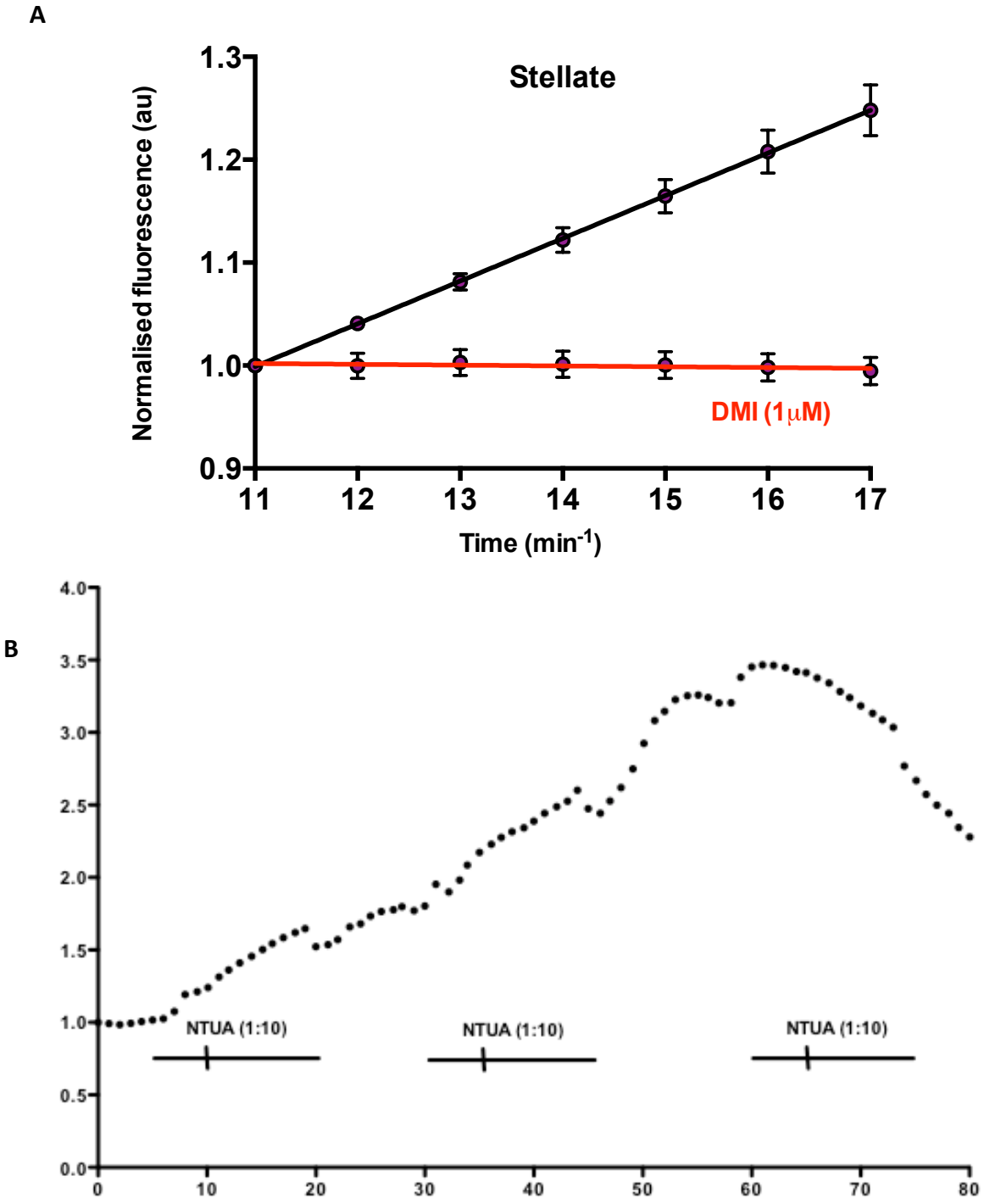

Figure 2.5: Rate of fluorescence increase in stellate neurons. Plotted as the gradient of the slope derived from y=mx+c. fluorescence increase blocked by DMI **A,** a reduction in uptake rate was observed with time (WKY n=18) **B,** Representative raw data trace of NET activity over a longer protocol of S1/S2/DMI as used during experiments carried out in chapter 6, looking at the pharmacological regulation of NET. S2 second NTUA hold when drug is present. Example from a time control trace where no drug was added.

A

Figure 2.6:

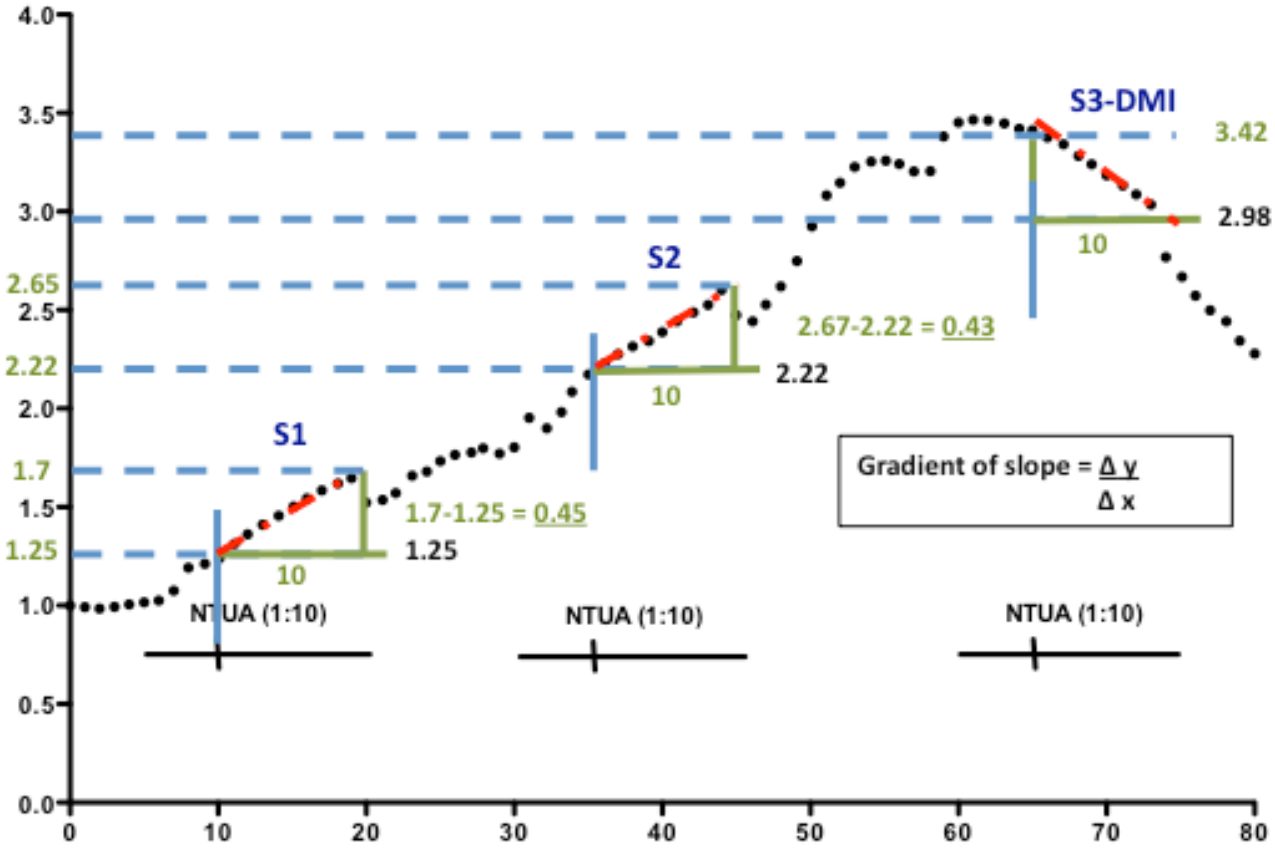

B

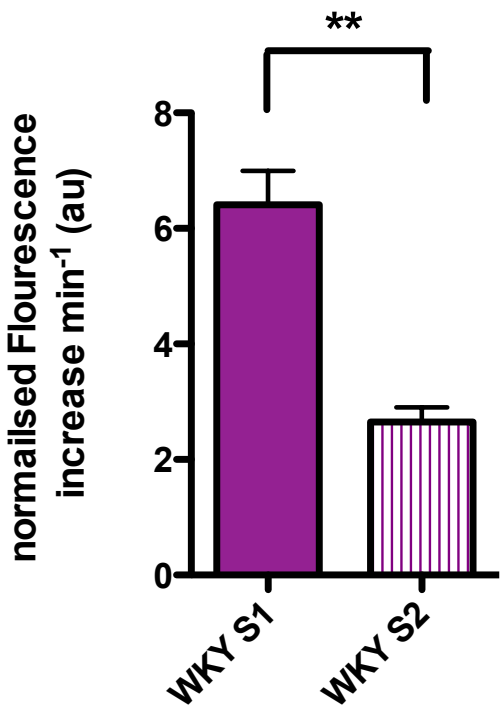

Figure 2.6: A, Representative raw data trace as shown in fig 2.5.B demonstrating how slope values were calculated and normalised to their starting fluorescence for S1/S2/S3-DMI. The ratio of change between S2 and S1 slope was plotted compared to time for all drug treatments. **B,** a reduction in uptake rate was observed with time (WKY n=18). Slope over time normalised to their starting fluorescence, difference in normalised slope rate is observed. However, S2/S1 ratio for paired results can normalise the difference in uptake rate observed allowing for a comparison between control and drug treatment at a given time. (**p<0.01).

experiments[158]. However, due to the inward kinetics of NET requiring the need for a number of ionic asymmetries and the concentration dependent nature of the transporter (as discussed in chapter one)[87, 97], time control experiments were performed to ascertain if the was any change in intracellular fluorescence accumulation rate over time of NTUA.

After an initial control recording (S1) cells were washed for a 15 minute period with Tyrode solution, followed by a five minute perfusion of Tyrode + NTUA (1:10) between 35-40min, corresponding with the maximum drug incubation time used within other protocols. The hold protocol was repeated from 40-50 minutes (S2), and an S2/S1 ratio for both groups of cells calculated to determine the role of time alone on change of uptake rate (figure 2.5.B).

Unsurprisingly due to the nature of the experiment, with all slopes normalised to their starting fluorescence, a reduction in uptake rate between S1 and S2 was observed S1: WKY: 6.66 ± 0.58 au/min^{-1}; S2: WKY: 2.65 ± 0.25 au/min^{-1}, WKY n=18,) (figure 2.6.B). This run down can be corrected for when data is presented as S2/S1 ratio (drug treatment/control) for all groups.

2.3.6. ELECTRICAL FIELD STIMULATION OF ISOLATED POSTGANGLIONIC NEURONS.

To test the effect of neuronal excitability on NET, cell depolarization was induced by electrical field stimulation (EFS) using a perfusion chamber adapted to contain parallel platinum electrodes inside the chamber below the water line of the perfusing solutions, connected to an external stimulator. Cells stimulated with EFS at 5Hz, 10V, 10ms pulse width, for 2.5min, from 7-9.5mins within the 10 minute NTUA

1:10 hold (S1) (red bar, figure 2.4). Parameters were chosen to match stimulation frequency and rate which shows submaximal noradrenaline release to right stellate stimulation in the isolated double atria preparation[162]. Stimulation parameters were confirmed to produce cell depolarisation using the Ca^{2+} indicator fura-2, Ca^{2+} transients were observed intracellularly in correlation with turning on of the electrical field stimulation.

2.4. Measurement of single cell norepinephrine release by amperometry.

Increased sympathetic nerve activity has been demonstrated by microneurography studies within patients with established and borderline hypertension[39-41]. By measuring single cell neurotransmitter release within isolated neurons, changes in sympathetic nerve transmission can be studied more directly.

Single cell noradrenergic neurotransmitter release can be detected by a number of electrophysiological or electrochemical methods. Although to date this has predominantly been carried out within cultures of small compact cells with known high catecholamine stores such as adrenal chromaffin cells (ACCs)[63, 65, 163]; due to the ease of cell shape and reliably high catecholamine release. Electrophysiology indirectly measures catecholamine release utilising the property of membrane capacitance (C_m). Either the whole cell or the secretory region of a cell are clamped using a patch pipette, and change in membrane capacitance due to cell activation is measured[164]. C_m which is proportional to the entire clamped surface area of the cell increases upon fusion of exocytotic vesicles with the plasma membrane, allowing the total cellular exocytosis that occurs within the clamped region to be measured. However, electrophysiological measurements can only be performed with a

successful cell surface clamp, therefore is not possible within complex structures such as neuron dendrites. Membrane retrieval of an exocytotic vesicle also counteracts the change in C_m due to vesicle fusion therefore can lead to an underestimation of total exocytosis. The nature of the membrane clamp also means that whole cell capacitance is recorded with no details on the distribution of release sites of composition of vesicles[165].

Alternatively, electrochemistry allows for the direct measurement of single cell neurotransmitter release by utilising the property that catecholamine molecules are oxidisable. The technique developed in the 1970's has now been optimised and used in a variety of preparations from ACC cell cultures to brain slices[64, 166, 167]. Catecholamines oxidise when they come into contact with a probe being held at a charge greater than their oxidation potential, resulting in a positive signal. The oxidation potential for NE is +780mV [168]. The advantages of electrochemical methods over electrophysical are that they allow for a quantifiable measurement of localised neurotransmitter release independent of cell geometry.

To date, due to challenges involved with electrochemical measurements from neurons, NE release from sympathetic nerve endings has been limited to measuring collective release from a number of varicosities in mature tissue. To directly ascertain a role for altered NE release within cardiac sympathetic neurons in hypertension an electrochemical amperometry based technique was developed to measure NE release between dissociated sympathetic neurons of the SHR and WKY.

2.4.1. VALIDATION OF CARBON FIBRE PROBE.

As discussed free NE will oxidise when it comes into contact with a carbon fibre probe held at an oxidation potential of +780mV[168]. Spatial resolution of electrochemical methods depends on the exposed carbon surface of the probe and the diffusion characteristics of the catecholamine in the tissue. Probes with a slightly extended cylindrical surface of exposed carbon fibre are regularly used for cyclic voltammetry and measurement within brain slices detecting catecholamine release within a greater area[169]. Where as, probes with an active discoid surface of about 5µm diameter positioned within about 0-5µm of a release site have been shown to allow for the resolution of single exocytotic release events[170].

Carbon fibre electrodes (CFE's) were originally purchased from ALA-Science (Farmingdale, NY) (figure 2.7.A.). The ALA-science CFE's are insulated with electrophoretic deposition paint (EDP), a method previously described[171] (pre-CFE). EDP has advantages over traditional methods of insulating carbon fibre probes by providing a thinner, more flexible coating around the carbon fibre than pulled glass capillary, Sylgard sealed probes. This allows for greater positioning accuracy within close proximity of the cells (figure 2.9.A). The low dielectric constant of EDP coated probes results in low capacitance and noise measurements compared to traditional methods. Where as, EDP compared to electropolymerization of phenol compounds has the significant advantage of greater simplicity, shorter processing times and lower toxicity of reagents involved[171].

CFE's were freshly cut to expose a discoid carbon surface and tested by low cyclic voltammetry (100mV/sec, 0.5V to -0.4V to 0.5V) in ferricyanide solution (1mM in 0.5M KCL, pH3[171]) (figure 2.7.B&C) before each experiment. Only cuts displaying

Figure 2.7:

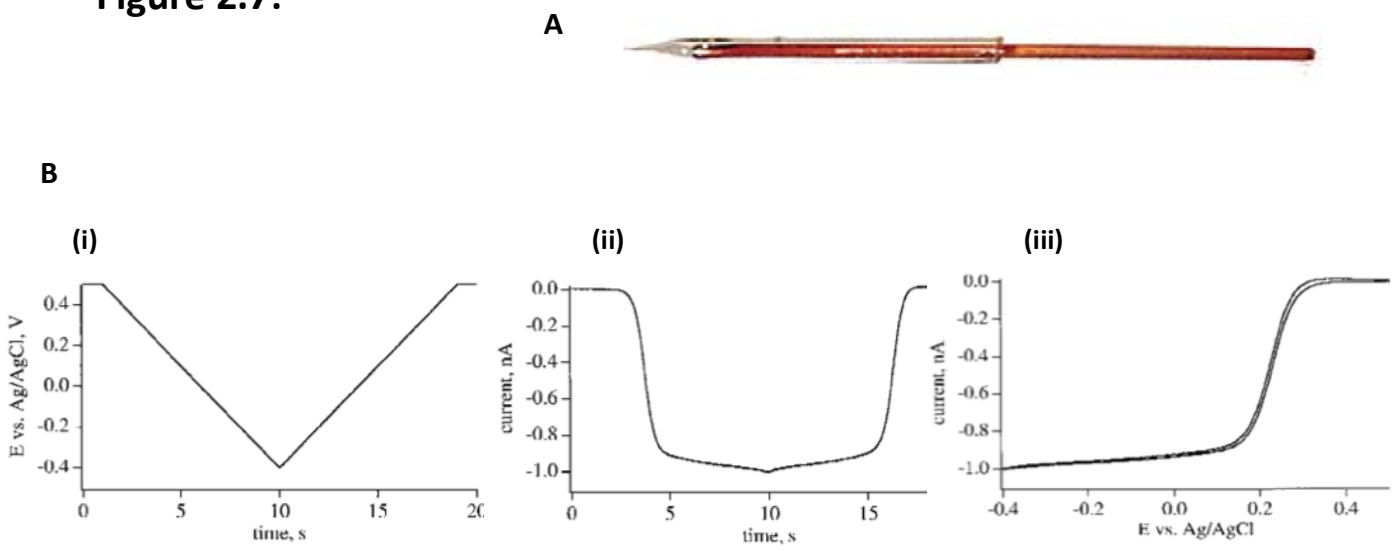

Figure 2.7: A, Carbon fibre electrode with electropaint deposition coated insulation as supplied from ALA-Scientific. **B,** Testing integrity of the insulation and seal around the discoid surface of the carbon fibre of a trimmed electrode. **(i)** Cyclic voltagram for the reduction of potassium ferricyanide (1mM) in 0.5M KCl, pH 3, scan rate 100mV/s. **(ii)** Corresponding current trace to cyclic voltagram in (i). **(iii)** combined image of the down and upstrokes of the current trace. A 'good' electrode is determined by a steep slope and overlapping curves as seen in (iii).

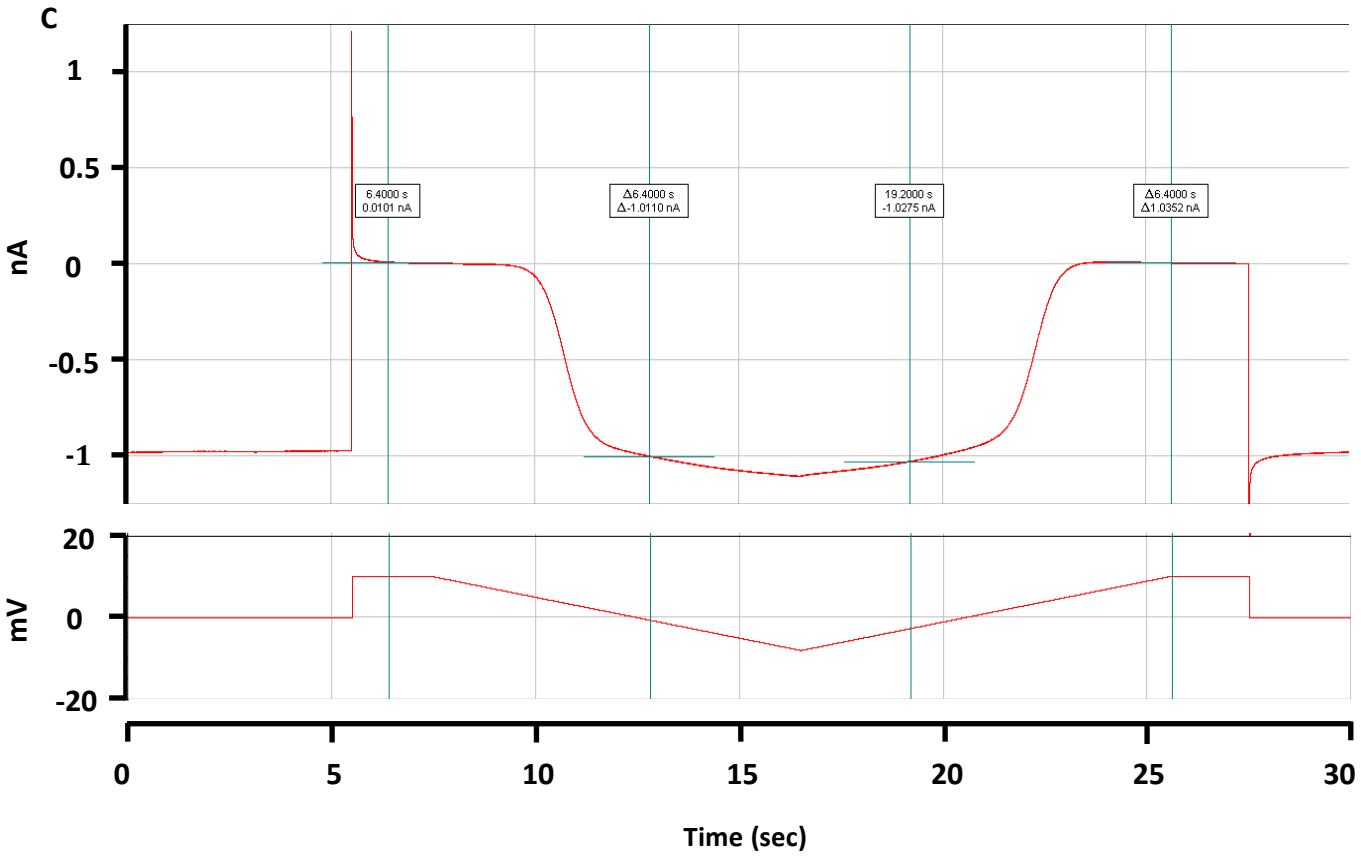

Figure 2.7: C, Example screen print pCLAMP software (Molecular Devices, Sunnyvale CA). Cyclic voltagram for the reduction of potassium ferricyanide (1mM) in 0.5M KCl, pH 3, scan rate 100mV/s, within our set up.

smooth, overlapping reductions curves with no hysteresis were used for experiments. The maximal reduction current in ferricyanide varied between cuts and is dependent on the total exposed surface of the carbon but does not affect recording of event properties[169].

2.4.2. Validation of the detection and oxidation potential of NE using CFE.

Within chamber norepinephrine voltage ramps

In order to test the system functionality and the ability of the CFE to detect a given concentration of NE slow voltage ramps (100mV-1000mV, 100mV, 4sec each step) were performed with the CFE held in a either Tyrode solution or 50µM NE (figure 2.8). Positive signals are detected upon oxidation of molecules on the exposed carbon fibre surface of the probe. The optimum oxidation potential for 50µM NE was observed to be at 800mV, consistent with the 780mV previously reported[168]. No oxidation was observed within Tyrode solution until very high potentials, confirming the specificity of the CFE to detect NE when held at a potential of 780mV.

To assess the sensitivity of the CFE to detect dynamic changes in NE concentration the slow volt ramps were repeated in solutions containing 10µM, 50µM, 100µM, and 500µM NE (figure 2.8.B). Increasing concentrations of NE resulted in a higher current detected at 800mV (880mV: 10µM NE, 0.054nA; 50µM NE, 0.096nA; 100µM NE; 0.135nA, and 500µM NE; 0,381nA), confirming the sensitivity of the CFE to detect NE.

Figure 2.8:

A

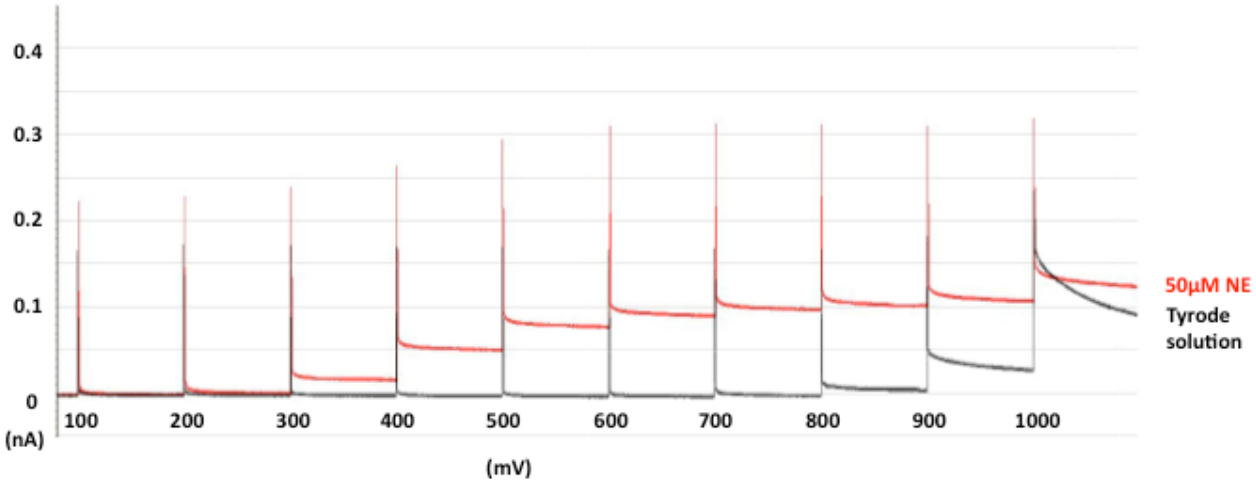

Figure 2.8: A, Voltage ramp, 100mV, 4 seconds per step. 50µM NA (red) and Tyrode solution (black). Optimum oxidisation potential for NA 800mV.

B

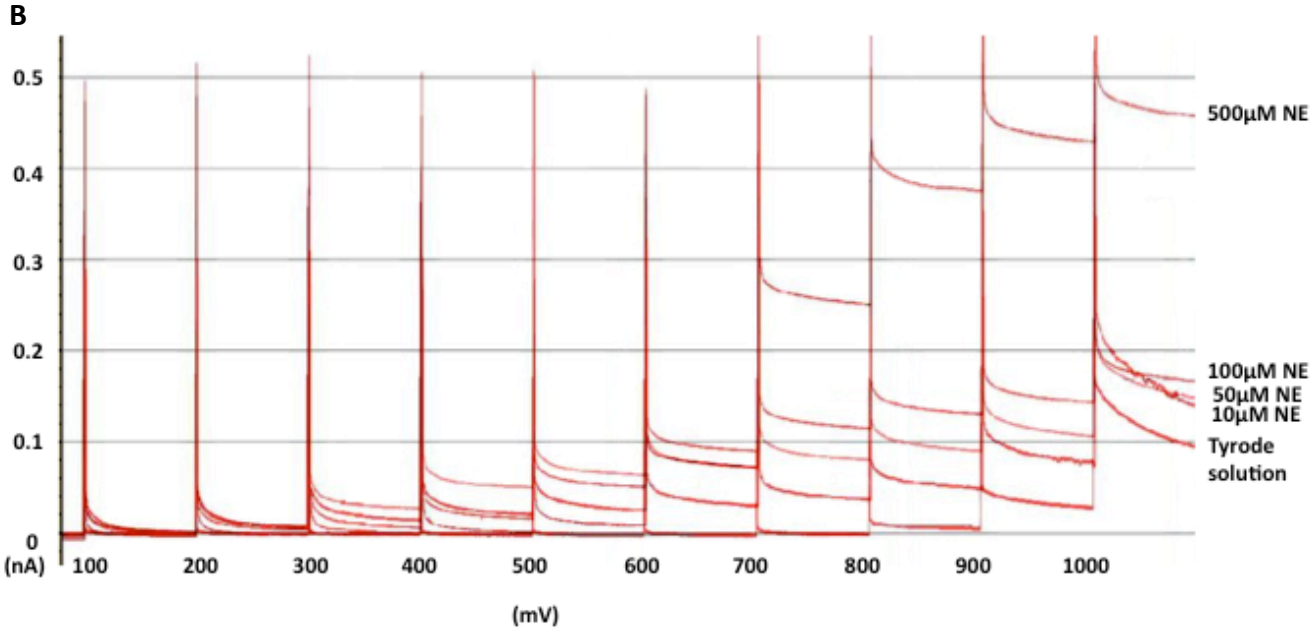

Figure 2.8: B, Voltage ramp, 100mV, 4 seconds per step. 10µM NE, 50µM NE, 100µM NE, 500µM NE, and Tyrode solution. Increased current detected upon oxidation of NE on carbon fibre probe with increasing concentrations of NE. Some oxidation is expected in Tyrode at very high electrical potentials.

Bath perfusion of norepinephrine

The ability of the CFE to detect changing concentrations of NE within the chamber and time course between change in perfusion solution and signal detection was tested. The CFE was positioned in the gravity fed perfusion chamber using a micromanipulator (Scientifica, UK) and charged to a driving voltage of 780mV. A general perfusion containing normal Tyrode solution was switched to one containing 50µM NE for 30 seconds, The current detected upon chamber perfusion of 50µM NE with a holding potential of 780mV was comparable to the current detected to 800mV in the voltage ramp in 50µM NE solution. Following 30sec 50µM NE perfusion was switched back to normal Tyrode, current returned to a steady base line. 50µM NE 30sec perfusion was repeated at three-minute intervals. Some reduction in the peak oxidation current occurred with repeated stimulations, however this is likely due to the un-physiologically high concentration of noradrenaline used. Detection of exocytotic release events within individual sympathetic neurons is expected to contain much lower concentrations of NE; therefore any detectable change in the measurement of spike concentrations or kinetics is unlikely to occur over the length of the experimental protocol[169].

2.4.3. Protocol refinement: change to pro-carbon fibre electrode

Great inconsistences occurred in the quality of the original pre-CFE's purchased from ALA-science that were previously described. Therefore to optimise the system a newly developed subtype of the carbon fibre microelectrode was tested, the Pro-CFE. The Pro-CFE is a polypropylene-insulated carbon fibre microelectrode

specifically designed to provide noise free fast and quantal secretion from single cells. The advantages of the Pro-CFE over paint type pre-CFE's are the reduced length of the carbon fibre tip of the Pro-CFE, reducing the mechanical instability, and degradation of the signal from the electrode over time (due to the paint isolation dissolving gradually into the bath solution during experiments)[172]. The Pro-CFE is also cheaper to manufacturer.

Pro-CFE's are manufactured by inserting a carbon fibre into a polypropylene pipette and heat pulling the pipette to produce a seal at the carbon fibre[172]. Electrical contact with the carbon fibre is made by backfilling the electrode with mercury which is then placed in contact with the input wire (Ag) of the headstage[172]. The Pro-CFE produced more reliable, consistent, results with less noise therefore was used in experimental studies.

2.4.4. Experimental protocol.

Postganglionic sympathetic neurons from the cardiac stellate ganglia of P_3 neonatal SHR and WKY rats were isolated, disassociated and plated onto 5mm coverslips as previously described in sections 2.2. Coverslips were then transferred to a gravity fed perfusion chamber (volume: 500µl) on the stage of a Nikon Eclipse TE200-U microscope.

Prior to the start of each experiment the CFE was positioned in the recording chamber using a micro-manipulator (Scientifica, UK) and charged to a driving voltage of 600mV. CFEs were manually positioned to touch a 4-5 cell sympathetic neuron

cluster (figure 2.9.A). A micro-puffer pipette was positioned on the other side of the cell for depolarisation.

A control period of 3-5 minutes in Tyrode perfusion was given at the start of each experiment to allow the trace to settle to a stable baseline. High K^+ (80mM) Tyrode was administered transiently in close spatial proximity to the cell by a patch electrode based glass puffer pipette (100mM K+, 2 secs) to trigger cell depolarisation based on a method previously described[168]. Detection of exocytotic release events of NE to cell depolarisation was detected as a positive signal. High K^+ induced cell depolarisation was repeated at 2-3 minute intervals.

2.4.5. TESTING RELIABILITY OF EVENT DECTECTION CORRELATES WITH NOREPINEPHRINE RELEASE.

To test if the release events detected in response to high K^+, were exocytotic release events and not noise, experiments were repeated with a proCFE holding potential of 600mV – 0 mV – 600mV. Noradrenaline will oxidise when it comes into contact with a probe held a 600mV, producing a positive signal. At 0mv NE does not oxidise therefore no positive signal in response to K^+ is seen. On return to 600mv the signals associated with the stimulation return (figure 2.9).

2.4.6. ACQUISITION AND ANALYSIS OF AMPEROMETRIC DATA.

Data were acquired using a VA-10X amplifier, gain 50, low pass filter 100 Hz, (npi electronic instruments, Tamm, Germany), driven through a Digidata 1440A data acquisition system (Molecular Devices, Sunnyvale, CA) by PCLAMP software

Figure 2.9:

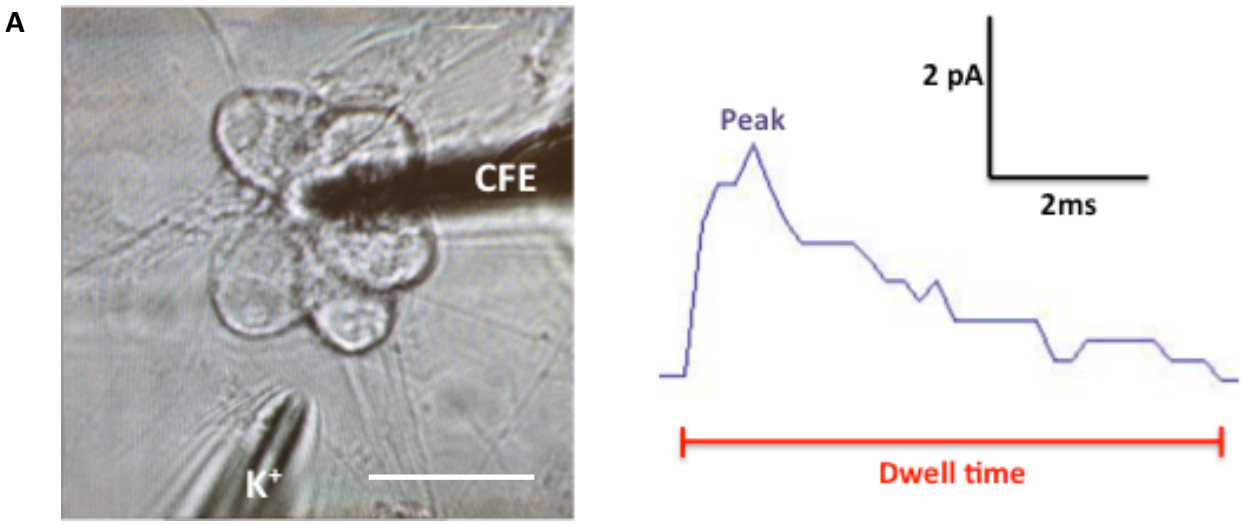

Figure 2.9: A, Carbon fibre electrode and depolarisation puffer pipette positioned close to postganglionic stellate neurons. **B,** Example trace of current spike detected in response to cell depolarisation (100mM K+). Parameters analysed, peak amplitude, dwell time of spike (red). Scale bar 50µm.

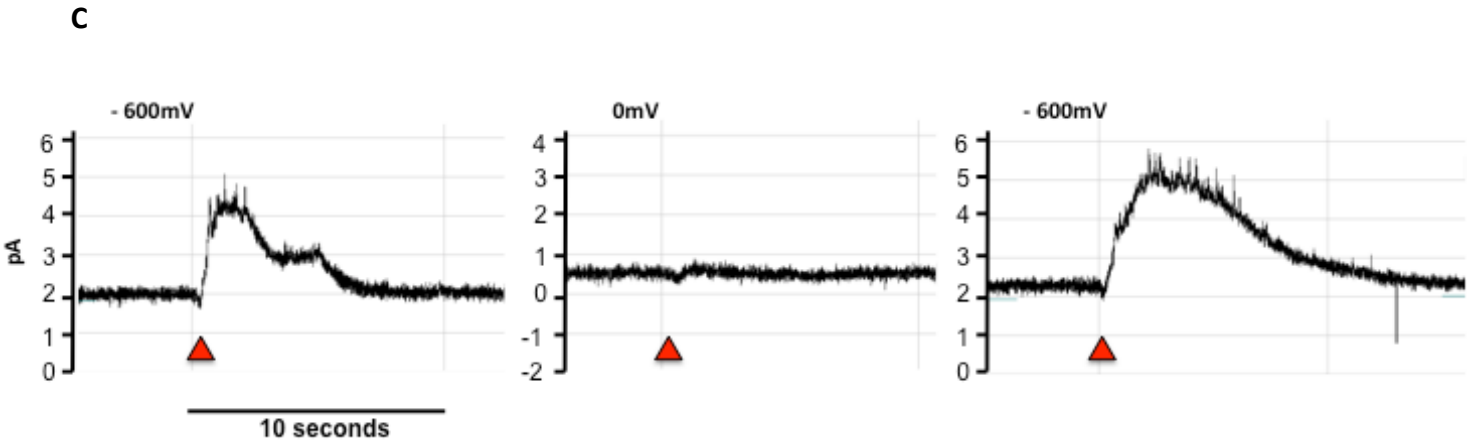

Figure 2.9: C, Raw data trace, high K^+ (80mM) puffed onto P_3 neonatal cell culture for 2 seconds at the red triangle, 10 secs post the start of each trace. Carbon fibre electrode held at a potential of 600mV – 0mV – 600mV respectively on the same cell culture. K^+ depolarisation is seen to produce positive signals at 600mV (the smaller spikes, not large displacement which is an artefact of the depolarisation) but not 0mV. This confirms that the spikes observed on the 600mV traces are due to oxidation of the CFE by a substance, consistent with literature likely to be NE.

(Molecular Devices Sunnyvale, CA). Recordings were stored for offline analysis, with a 30Hz high pass filter applied.

Analysis was performed using the clampfit application within pCLAMP. Peaks were detected using a semi-automatic event detection function after the setting of baseline and peak parameters. Any peaks detected were visually inspected to confirm time course and kinetics were consistent with an exocytotic release event. Any records detected with kinetics that did not seem consistent with a typical release event were discarded from analysis. Peak amplitude, abd time course (dwell time), were calculated for each spike (figure 2.9).

2.5. Measurement of [^{3}H]- norepinephrine release.

Spontaneously beating double atria were isolated and transferred to a pre-heated (37±0.2^{o}C), water jacketed, carbogen-aerated water bath containing 3ml Tyrode solution, where the atria were pinned flat over a silver stimulating electrode. The method for determining local NE release was based on one previously described[173]. Following a 20min equilibration period, Tyrode solution replaced every 10min; the double atria preparation was incubated with 5µM ^{3}H-NE (0.185 MBq, ARC) and ascorbic acid (30µM/L, Sigma). The atria were stimulated at 5Hz (15 V, 1ms pulse width) for 10 s every 30 s, for 30min to facilitate uptake of ^{3}H-NE into the transmitter stores of the pre-synaptic terminal. Following ^{3}H-NE incubation excess radioactivity was washed from the preparation with Tyrode's solution superfusion for 45min, at a rate of 3ml/min. Bath solution was then replaced every three min for 60min. A 0.5ml sample from each solution change was added to 4.5ml scintillation liquid (Ecoscint A, National Diagnostics) and the amount of radioactivity measured (counts per minute,

CPM) using a liquid scintillation counter (Tri-Carb 2800TR, Perkin-Elmers life science). At 16min the atria were stimulated at 5Hz for one min (stimulation 1, S1). The bath solution from 27min onwards was changed to contain one drug (desipramine 1µM, Sigma, or yohimbine 1µM, Sigma). A second stimulation (S2) was applied at 49min. The ^{3}H-NE outflow was calculated as a proportional percentage increase:

$$^{3}\text{H-NE outflow} = [(CPM_{(y)} - CPM_{(x)})/CPM_{(x)}]x100$$

($CPM_{(x)}$ = CPM immediately before stimulation; $CPM_{(y)}$ = CPM immediately after stimulation.)

A control experiment demonstrated no significant change in the magnitude of the response over two stimulations (n = 4)[173].

2.6. HEART RATE AND BLOOD PRESSURE RECORDING.

2.6.1. IN VIVO HEART RATE AND BLOOD PRESSURE RECORDING.

Heart rate and blood pressure *in vivo* is often measured within rodents using a tail cuff method by inflating the cuff around the rodents tail to occlude blood flow. Haemodynamic measurements are then recorded upon deflation by one of several types of blood pressure sensor placed distal to the cuff. Although, this technique is non invasive, and great advances within volume pressure recording (VPR) have been made[174], tail cuff recordings can still be subjected to more movement and temperature artefacts with measurement of blood pressure through carotid artery cannula still being considered the gold standard[175].

In order to achieve a simultaneous recording of blood pressure and heart rate *in vivo* the left carotid artery was cannulated with a 3F portex cannula connected to a pressure transducer and data acquired using a biopac M150 system (AcqKnowledge 3.9.2 software)[173]. Rats were ventilated under anaesthesia (3% isoflurane, 100% oxygen) throughout the procedure. Experiments were carried out under a heat lamp, with the animal resting on a 37^{o}C heat mat to maintain appropriate body temperature. An equilibration period of 5 minutes allowed the system to stabilise before heart rate and blood pressure readings were taken. The *in vivo* set up also allowed for the direct cannulation of the vena cava for the administration of drugs to assess their affect on haemodynamic parameters between the different animal models and in response to direct vagal nerve stimulation (figure 2.10).

2.6.2. IN VITRO HEART RATE RECORDING.

In vitro heart rate recording has been used to measure the effect of sympathetic stimulation on heart rate within an isolated double beating atria preparation as previously described[162, 176]. The mediastinum and thorax were immediately removed from terminally anesthetised rats and the ventricles perfused with heparinized Tyrode solution (1,000U/ml) to prevent blood clots forming in the atria. Both atria and the right stellate ganglion were dissected free from the ventricles and a suture placed on the lateral edges of both atria. Within a preheated (37^{o}C) water jacketed bath the left atrium was connected to a stainless steal hook, and the right atrium was connected to a force transducer for the recording of heart rate. The right stellate ganglion was placed through a pair of platinum electrodes and connected to a stimulator (figure 2.10.C).

Figure 2.10:

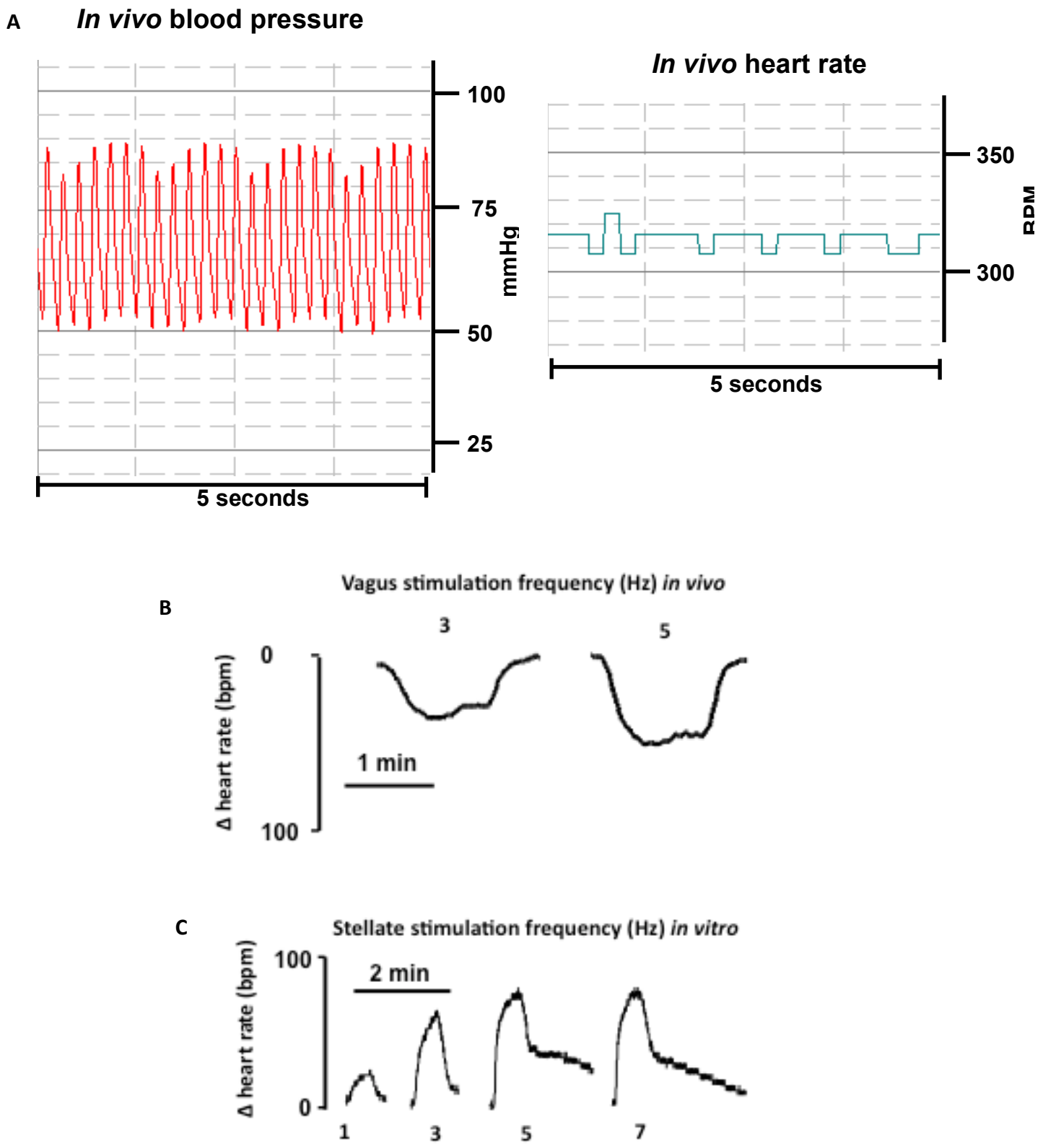

Figure 2.10. A, Raw data of *in vivo* blood pressure and heart rate of anesthetised WKY rat. Recorded using a biopac M150 system connected to a Dell computer running AcqKnoledge 3.9.2 software. **B,** vagal stimulation *in vivo* decreases heart rate. **C,** *ex-vivo* double atria with attached stellate preparation. Stellate stimulation increases heart rate.

Before starting each protocol, mounted atria were allowed to equilibrate for 45 min in Tyrode solution until beating rate stabilized (±5 beats per minute). The stellate was stimulated at 1,3,5 and 7 Hz (20V, 1ms pulse duration for 30s). Tyrode solution was replaced approximately every 30min throughout each protocol. Data was obtained using a biopac M150 system connected to a Dell computer running AcqKnowledge 3.9.2 software.

2.8. IMAGING OF ISOLATED POSTGANGLIONIC SYMPATHETIC NEURONS- IMMUNOHISTOCHEMISTRY.

Immunohistochemistry was used to confirm that postganglionic neurons isolated from major sympathetic ganglia were sympathetic in origin and remained sympathetic post isolation. Animals were terminally anaesthetised by 3% isoflurane, then humanly killed by the approved home office schedule 1 method of overdoes of pentobarbital followed by exsanguination. Sympathetic ganglia were removed and postganglionic neuronal cells isolated and plated on laminin-coated coverslips as previously described.

Two-Three days post culture (to mirror the time period in which cells are used for experimental protocols); coverslips were first washed once in phosphate buffered saline (PBS)(Sigma) to remove any cell medium. Cells were then fixed with 2% paraformaldehyde (Sigma) for 10 minutes at room temperature, followed by three x five-minute washes in PBS. Neurons were permeabilized using a permeabilization and blocking solution containing 0.1% Triton-20 (Sigma) + 1% bovine serum albumin (BSA) in PBS for 20-30min at room temperature followed by two x washes in PBS.

Neurons were then incubated in primary antisera, rabbit anti-TH (1:200) in 1%BSA/PBS for one hour, 37^{o}C. Following incubation neurons were then washed three x five-minute in PBS and incubated in the secondary antisera Alexa Fluor 647 goat anti-rabbit IgG (1:200)(Invitrogen) in 1%BSA/PBS for one hour, 37^{o}C. Neurons were washed once in PBS before incubating in DAPI (1:1000) a nuclear stain for three min, room temp, followed by three x five-minute washes in PBS (figure 2.11).

Sympathetic labelling was viewed using a Nikon Eclipse TE200-U microscope excitation wavelength 640nm, emissions 700±75nm.

2.9. Quantification of protein expression levels in sympathetic neurons- Western Blot analysis

Protein expression levels within the SHR and WKY sympathetic ganglia were determined using western blot. Western blotting can detect the presence and to some degree the expression level of the protein within a given sample. By loading equally amount of protein into each well, and by normalising the optical density of the band of the desired protein to a loading control differing protein expression levels between samples can be measured.

Stellate ganglia were dissected placed in ice-cold L-15 medium and carefully cleaned of connective tissue before rapidly preserving in liquid nitrogen. Frozen tissue was homogenized in lysis buffer (CelLytic) and a cocktail of protease inhibitors at a ratio of 40:1 (Sigma, U.K.) followed by four freeze-thaw cycles. Homogenized tissue was centrifuged at 14,000 r.p.m, 10 minutes, 4^{o}C and the supernatant collected. Protein concentrations were measured using the Bio-Rad DC protein assay kit. 40μg of

Figure 2.11:

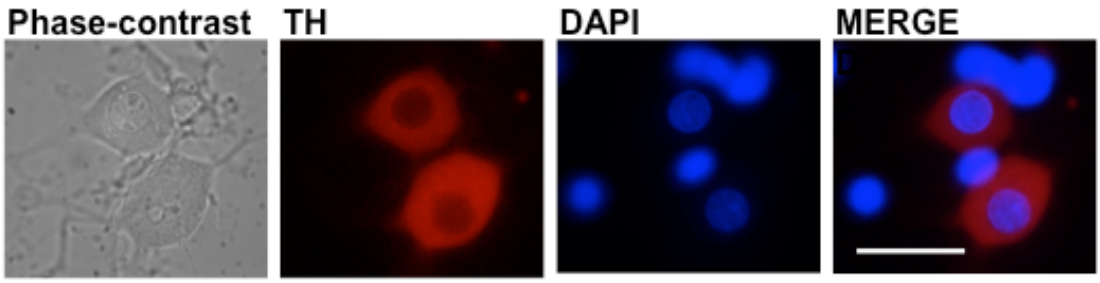

Figure 2.11, Positive immunoreactivity to sympathetic marker tyrosine hydroxylase in WKY sympathetic neurons. DAPI is a nuclear stain. Scale bar: 50µm.

Figure 2.12:

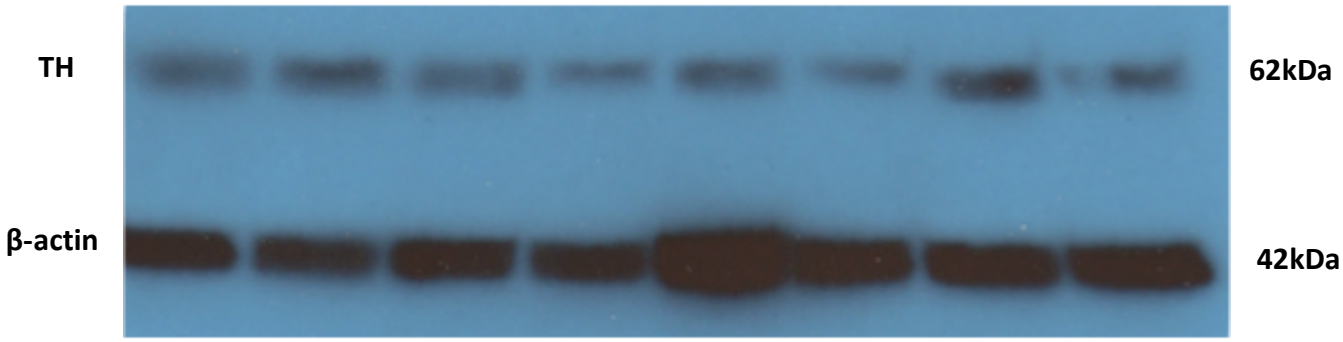

Figure 2.12, Expression levels, using western blot, of loading control β-actin and tyrosine hydroxylase in homogenised stellate ganglia.

stellate protein was separated on 4-15% gradient Tris-HCL gel (Criterion, BIO-RAD) and resolved proteins transferred to a PVDF membrane (Immobilon-P 0.45µm, Millipore) by electroblotting. Membranes were blocked in 5% non-fat dried milk in PBS/0.05% Tween-20 (Sigma) at room temperature, then incubated overnight in primary antiserum (1:1000 rabbit pAb anti-tyrosine hydroxylase and 1:200 rabbit pAb β-actin, abCam) PBS/0.05% Tween-20 solution at 4^{o}C. Reactive bands were visualized with Plus-ECL reagent (Perkin Elmer). Results are normalized to the GAPDH loading control (figure 2.12).

Analysis of the exposed reactive bands needs to be taken with caution. As with immunohistochemistry, any membrane exposed for long enough will fluoresce due to the intrinsic auto-fluorescence of proteins. Therefore, the intensity and duration of exposure for western blot membranes has to be carefully monitored. Over exposure of a loading control to expose the desired band can lead to a non-linear interpretation of protein concentration between bands during normalisation.

CHAPTER 3.

EXAGGERATED PERIPHERAL SYMPATHETIC CONTROL OF HEART RATE IN THE PRE-HYPERTENSIVE SPONTANEOUSLY HYPERTENSIVE RAT

3.1. INTRODUCTION.

Sympathetic hyperactivity is a key feature of essential hypertension [39-41, 43, 44, 177] and may arise at several distinct neuroanatomical sites. Recently major changes have been reported at the end organ level in peripheral cardiac sympathetic neurotransmission in the adult spontaneously hypertensive rat (SHR) compared to normotensive Wistar Kyoto rats (WKY) [1, 35, 37, 77, 162, 178]. At 16 weeks of age there is evidence of significantly elevated heart rate and mean arterial pressure within the SHR [162], indicating that the SHR have established hypertension by this age. The SHR at 16 weeks also display evidence of left ventricular hypertrophy [162], and increased NE release [37] which are phenomena associated with both human and animal models of hypertension[179-181]. A larger tachycardia on stimulation of the right stellate ganglion [162] is also observed in the adult SHR. Cultured neurons from the stellate ganglion of adult SHRs have larger depolarisation induced calcium transients compared to WKYs [1], and this may drive a greater calcium dependent exocytotic release of NE. Increased NE release appears to be further exacerbated by an observed reduction in the autoinhibtory action of the pre-synaptic α_2 adrenoceptor [77]. Alongside the end organ sympathetic signalling dysfunction observed in the adult SHR, the heart rate response to stimulation of the cervical vagus nerve is diminished in the SHR compared to age matched WKYs [34].

A number of recent studies provide evidence that dysregulation of cardiac sympathetic neurotransmission may arise before the onset of hypertension in the SHR. At around four weeks of age when the SHR is still normotensive compared to

age matched WKY animals an increased intracellular calcium transient in response to neuronal depolarisation has been described in stellate and superior cervical ganglia (SCG) neurons[1]. Dysregulation in the action of the norepinephrine re-uptake transporter (NET) has also been observed in a number of studies of young and older SHR compared to WKY (see chapters four and five)[140, 182]. However, the functional significance of these observations in terms of NE release and peripheral cardiac sympathetic control of heart rate is unknown. It is also currently unknown the degree to which SHR display compensatory mechanism to hypertension, such as left ventricular hypertrophy or reduced α_2 receptor auto-inhibition at this developmental age.

I therefore hypothesised that end organ cardiac sympathetic neurotransmission may be altered in the young four week pre-hypertensive SHR, before the animal develops the higher resting heart rate and elevated arterial blood pressure that is associated with hypertension.

3.2 METHODS

3.2.1. ANIMALS.

Age and weight matched four to five week (60g-110g) male SHR and WKY rats were purchased from Harlan (Biscester, UK), and housed under standard laboratory conditions. All experiments were performed under British Home Office license requirements (PPL 30/2360) in accordance to the Guide for the Care and Use of Laboratory Animals published by the US National Institutes of Health (NIH

Publication No. 85-23, revised 1996) and the Animals (Scientific Procedures) Act 1986 (UK).

3.2.2. VENTRICULAR WEIGHT: BODY WEIGHT RATIO

To determine the degree of left ventricle hypertrophy as a measure of cardiac remodelling during hypertension[180] between the two groups the whole body weight and then the dissected ventricular weight of each rat was measured, and the ventricular weight:body weight ratio was calculated.

3.2.3. HAEMODYNAMIC MEASUREMENTS AND HEART RATE RESPONSES TO VAGUS NERVE STIMULATION IN-VIVO.

Baseline haemodynamic measurements of heart rate and blood pressure within the SHR and WKY rats, as well as monitoring heart rate change to *in vivo* vagus nerve stimulation, was measured in rats that were ventilated under anaesthesia (3% isoflurane and 97% oxygen) as a terminal procedure. The left carotid artery was cannulated with a 3F portex cannula, based on a method previously described[173]. The cannula was connected to a calibrated pressure transducer and data acquired using a biopac M150 system and data acquired using a Macbook Pro computer running AcqKnolege 3.9.2. software. Following an equilibration period of 5-10 minutes, heart rate and blood pressure recordings were taken as an average over 30 seconds, at a rate of 200 Hz. In a subset of experiments the right vagus was isolated, crushed distal to the heart and stimulated at 3Hz and 5Hz (20V, 1msec pulse duration for 30s) and heart rate response recorded.

3.2.4. Measurement of heart rate response to right stellate stimulation in vitro

In order to measure heart rate responses to sympathetic nerve stimulation (SNS), spontaneously beating atria with intact sympathetic innervations and right stellate ganglia were isolated and responses to SNS measured based on a method previously described[162, 176]. For methods see chapter two.

3.2.5. MEASUREMENT OF LOCAL ^{3}H-NE RELEASE FROM ISOLATED DOUBLE ATRIA.

Spontaneously beating double atria were isolated and transferred to a pre-heated (37±0.2^{o}C), water jacketed, carbogen-aerated water bath containing 3ml Tyrode solution, where the atria were pinned flat over a silver stimulating electrode. The method for determining local NE release was based on one previously described[173]. Briefly following a 20min equilibration period, Tyrode solution replaced every 10min, the double atria preparation was incubated with 5µM ^{3}H-NE (0.185 MBq, ARC) and ascorbic acid (30µM/L, Sigma). The atria were field stimulated at 5Hz (15 V,1ms pulse width) for 10 s every 30 s, for 30 min to facilitate uptake of ^{3}H-NE into the transmitter stores of the pre-synaptic terminal. Following ^{3}H-NE incubation excess radioactivity was washed from the preparation with Tyrode solution superfusion for 45min, at a rate of 3ml/min. Bath solution was then replaced every 3min for 60 min. A 0.5ml sample from each solution change was added to 4.5ml scintillation liquid (Ecoscint A, National Diagnostics) and the amount of radioactivity measured (counts per minute, CPM) using a liquid scintillation counter (Tri-Carb 2800TR, Perkin-Elmers life science). At 16 min the atria were stimulated at 5Hz for 1min (stimulation 1, S1). The bath solution from 27 min onwards was changed to contain one drug (desipramine 1µM, Sigma, or yohimbine 1µM, Sigma). A second stimulation (S2) was

applied at 49 min. The ^{3}H-NE outflow was calculated as a proportional percentage increase, see chapter two.

3.2.6. MEASUREMENT OF CELLULAR NOREPINPEHRINE RELEASE USING CARBON FIBRE AMPEROMETRY

Stellate neurons were isolated from SD, SHR and WKY P_3 neonatal rats, by methods previously described in chapter two. Neonatal rats, rather than four week old rats were used for amperometry experiments as the isolation of neurons at this age results in the formation of multi-cell clusters. With extensive testing it was found that consistent reproducible NE detection was not possible from single isolated cells, therefore cells forming in 4-5 cell clusters were used. This offers limitations as clusters would contain slightly varying number of cells, which could effect results. These were preliminary tests, with further work can be corrected for in the future.

6mm diameter coverslips with neonatal stellate cells were left for 3 days post culture (consistent with testing for reliable NE release). Coverslips were transferred into a 500µl gravity perfused chamber on top of a microscope stage with two micromanipulators. The micromanipulators were used to position one pro-CFE (held at a potential of -600mV) and one micro-puffer pipette within close proximity of the cell cluster. Following an equilibration period cells were depolarised by high K^{+} (80mM), two seconds, administered via the micro-puffer-pipette.

Data were acquired using a VA-10X amplifier, gain 50, lowpass filter 100 Hz, (npi electronic instruments, Tamm, Germany), driven through a Digidata 1440A data

acquisition system (Molecular Devices, Sunnyvale, CA) by PCLAMP software (Molecular Devices Sunnyvale, CA). Recordings were stored for offline analysis, with a 30Hz filter applied. Analysis was performed using the clampfit application within pCLAMP. Peak amplitude, dwell time (time course), were calculated for each spike.

3.2.7. Measurement of tyrosine hydroxylase protein expression by western blot analysis.

Dissected stellate ganglia were carefully cleaned of connective tissue before rapidly preserving in liquid nitrogen. Frozen tissue was homogenized in lysis buffer (CelLytic) and a cocktail of protease inhibitors at a ratio of 40:1 (Sigma, U.K.) followed by four freeze-thaw cycles. The homogenized stellate ganglion tissue was then centrifuged at 14,000 r.p.m, 10 minutes, 4^{o}C from which the supernatant collected. Protein concentrations were measured using the Bio-Rad DC protein assay kit. 40μg of stellate protein was separated on 4-15% gradient Tris-HCL gel (Criterion, BIO-RAD) and resolved proteins transferred to a PVDF membrane (Immobilon-P 0.45μm, Millipore) by electroblotting. Membranes were blocked in 5% non-fat dried milk in PBS/0.05% Tween-20 (Sigma) at room temperature, then incubated overnight in primary antiserum (1:1000, rabbit pAb anti-tyrsosine hydroxylase, and 1:200 rabbit pAb β-actin,, abCam) PBS/0.05% Tween-20 solution at 4^{o}C. Reactive bands were visualized with Plus-ECL reagent (Perkin Elmer). Results are normalized to the β-actin loading control. See chapter two.

3.2.8. Plasma Neuropeptide Y (NPY) levels.

Another method of determining the level of cardiac sympathetic activity within the young SHR and WKY rats is to measure the level of free circulating sympathetic co-transmitters, such as NPY, that are released in unison with NE from the postganglionic neuron during high sympathetic drive.

In a subset of animals immediately following terminal anaesthesia, on opening the thorax a 26-gauge needle was inserted through the right ventricle to the level of the right atria and 0.5ml blood sample obtained. The sample was immediately centrifuged (10min, 13,000rpm) to isolate plasma and snap frozen at -80^{o}C. NPY concentration was measured using a commercially available ELISA (S 1346, Peninsula Laboratories, Bachem) against serially diluted protein standards.

3.2.9. Solutions and drugs.

Rat Tyrode's solution for the isolated atria preparation contained (mmol/L NaCl 120, KCl 4.7, $MgSO_4$ 1.2, KH_2PO_4 1.2, $NaHCO_3$ 25, $CaCl_2$ 2 and glucose 11), constantly aerated with carbogen (5% CO_2 95% O_2) to maintain pH 7.4. Experiments using ^{3}H-NE and ascorbic acid were carried out in the dark due to the light sensitivity of the drug. Desipramine (1µM, Sigma) was used at a concentration previously shown to completely inhibit NET[35], and yohimbine (1µM, Sigma) at a concentration used to completely block α_2 in a similar preparation[183]. Drugs were made up and stored as stock solutions (1mM) and diluted to the desired concentration on the day. All drugs under went no more than one freeze thaw cycle.

3.2.10. STATISTICS.

All statistical analysis was carried out using GraphPad Prism (GraphPad Software, San Diego, CA, USA). Data was presented as means±SEM and all data passed a normality test. Analyses between groups of data were done using an unpaired Student *t* test assuming unequal variance. For all experiments, statistical significance was accepted at $P<0.05$.

3.3 RESULTS:

3.3.1 BASELINE HAEMODYNAMIC CHARACTERISTICS

At four weeks of age the SHR (n=19) did not show any change in *in vivo* systolic, diastolic or mean arterial blood pressure compared to WKY rats (n=20), measured under general anaesthesia. However, the SHR displayed a small but significant resting tachycardia compared to WKY under these conditions (figure 3.1). After the removal of the spontaneously beating atria and equilibration of the organ within water bath no difference in *in vitro* baseline atrial rate between SHRs (n=9) and WKYs (n=7) was observed. At four weeks there was no difference in the ventricular weight: body weight ratio between the SHR (n=19) and WKY (n=21), indicating no left ventricular hypertrophy within the SHR. Animals were age matched and were of a similar weight as shown in Table 3.1.

Although these results present a lower blood pressure than in awake animals, the mean arterial blood pressures are still physiological. Telemetry and tail cuff introduces a lot of variability into measure of blood pressure and heart rate. Even

Table 1.

Baseline haemodynamic measurements

	WKY	SHR
***In vivo* Systolic Blood Pressure (mmHg)**	88±3 (n=20)	89±2 (n=18)
***In vivo* Diastolic Blood Pressure (mmHg)**	49±4 (n=20)	51±3 (n=18)
***In vivo* Mean Arterial Blood Pressure (mmHg)**	66±3 (n=20)	69±3 (n=18)
***In vivo* Heart rate (bpm)**	298±11 (n=20)	**334±9*** (n=19)
***In vitro* Heart rate (bpm)**	286±9 (n=16)	298±7 (n=19)
Body weight (g)	97± 4 (n=48)	96± 3 (n=53)

Table 1. No statistical difference in *in vivo* systolic, diastolic or mean arterial blood pressure, or *in vitro* atrial rate is observed between 4 week old SHRs and WKYs, which are also of a similar weight. However, *in vivo* heart rate was significantly increased in the SHR (*P<0.05, unpaired t test).

under general anesthesia the increase in heart rate is small, power analysis calculated prior to experiments revealed n=20 was required for each group to reveal a statistical significance. Another recent study by Komolova *et. al.*[184], supports these general anesthetic findings with telemetry results.

3.3.2 In vivo heart rate response to parasympathetic stimulation

There was no difference in the heart rate (bpm) response to right vagal stimulation between the SHR and WKY at either 3 or 5Hz (3Hz: SHR, n= 9, WKY, n= 6. 5Hz: SHR, n= 12, WKY, n= 10) *in-vivo* (figure 3.2).

3.3.2 In vitro heart rate response to sympathetic stimulation

The heart rate response to stimulation of the right stellate ganglia in the isolated atria preparation was significantly higher in the pre-hypertensive SHR compared to age matched WKYs at 5 and 7Hz (5Hz: SHR, 96.75±4.4 bpm, WKY, 81.71±5.4 bpm. 7Hz: SHR, 108.6±6.5 bpm, WKY, 80.60±4.5 bpm, n=7; figure 3.3).

3.3.3 Sympathetic neurotransmitter release

The level of ^{3}H-NE release in response to field stimulation of double atrial preparations was significantly higher in the pre-hypertensive SHR compared to age matched WKYs (SHR: 82.14±10.5 %, n=17 Vs WKY: 56.05±7.0 %, n=16; figure 3.4). Similarly, plasma levels of the sympathetic co-transmitter NPY sampled from the right atria, were also significantly elevated in the SHR (SHR: 15.70±3.1 nM, n=12. WKY: 8.46±1.4 nM, n=12) (figure 3.4.C).

Figure: 3.1

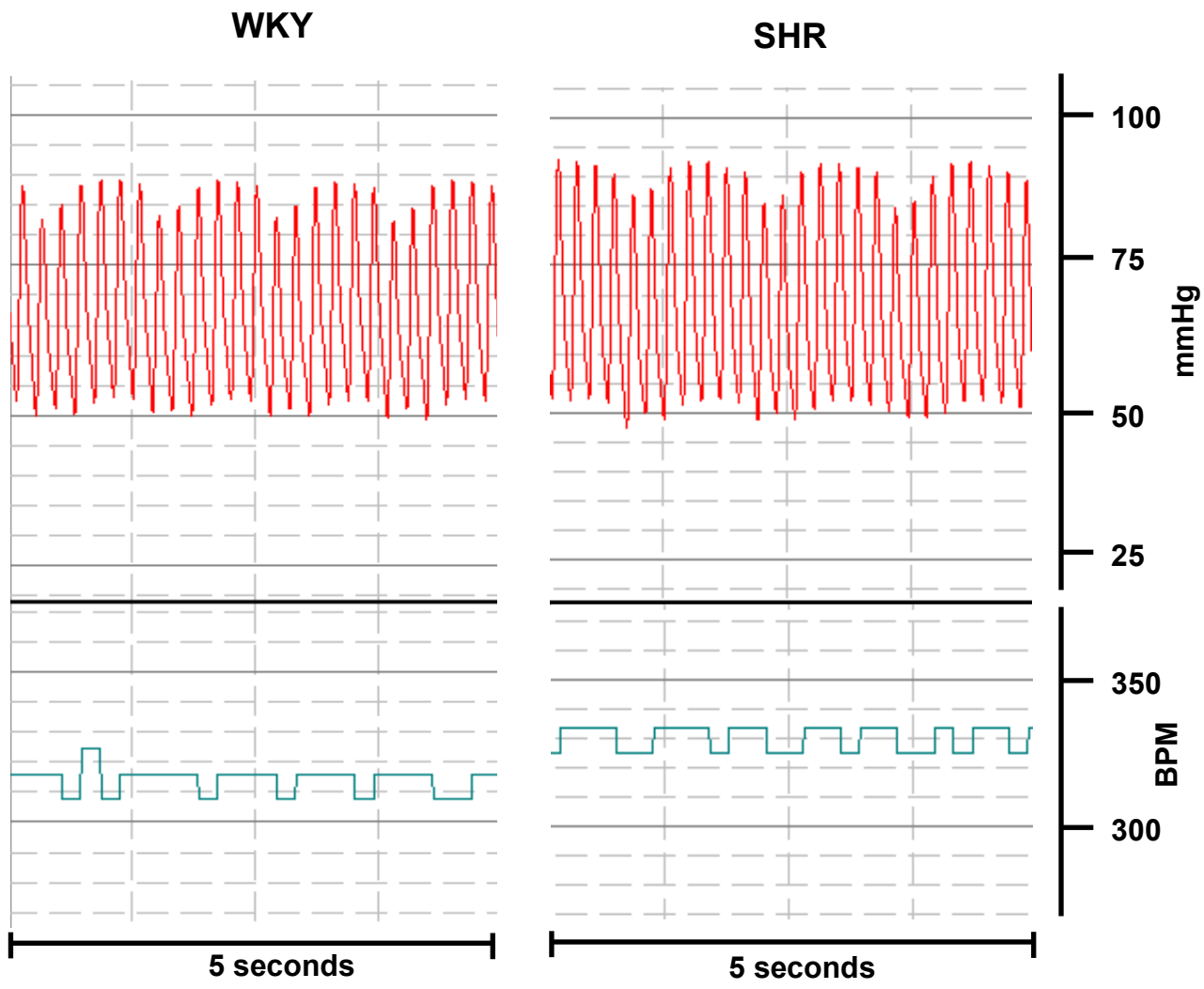

Figure 3.1: Raw data traces obtained from four week SHR and WKY under 3% isoflurane anaesthesia, recorded using a biopac M150 system connected to a Dell computer running AcqKnowledge 3.9.2 software. Top red trace blood pressure measured in mmHg, oscillations in blood pressure can be seen consistent with breathing. No change in mean arterial blood pressure between SHR and WKY. Lower blue trace, heart rate in beats per minute (BPM), SHR displayed a small but significant tachycardia compared to WKY at this age.

Figure: 3.2

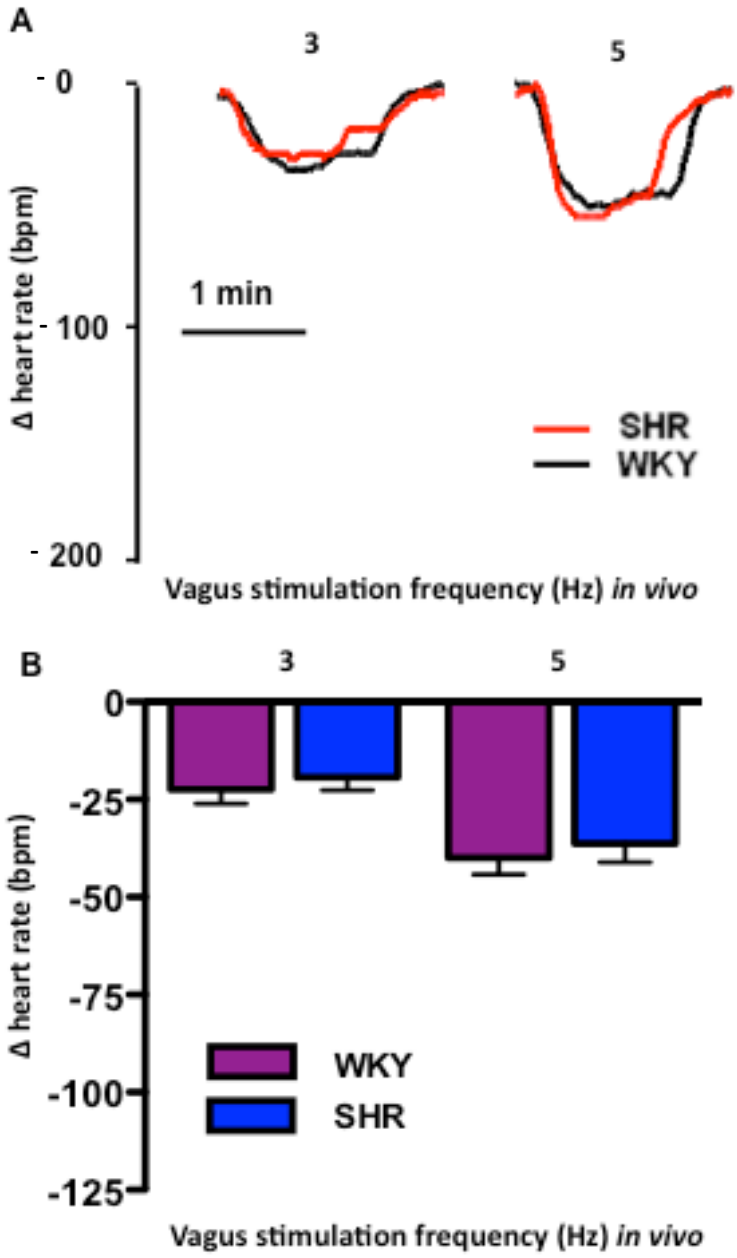

Figure 3.2 : A, Representative raw data trace and **B,** group mean data demonstrating that the heart rate response to vagal nerve stimulation was similar in the pre-hypertensive SHR (3Hz: n= 9, 5Hz: n= 12) compared to WKY (3Hz: SHR, n= 6. 5Hz: n= 10).

Figure: 3.3

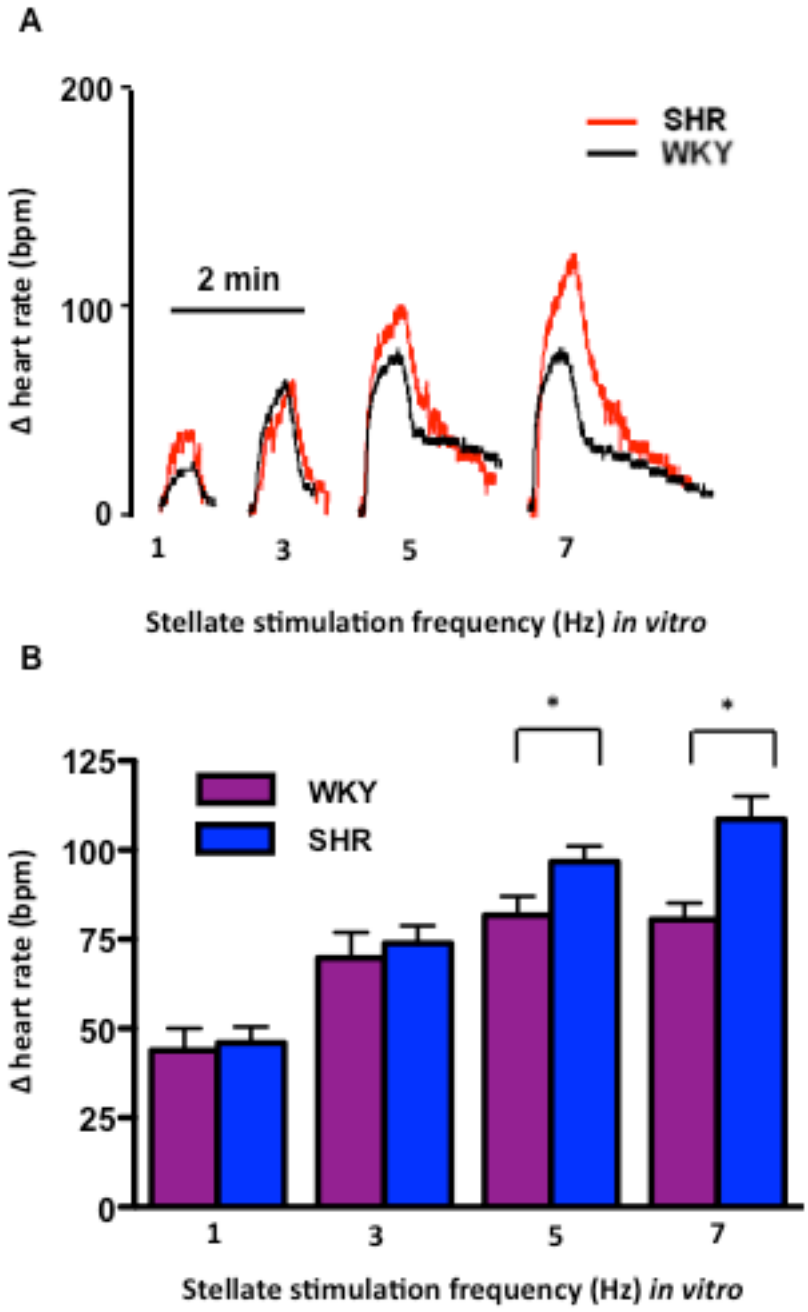

Figure 3.3 : A, Representative raw data trace and **B,** group mean data demonstrating that the heart rate response to right stellate ganglion stimulation was significantly larger in the pre-hypertensive SHR (n=9) compared to WKY (n=7), significant at 5 (**P*<0.05, unpaired *t* test) and 7Hz (***P*<0.01, unpaired *t* test).

Figure: 3.4

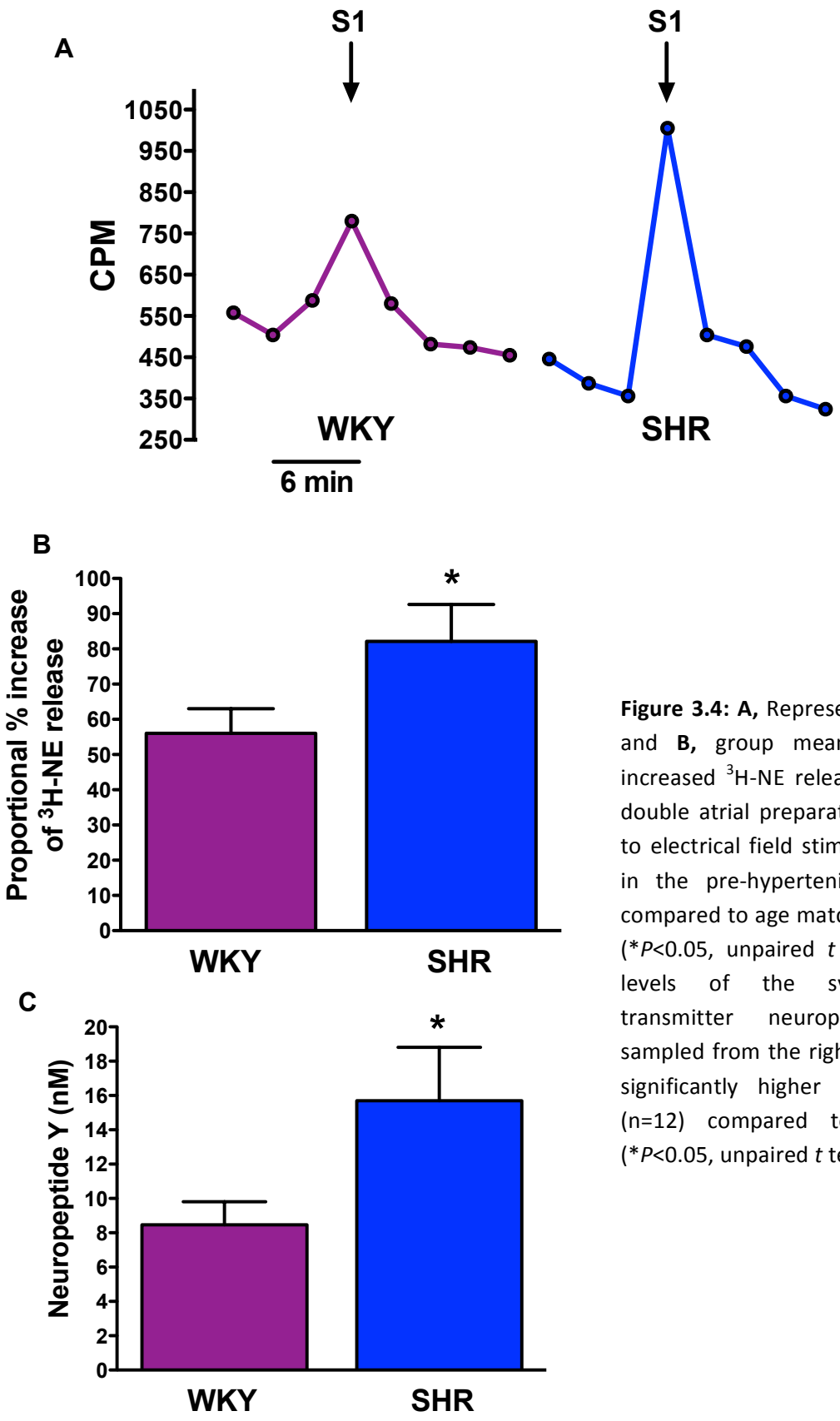

Figure 3.4: A, Representative raw data and **B,** group mean data showing increased ^{3}H-NE release from isolated double atrial preparations in response to electrical field stimulation (S1, 5Hz) in the pre-hypertenisve SHR (n=17) compared to age matched WKY (n=16), (**P*<0.05, unpaired *t* test). **C,** Plasma levels of the sympathetic co-transmitter neuropeptide-Y (NPY) sampled from the right atria were also significantly higher within the SHR (n=12) compared to WKY (n=12), (**P*<0.05, unpaired *t* test).

3.3.4 Re-uptake and autoinhibition of NE release

To determine whether the rate of the NE re-uptake contributed to the increased NE release observed in the SHR, despiramine was used as an inhibitor of NET. Desipramine normalised the difference in release of ^{3}H-NE to field stimulation between the SHR and WKY (SHR: 97.19±7.8 %, n=10. WKY: 106.0±11.5 %, n=8) (figure 3.5). To determine if reduced levels of α_2 adrenoceptor auto-inhibition may contribute to the increased NE release observed in the SHR, yohimbine was used a potent and selective α_2 antagonist. Yohimbine did not normalise the difference in ^{3}H-NE release between pre-hypertensive SHRs (n=7) and WKYs (n=8). In fact the difference in ^{3}H-NE release between the SHR and WKY was significantly increased (figure 3.6).

3.3.5 SINGLE CELLS NEUROTRANSMITTER RELEASE

To further study differences in kinetics of neurotransmitter release between the SHR and WKY, an amperometry technique was developed to measure NE release from stellate neuron clusters.

Preliminary tests using cultures from SD rats, demonstrated that upon depolarisation with high K^{+}, the cell released NE which was detected on the traces as a positive signal (figure 3.7). The results of this data are then plotted into histograms of peak amplitude and dwell time as previously described in chapter 2 (figure 3.7). Both amplitude and dwell time show distributions screwed to the lower end of the scales, indicating most events are of a similar size with some larger ones.

Figure: 3.5

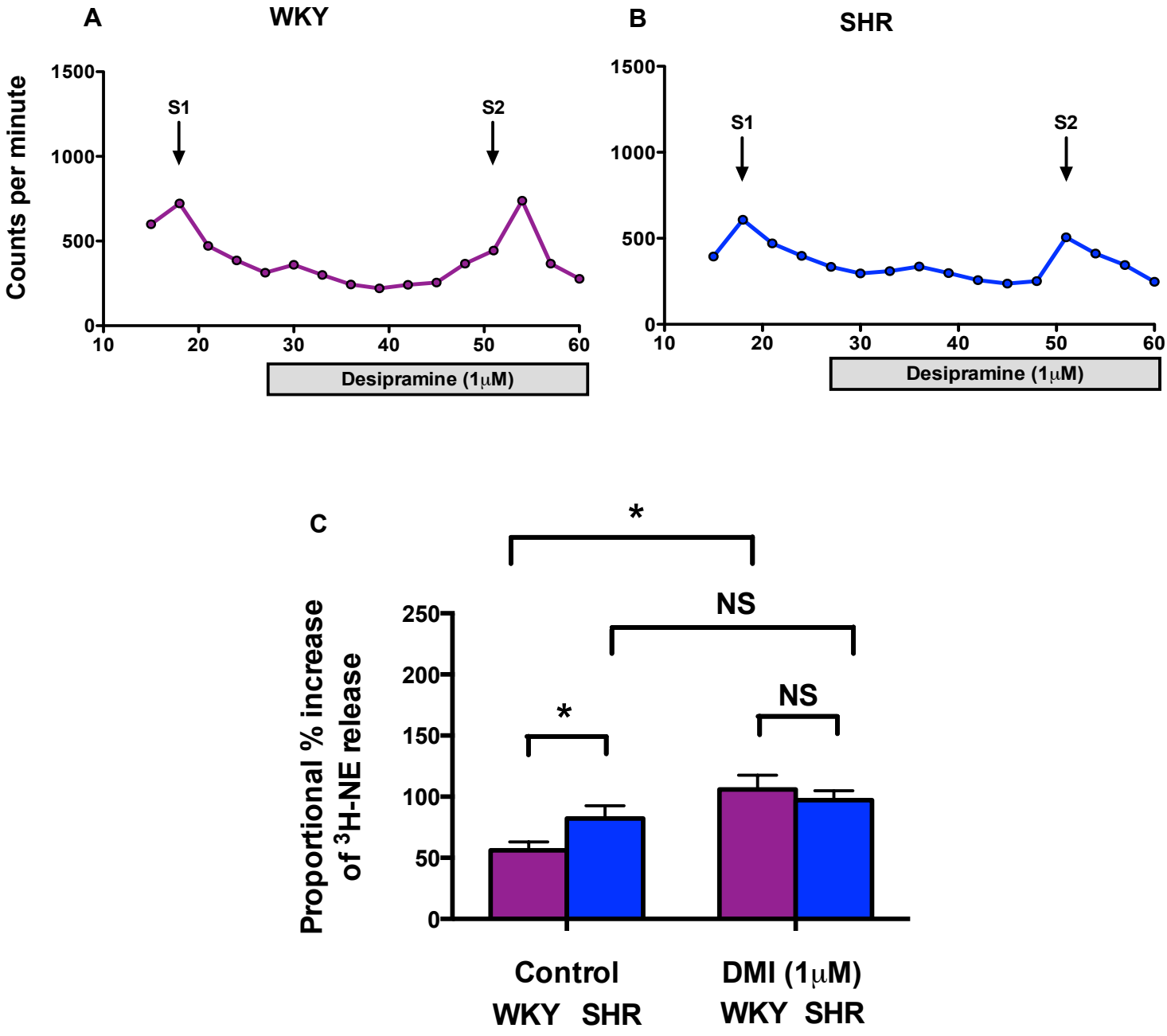

Figure 3.5 : The neuronal norepinephrine reuptake transporter (NET) inhibitor desipramine (DMI) (1μM) significantly increased ^{3}H-norepinephrine (NE) release in response to electrical field stimulation (S1 v's S2, 5Hz) of isolated atria in the WKY (n=8, raw data (A); *P*<0.01, paired *t* test) and SHR (n=10, raw data (B); *P*<0.01, paired *t* test). However, after desipramine pre-treatment the difference in ^{3}H-NE release between the SHR and WKY was abolished, group mean data (C) (**P*<0.05, unpaired *t* test).

Figure: 3.6

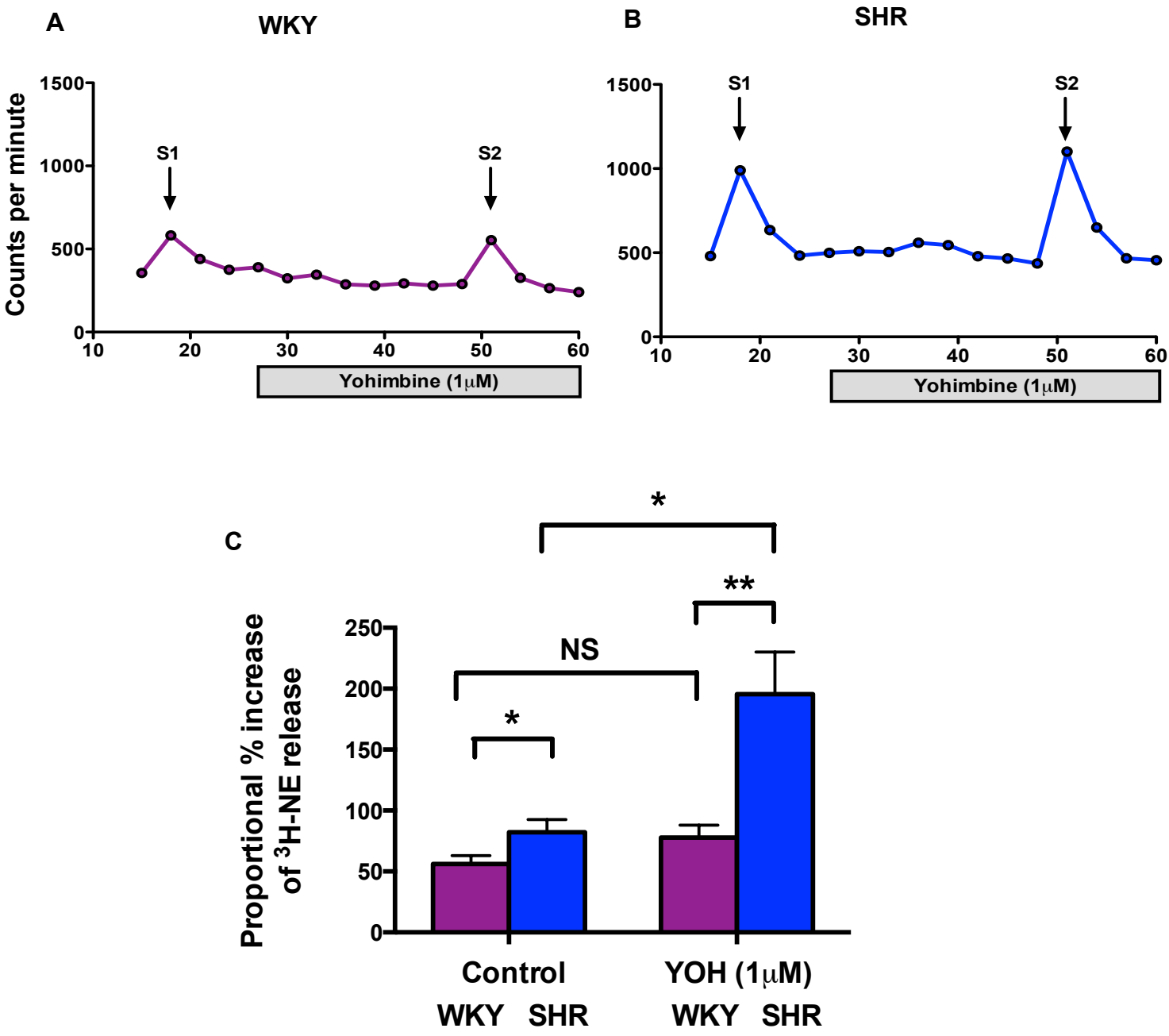

Figure 3.6 : The α_2 receptor antagonist yohimbine (1μM) had no effect on ^{3}H-NE release in the WKY (n=8, raw data trace (A)) but slowed down pre-synaptic inhibition resulting in more release of ^{3}H-NE in the SHR (n=7, raw data trace (B); *P*<0.001, paired *t* test), The difference in ^{3}H-NE release in response to field stimulation between the SHR and WKY increased significantly in the presence of yohimbine, group mean data (C) (**P*<0.01, unpaired *t* test).

Figure: 3.7

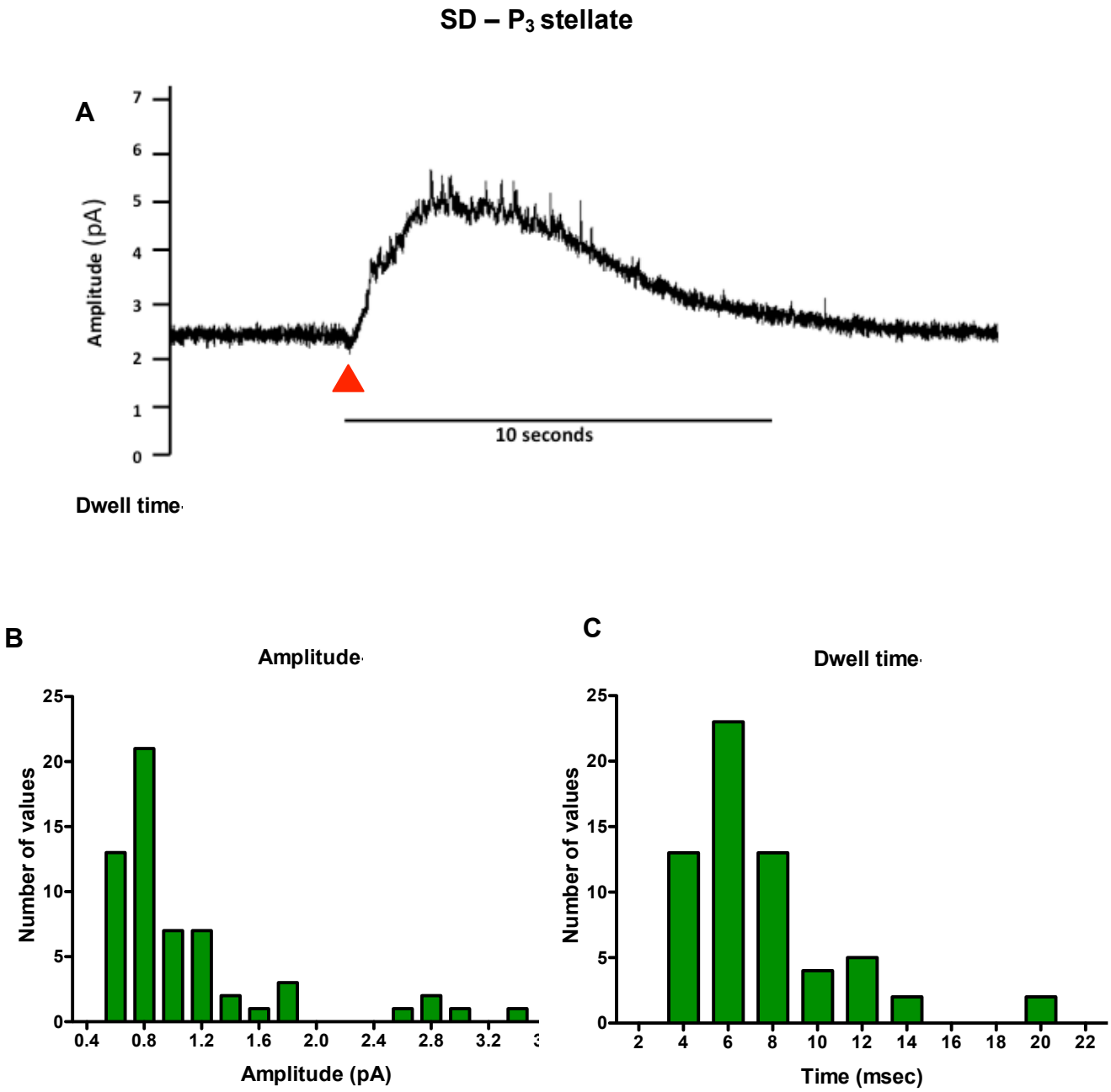

Figure 3.7: A, raw data trace from SD neonatal stellate culture stimulated with K^+ (80mM) (red arrow) shows large displacement artefact post stimulation and positive deflections in the current of the trace, seen as spikes, representing detection of quanta's of NE release. **B,** histogram representing amplitudes of events detected from SD neonates (n= 6 cells, 59 depolarisations). **C,** histogram representing the dwell time (time course) of events detected from SD neonates (n= 6 cells, 59 depolarisations).

Figure: 3.8

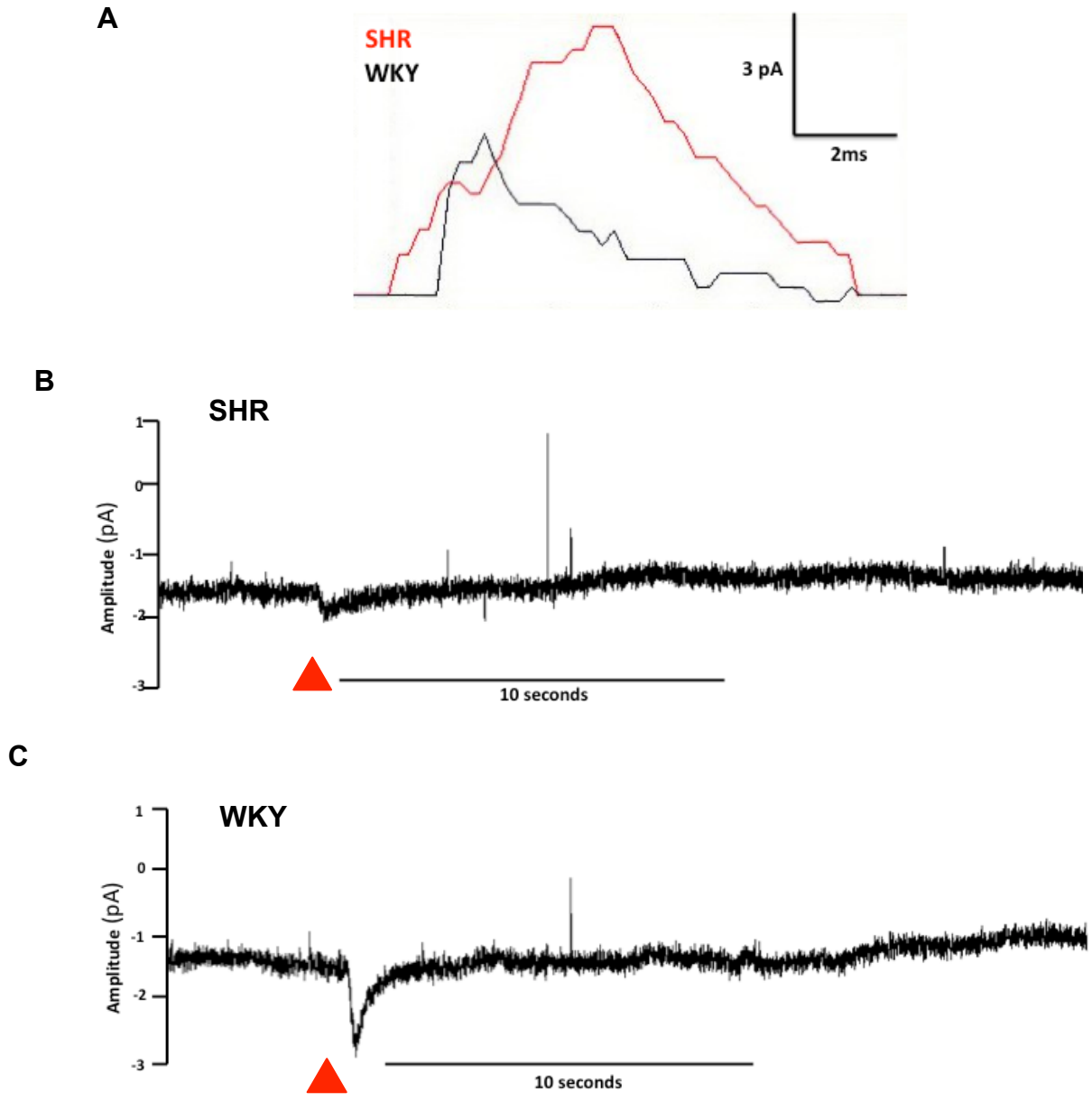

Figure 3.8: A, Raw data of events detected from SHR and WKY neuronal cultures. **B,** raw data trace of SHR culture stimulation with high K^+ **C,** raw data trace of WKY culture stimulation with high K^+ (red arrows).

Figure: 3.9

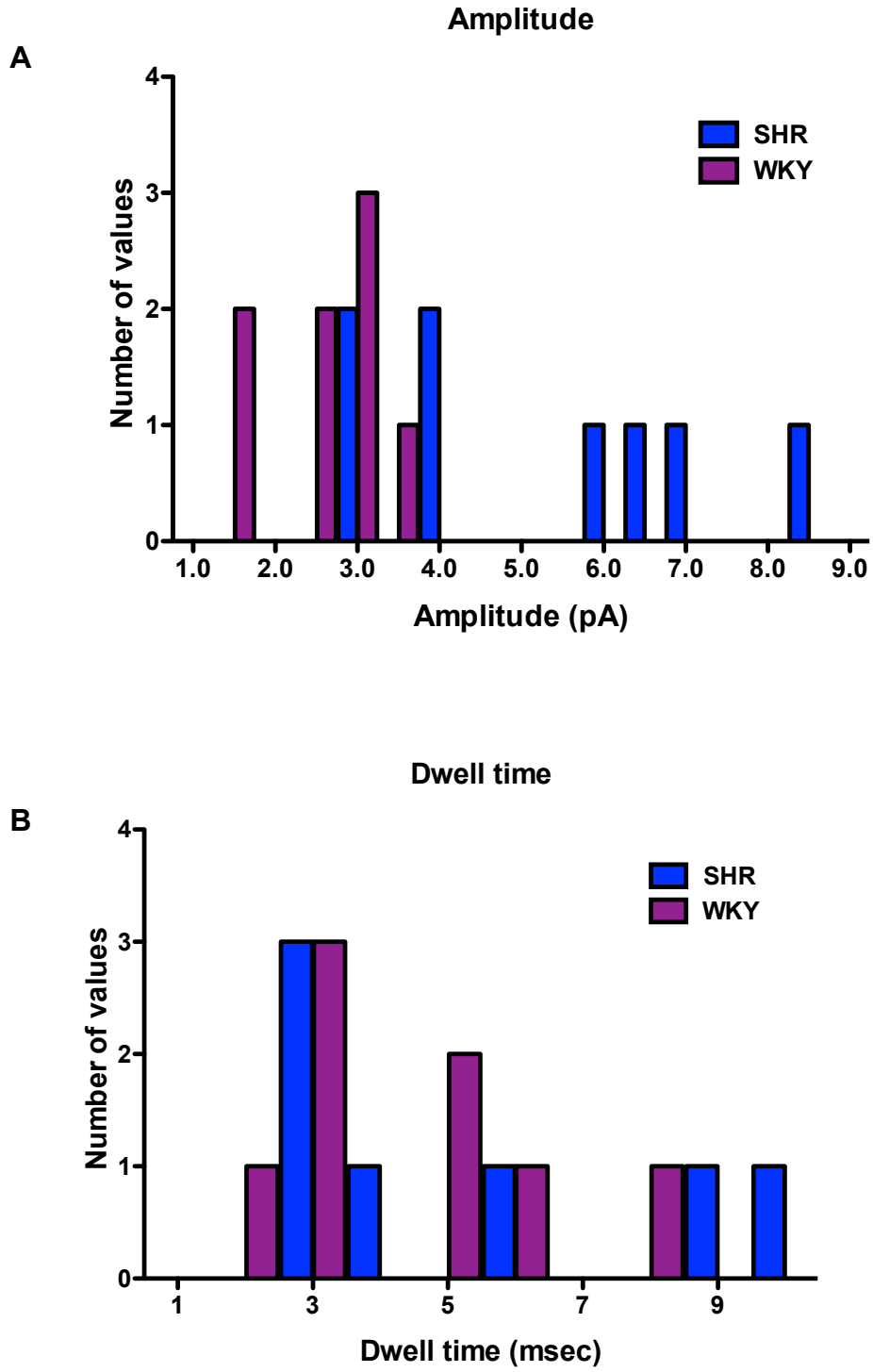

Figure 3.9: A, histogram representing amplitudes of events detected from SHR and WKY neonates (SHR n= 5 cells, 8 depolarisations; WKY n= 3 cells, 8 depolarisations). **B,** histogram representing the dwell time (time course) of events detected from SHR and WKY neonates (SHR n= 5 cells, 8 depolarisations; WKY n= 3 cells, 8 depolarisations).

Figure: 3.10

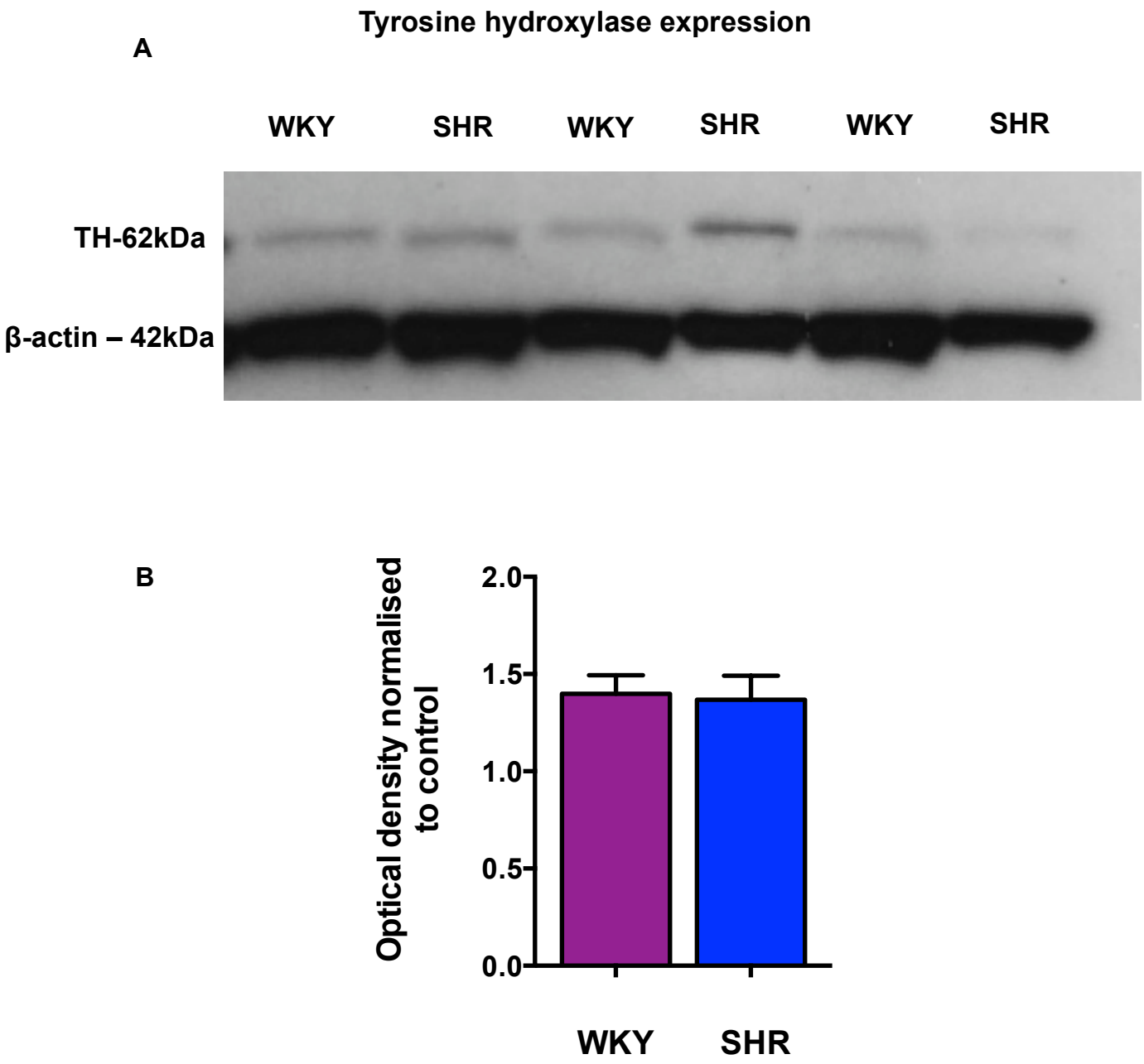

Figure 3.10: Tyrosine hydroxylase expression levels as recorded using western blot analysis between stellate ganglia tissue of the four week SHR and WKY, show no difference in expression levels of tyrosine hydroxylase. Therefore the increased sympathetic drive in the young SHR is unlikely to be due to higher NE synthesis. Although, due to the lack of positive and negative controls for TH this data has to be interpreted with care **A,** Raw data showing β-actin loading control. **B,** Average optical density of TH staining within each group.

Amperometry experiments with clusters of SHR and WKY neonates proved technically very difficult, therefore the results presented here are only very preliminary (figure 3.8). Although amperometry is a well established technique within brain slices and adrenal chromaffin cells, if had never successfully been carried out in isolated stellate neurons in the past. The results for the SHR and WKY suggest that SHR neurons may have greater amplitude of release even at this very young neonatal age (figure 3.9), although firm conclusions cannot be drawn from this data.

3.3.6 Sympathetic ganglia tyrosine-hydroxylase expression levels

To determine if the increased NE release in the SHR could be due to greater synthesis of NE, therefore resulting in a higher concentration of NE intracellularly, ganglia concentration of the NE synthesis enzyme tyrosine hydroxylase was measured. In this experiment no difference in tyrosine hydroxylase expression in stellate ganglia was observed between the SHR and WKY (optical density, SHR: 1.37±0.12, n=6, WKY: 1.40±0.10, n=6; figure 3.10). This western blot was performed with a well characterised TH antibody, therefore the band at 62kDa is likely to be TH, although without the specific positive and negative controls this can not be said for certain.

Additionally, a *post hoc* statistical power analysis of the TH western data was carried out. It returned a power of 6.8% for the experiment showing that the experiment was greatly underpowered for detecting any difference in TH expression levels between the WKY and SHR. This could lead to false conclusions being drawn from the data due to a type II error. Additionally due to the high exposure needed to

expose the 62kDa TH band the β-actin control is over exposed. This is likely to be due to the very low level of TH protein obtained from the stellate ganglia, but means that normalisation of the protein bands needs to be taken with caution as discussed in section 2.9.

3.4. DISCUSSION

Novel findings of this chapter are:

- SHR show a small but significant *in vivo* tachycardia compared to age and weight matched WKY, despite the intrinsic heart rate of isolated atria, and the ability of the vagus nerve to lower heart rate remaining unchanged.
- Sympathetic stimulation induced tachycardia was significantly greater in the SHR.
- The release of NE and the sympathetic co-transmitter NPY were also significantly elevated in the SHR.

When these results are taken together with other reports previously published[1], they indicate that the impaired cellular signalling in the SHR translates to impaired cardiac excitability before hypertension develops.

3.4.1 DISRUPTED AUTONOMIC BALANCE IN THE PRE-HYPERTENSIVE SPONTANEOUSLY HYPERTENSIVE RAT.

Hypertension is associated with well-characterised physiological changes, including cardiac remodelling due to stresses in the myocardium resulting in left ventricular hypertrophy, and an increase in sympathetic nervous system activity[11]. Within the four-week-old SHR, arterial blood pressure was not different from age and weight matched WKY controls. In addition, ventricular weight/body weight ratios were also no different[1], suggesting no evidence of left ventricular hypertrophy. However, there was a small but significant increase in resting heart rate *in vivo* in the pre-

hypertensive SHR, as has previously been observed in the adult animal[1]. The fact that there was no difference in the beating rate of isolated atria from both the SHR and WKY at this age suggests that the difference observed *in-vivo* was due to a change in autonomic balance. The magnitude of vagally mediated bradycardia is small in both the SHR and WKY when compared to the tachycardia mediated by sympathetic stimulation as has been previously reported in adult animals[34, 162]. Unlike the adult SHR which has a smaller heart rate response to vagus nerve stimulation than the WKY, we observe no difference in the degree of bradycardia at four-weeks of age, suggesting there is no functional cardiac parasympathetic impairment at this developmental state. Others have reported a slight increase in the heart rate response to vagal nerve stimulation at around six weeks of age, which quickly normalises as the animal ages[185]. It is therefore unlikely that a change in vagal tone is responsible for the difference in *in-vivo* heart rate we observe. To confirm this experiments would need to be repeated in the presence of atropine the muscarinic acetylcholine receptor antagonist. If vagal tone were unaffected within animals at this age, then atropine parasympathetic blockade would cause no change in resting heart rate, between the two groups.

Direct stimulation of the right stellate ganglion at 5 and 7Hz produced a greater tachycardia in the SHR than the WKY. This was not as marked as seen in the adult animal where stimulation frequencies between 1 and 7Hz produce significantly larger responses[162]. However, at this age (16-weeks) both ^{3}H-NE release and beta-adrenergic receptor responsiveness are greatly increased[162]. A greater release of NE during field stimulation at 5Hz was also observed, and plasma levels of the

sympathetic co-transmitter NPY (sampled from within the right atria) were elevated in the pre-hypertensive SHR compared to the WKY. NPY is a slowly diffusing co-transmitter with a long half-life. Plasma levels have little diurnal variation compared to circulating catecholamines and cortisol, therefore providing for a more accurate indicator of sustained sympathetic hyperactivity[186-188]. NPY is also able to cross talk and inhibit vagal acetylcholine release following high frequency sympathetic stimulation[189, 190]. No difference was observed in the size of the vagal responses in the young SHR despite higher circulating NPY levels. This suggests the NPY levels were not at functionally significant concentrations, although both these measurements were taken in the resting state under general anaesthesia, rather than following high-level sympathetic stimulation where NPY release may increase further. Nevertheless it is conceivable that elevated cardiac NPY levels may contribute to resting vagal impairment in the adult animal when very high levels of sympathetic hyperactivity have become established[34].

3.4.2 Regulation of cardiac sympathetic neurotransmission in the pre-hypertensive spontaneously hypertensive rat.

The adult SHR has evidence of larger calcium transients on depolarisation of cultured stellate neurons[1], larger plasma concentration of ^{3}NE spill over[162], and impaired α_2 adrenoceptor autoinhibition of NE release[77] (summary figure 3.11). The stroke prone SHR also has increased sympathetic innervation of the left ventricle with higher tyrosine hydroxylase positive nerve fibre density[178]. We observed that inhibition of NET with desipramine normalises the difference in NE release between pre-hypertensive SHRs and WKYs. However, the difference in NE release between the

Figure: 3.11

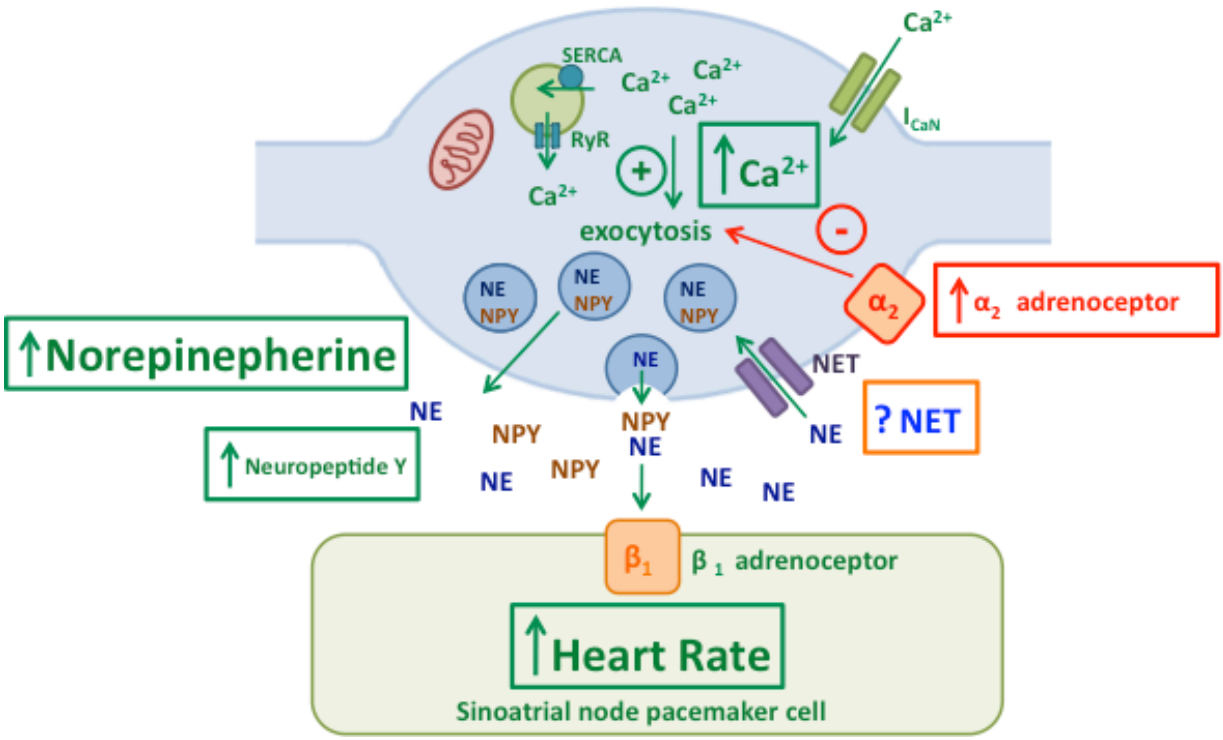

Figure: 3.11: A schematic diagram of a cardiac peripheral sympathetic nerve terminal within the 4 week pre-hypertensive SHR. Increased depolarization induced intracellular Ca^{2+} transients (Li, et.al. 2012) and reduced norepinephrine reuptake via NET (Shanks, et.al. 2013) facilitate greater release of NE and the co-transmitter neuropeptide-Y (NPY) at the neuroeffector junction. The increased intracellular calcium transient is due to reduced mitochondrial buffering of intracellular calcium rather than changes in endoplasmic reticulum ryanodine receptor (RyR) function, despite a more rapid uptake into the endoplasmic reticulum by the smooth endoplasmic reticulum ATPase (SERCA) (Li, et.al. 2013). An increase in the action of α_2 receptor autoinhibtion may act as a compensatory mechanism within the pre-hypertensive SHR to limit NE release, although this is lost in the adult animal. The increase in NE release to stimulation of the right stellate ganglion leads to a greater increase in the beating rate of the sinoatrial node. Green represents stimulatory pathways and red inhibitory pathways of neurotransmission.

young SHR and WKY became significantly larger following administration of the α_2-AR antagonist yohimbine suggesting that increased α_2-AR autoinhibition may be a compensatory mechanism limiting increased sympathetic neurotransmission at this developmental stage. This indicates that the increase NE release observed in the young SHR may be in part due to impaired re-uptake of NE through NET rather than through reduced α_2 adrenoceptor auto-inhibition.

Amperometric data were technically very challenging to obtain. This was particularly difficult from SHR neonatal neuron clusters, which appeared structurally unstable and often would not survive well in clusters for more than three days in culture. Greater data has been obtained from isolated SD neurons demonstrating that the technique is functional and opens up possibilities to study dynamics of neurotransmitter release within these settings in the future. The data presented here for the peak amplitude and dwell time of release current from SHR and WKY suggests that the SHR may have greater peak amplitudes compared to age matched WKY, also that the dwell time, or time course, of SHR NE release responses may be longer. This compliments the results achieved using ^{3}H-NE, which is often used as the 'gold standard' measurement for neurotransmitter release. The dwell time data also appears to fall into three distinct groups, around 3ms, 6ms and 9ms, potentially demonstrating, single, double and triple vesicle release.

Baroreceptor control has previously been shown to be dysregulated in the older SHR, where as renal sympathetic response and mean arterial pressure are no different in 5-10 week SHR compared to control when the 4 major baroreceptors have been removed[191]. Moreover between age matched WKY and SHR baroreceptor

gain has been shown to progressively increase in the WKY and decrease in the SHR with age, with the major alteration in baroreflex-heart rate reflex developing after the onset of hypertension[192]. These studies suggest that there is no difference in baroreceptor control between the SHR and WKY at four weeks of age.

3.4.3. Previous implications of NET dysregulation in hypertension

Dysregulation of NET has previously been implicated in clinical studies of hypertension[3, 43, 193], where NET impairment has been associated with essential hypertension, but not obese related[3]. A knock out model $NET^{-/-}$ mice also displays an elevated mean atrial blood pressure, displaying the importance of NET in blood pressure regulation[79]. The role of neurotransmitter release and its action on post synaptic receptors are the factors of sympathetic regulation that have most extensively been studied within cardiovascular diseases. However, the previous observations into NET dysregulation in hypertension mentioned above, suggest that studying the role of NET in norepinephrine regulation, particularly at the cellular level, may facilitate further understanding of cardiac control of the sympathetic nervous system in hypertension.

There is evidence in this study that dysregulation in cardiac adrenergic signalling in the SHR develops before the onset of hypertension and functionally translates to a small but significant resting tachycardia and larger increases in heart rate on stimulation of the right stellate ganglion. Sympathetic dysfunction may therefore be an early marker of the disease and contribute to its pathogenesis rather than being an epiphenomenon that develops once hypertension has set in.

3.4.5. SUMMARY

Evidence that the cardiac sympathetic dysfunction identified in the established hypertensive SHR model is present in the younger pre-hypertensive SHR has been confirmed by measuring a number of sympathetic factors. At four weeks of age no difference in systolic blood pressure, diastolic blood pressure, *in vitro* heart rate or ventricular weight: body weight ratio is observed between SHR and WKY rats. Indicating that SHR are still phenotypically normotensive at this age. However, a small but significant *in vivo* tachycardia is observed in the SHR, alongside greater ^{3}H-NE release, heart rate change in response to sympathetic stimulation, and greater plasma concentrations of the slowly diffusing sympathetic co-transmitter NPY. Moreover, no difference in heart rate change to vagal stimulation *in vivo* was observed between young SHR and WKY. Greater identification of early hallmarks of hypertension may help develop therapies that prevent the progression of hypertension. The role for NET dysfunction in hypertension has previously been unknown, the ^{3}H-NE results within this study in the presence of DMI suggest that NET may be dysfunctional in the young SHR. A more direct method of studying NET action within isolated neurons is needed to draw any firm conclusions from this.

CHAPTER 4:

SITE-SPECIFIC ROLE OF NET IN THE SYMPATHETIC HYPERACTIVITY OF HYPERTENSION

4.1. INTRODUCTION

Increased activity of the sympathetic nervous system is a well-established component of the pathophysiology of hypertension[39-44], although the exact mechanisms underlying this remain unknown. Both clinical cases and the SHR model of hypertension have been associated with enhanced cardiac norepinephrine (NE) release[3, 37, 77]. Impaired NE re-uptake by the norepinephrine re-uptake transporter (NET) may potentiate this, although previous studies in support of this hypothesis have been inconclusive[3, 43, 77, 139, 148]. Within human hypertensives NET has been shown to be either reduced[3, 43] or unaltered [194] in comparison to normotensive subjects. Whereas, in the SHR NET has been reported to be either down regulated[139], unaffected[182, 195] or up regulated[182, 196] compared to age matched WKY controls.

The inconsistences in previous results are likely to be due to the indirect nature of experimental methods used and differences in tissue populations studied[77, 139, 182, 195]. Conventional methods of monitoring NET activity by measuring plasma levels or tissue accumulation of pre-administered triturated NE and its metabolite 3,5-Dihydroxyphenylglycine (DHPG) in the presence of NET inhibitors[3, 43, 197], only indirectly asses transporter activity giving a global overview of NET function rather than ascertaining the dynamic kinetics of the transporter itself. Moreover, studies have often been carried out within diverse tissue populations [194, 195] and results then used to draw conclusions into the role of NET in hypertension as a whole.

The aim of this chapter was to determine if there were any differences in NET activity within sympathetic neurons isolated from three major sympathetic beds previously implied in hypertension[44, 162, 198] between the hypertensive SHR and age matched WKY controls.

4.2. METHODS

4.2.1 ANIMALS

All experiments were performed under British Home Office license requirements (PPL 30/2360) in accordance to the Guide for the Care and Use of Laboratory Animals published by the US National Institutes of Health (NIH Publication No. 85-23, revised 1996) and the Animals (Scientific Procedures) Act 1986 (UK).

Age and weight matched 16 to 17 week (340g-365g) male SHR and WKY rats were purchased from Harlan (Biscester, UK) and Charles River (Sulzfeld, Germany), and housed under standard laboratory conditions. SHR has established hypertension at this age[138].

4.2.2 ANATOMY

Isolation and preparation of sympathetic post ganglionic neurons

Animals were rendered unconscious using general anaesthesia (3% isoflurane and 97% oxygen) then humanely killed by an approved Home Office schedule 1 method: overdose of pentobarbital followed by exsanguination. Sympathetic neurons were isolated from three major sympathetic ganglia implied in hypertension[44, 162, 199], the

cardiac stellate ganglion (which innervates the heart[162]), superior cervical ganglion (SCG: which predominantly innervates the head and neck region[143]) and the celiac ganglion, superior mesenteric ganglion and autonomic sympathetic chain (CG/SMG/SC) that innervate the kidneys and other abdominal organs[144, 145].

Isolation and culture of the sympathetic ganglia were carried out using the method previously described[147, 200]. Briefly sympathetic stellate, SCG and CG/SMG/SC ganglia were dissected separately, placed in cold L-15 medium and desheathed carefully under a dissecting microscope removing all connective tissue. Ganglia were cut into pieces and digested using a combination of collagenase type 4 (1mg/ml in Ca^{2+} and Mg^{+2}-free phosphate-buffered saline (PBS)) for 40 min, 37^{o}C in a shaking water bath and trypsin TRL3 (2mg/ml in PBS) 42 min, 37^{o}C. The ganglia were then rinsed twice in L-15 blocking medium (96.8% L-15 medium supplemented with 0.6% D-(+)-Glucose solution, 2 mmol/L L-glutamine, 100 units/ml penicillin, 100 ug/ml streptomycin, 10% fetal bovine serum), and rinsed two more times in L-15 plating medium (L-15 incomplete medium, 90% (v/v); NaHCO3, 24mM; Glucose, 38mM; Penicillin (10,000 units/ml), 50 units/ml; Streptomycin (10,000 µg/ml), 50 µg/ml; Nerve growth factor, 25ng/ml; Foetal bovine serum, 10% (v/v)), to remove any residual enzyme.

Ganglia were titrated into a single-cell suspension and plated on Poly-D lysine and laminin coated cover slips (5mm), placed at 37^{o}C 5% CO_2 for 1-2 days before use, as outlined in methods 2.1.3.

Immunohistochemistry

Cultured cardiac stellate neurons and renal CG/SMG/RSC neurons were fixed with 4% Paraformaldehyde and permeabilised with 0.1% Triton X100 and 1% BSA. Cells were then processed for immunoreactivity to the sympathetic marker tyrosine hydroxylase with mouse anti tyrosine hydroxylase (TH), 1:200 (sigma), and Alexa Fluor 647 goat anti-mouse IgG, 1:100-1:200 (invitrogen, A21236).

4.2.3 Experimental Protocol

Measurement of Norepinephrine uptake rate.

NET activity was dynamically recorded using a novel fluorescent assay of the monoamine transporters developed to temporally monitor transporter kinetics within living sympathetic tissue[158]. To assess NET transporter function we used a commercially available assay (neurotransmitter transporter uptake assay; NTUA) (Molecular devices: Sunnyvale,CA) which has been validated to monitor NET transport rates in cell culture systems[157] and intact tissue samples[158]. The NTUA assay contains two compounds, a fluorescent NET substrate and a masking dye that conceals extracellular fluorescence (http://www.moleculardevices.com/Products /AssayKits/Transporters/Neurotransmitter .html). For details see chapter two.

Assay preparation

The NTUA kit was purchased from MDS Analytical Technologies (catalogue R8173; Wokingham, Berkshire, UK) and diluted with Tyrode solution (10 mL per unit) to

make a stock solution. This was divided into 1 mL aliquots that were then stored at -20^{o}C for subsequent use. All drugs only underwent one freeze-thaw cycle.

Protocol

Prior to the start of the experiment cells were pre-incubated in a low 1:100 concentration of the assay in cell plating medium for 20 min, 37^{o}C, 5% CO_2. Cells selected for imaging and expressing the transporter were selected if a basal level of fluorescence was observed (a strong fluorescent signal was observed in 95%-100% of cells). They were then transferred to a temperature controlled (37^{o}C) gravity fed perfusion chamber (volume 500µl); flow rate 3ml/min on the stage of a Nikon Eclipse TE200-U microscope. Cells were selected for study based on physical appearance and intact cell membranes under bright field conditions using a 10x/0.30 air objective.

A control period of 5 minutes perfusion (3ml/min) in Tyrode solution to allow the cells to equilibrate within the system, was followed by a 5 minute perfusion with Tyrode + NTUA (1:10) assay. The perfusion system was then stopped, and cells held stationary in the NTUA containing buffer at 37±0.5^{o}C for 10 minutes, where the rate of increase in fluorescence within the cell was recorded.

The rate of increase in intracellular fluorescence was recorded by selecting a region of interest (ROI) around the isolated postganglionic cell. Images were acquired every 2 seconds using a photometrics CoolSNAP HQ^{2} camera, excitation wavelength 440nm, emissions band 535±35nm, analysed in EasyRatio pro (Molecular Devices, Sunnyvale CA).

Results are presented as increase in fluorescence over time, normalised to the starting intracellular fluorescence of the cell at t=10 min (when perfusion was stopped), which allowed for comparison of changes in rate that were independent of the starting fluorescence.

Inhibition of the norepinephrine re-uptake transporter.

In order to assess the validity of the NTUA assay, and confirm its specificity to NET. The tricyclic antidepressant NET inhibitor[82] desipramine (DMI 1μM-concentration previously shown to inhibit the NET[158]) was added to the perfusing Tyrode after the initial slope was recorded as described in chapter two. Any cell in which the increase in fluorescence was not blocked by DMI was excluded from analysis, as any previous rate of uptake of the assay could not be confirmed to be NET specific.

Electrical Field stimulation of isolated sympathetic post ganglionic neurons

Cell depolarisation was induced by electrical field stimulation (EFS) (5Hz, 10V, 10ms) for 2.5min at 17min and 47min (during both the control NTUA (1:10) and NTUA (1:10) + DMI (1μM) holds) by a pair of parallel horizontal platinum electrodes mounted within the perfusion chamber. Parameters were chosen to match stimulation frequency and rate which shows submaximal noradrenaline release to right stellate stimulation in the isolated double atria preparation[162].

4.2.4. Solutions and Drugs

Tyrode solution for isolated postganglionic sympathetic neuron experiments contained (mmol/L NaCl 145, KCl 5, HEPES 10, glucose 10, $CaCl_2$ 2 and $MgCl_2$ 1) (pH

7.38-7.42, 37±0.5^{o}C). NTUA was purchased from MDS Analytical Technologies (catalogue R8173; Wokingham, Berkshire, UK) prepared as described in chapter two. Desipramine (Sigma, UK) was stored as stock solution (1mM in distilled H_2O). Desipramine was made to the desired concentration (1µM) on the day. All drugs under went no more than one freeze thaw cycle.

4.2.5. STATISTICS

All statistical analysis was carried out using GraphPad Prism (GraphPad Software, San Diego, CA, USA). Data are presented as means±SEM. Analysis was performed using paired or unpaired Student *t* test as appropriate. For all experiments, statistical significance was accepted at $P<0.05$.

4.3. RESULTS

4.3.1. MEASUREMENT OF NET RATE IN ISOLATED SYMPATHETIC NEURONS USING A FLUORESCENT INDICATOR.

Cultured cells were confirmed to be sympathetic specific by positive immunoreactivity to anti-tyrosine hydroxylase (figure 4.1.) A linear increase in intracellular fluorescence was observed in the cells when incubated in a solution containing the NTUA assay (see figure 2.4. in methods) The rate of increase in fluorescence within the neuronal cell was recorded over time, and the gradient of the slope (y=mx+c) was normalised to the starting fluorescence.

Figure 4.1

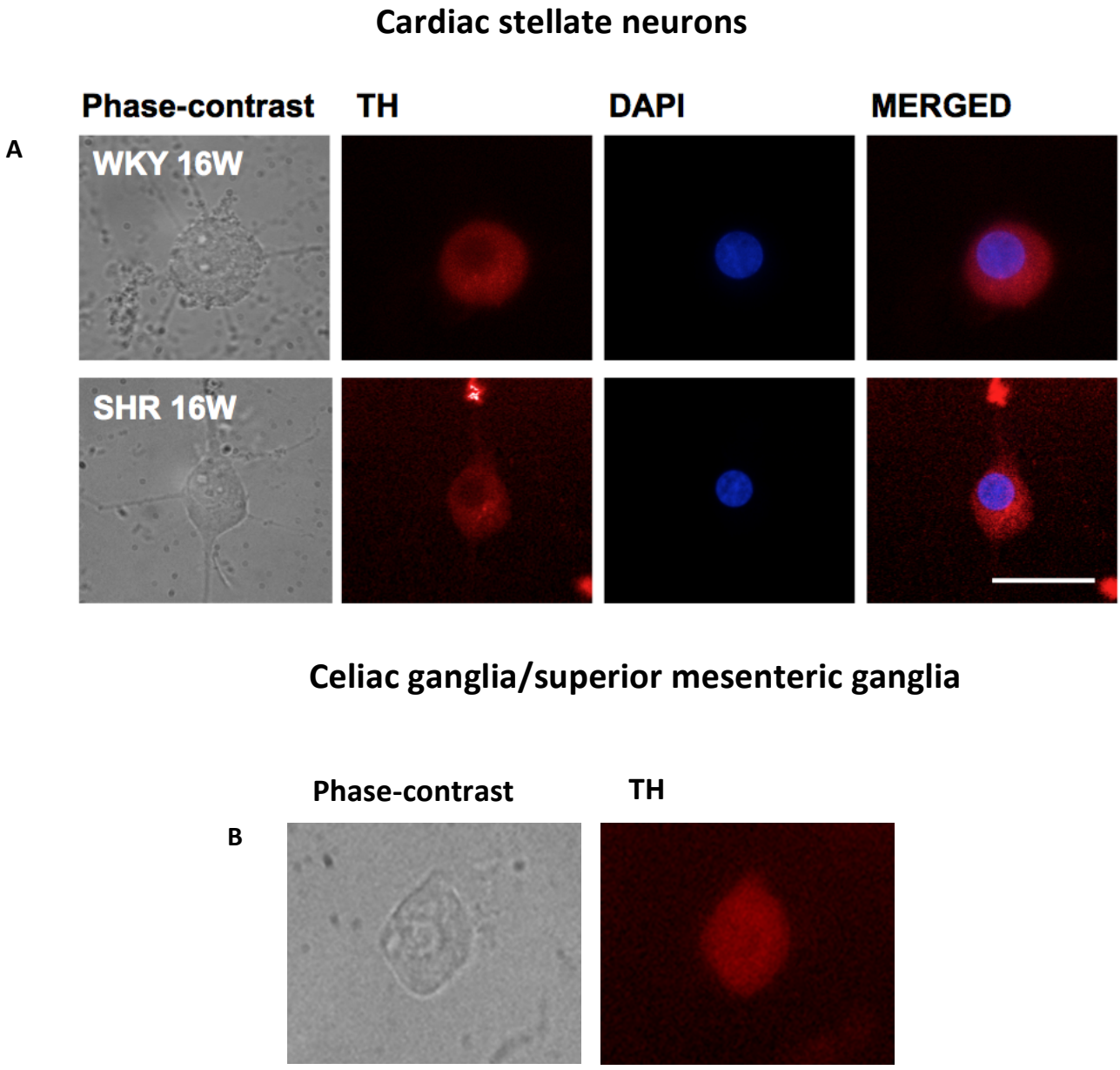

Figure 4.1: A, Positive immunoreactivity to sympathetic marker tyrosine hydroxylase in cardiac stellate neurons. DAPI is a nuclear stain. Scale bar: 50μm. **B,** Positive immunoreactivity to sympathetic marker tyrosine hydroxylase in celiac ganglia/superior mesenteric ganglia neurons. Scale bar: 50μm. Tyrosine hydroxylase positive immunoreactivity of SCG neurons has previously been reported (Li, et.al. 2012).

4.3.2. Norepinephrine re-uptake within major sympathetic ganglia of the SHR and WKY.

In cells from hypertensive animals NET transporter activity was significantly reduced in cardiac stellate neurons of the SHR compared to age matched normotensive WKY rats (figure 4.2)(SHR: 2.82±0.25 au/min, n=20, WKY: 3.69±0.33 au/min, n=19, $P<0.05$, unpaired *t* test; figure 4.5). Moreover no difference in uptake rate was observed between sympathetic neuronal cells of the hypertensive SHR SCG compared to age matched WKY (figure 4.3.)(SHR: 2.59±0.19 au/min, n=24, WKY: 2.54±0.27 au/min, n=24; figure 4.5), nor hypertensive SHR CG/SMG/SC compared to age matched WKY (figure 4.4)(SHR: 2.14±0.21 au/min, n=18, WKY: 2.18±0.20 au/min, n=23; figure 4.5). DMI (1μM) blocked the action of the NET fluorescence in all groups of neurons.

4.3.3. Effect of cell depolarisation on norepinephrine uptake rate within stellate neurons.

To test the effect of neuronal excitability on NET activity preparations were depolarised by electrical field stimulation (EFS). Electrical field stimulation potentiated the difference in NET rate observed within stellate neurons of the hypertensive SHR and age matched WKY. (SHR: 2.59±0.30 au/min, n=20, WKY: 4.25±0.47 au/min, n=19, $P<0.01$, unpaired *t* test; figure 4.6). The increase in transporter rate observed in WKY stellate neurons was significantly greater during electrical field stimulation compared to control (WKY n=19, $P<0.05$, paired *t* test). With no observed difference in NET rate with field stimulation in hypertensive SHR (SHR n=20, $P=0.20$).

Figure 4.2

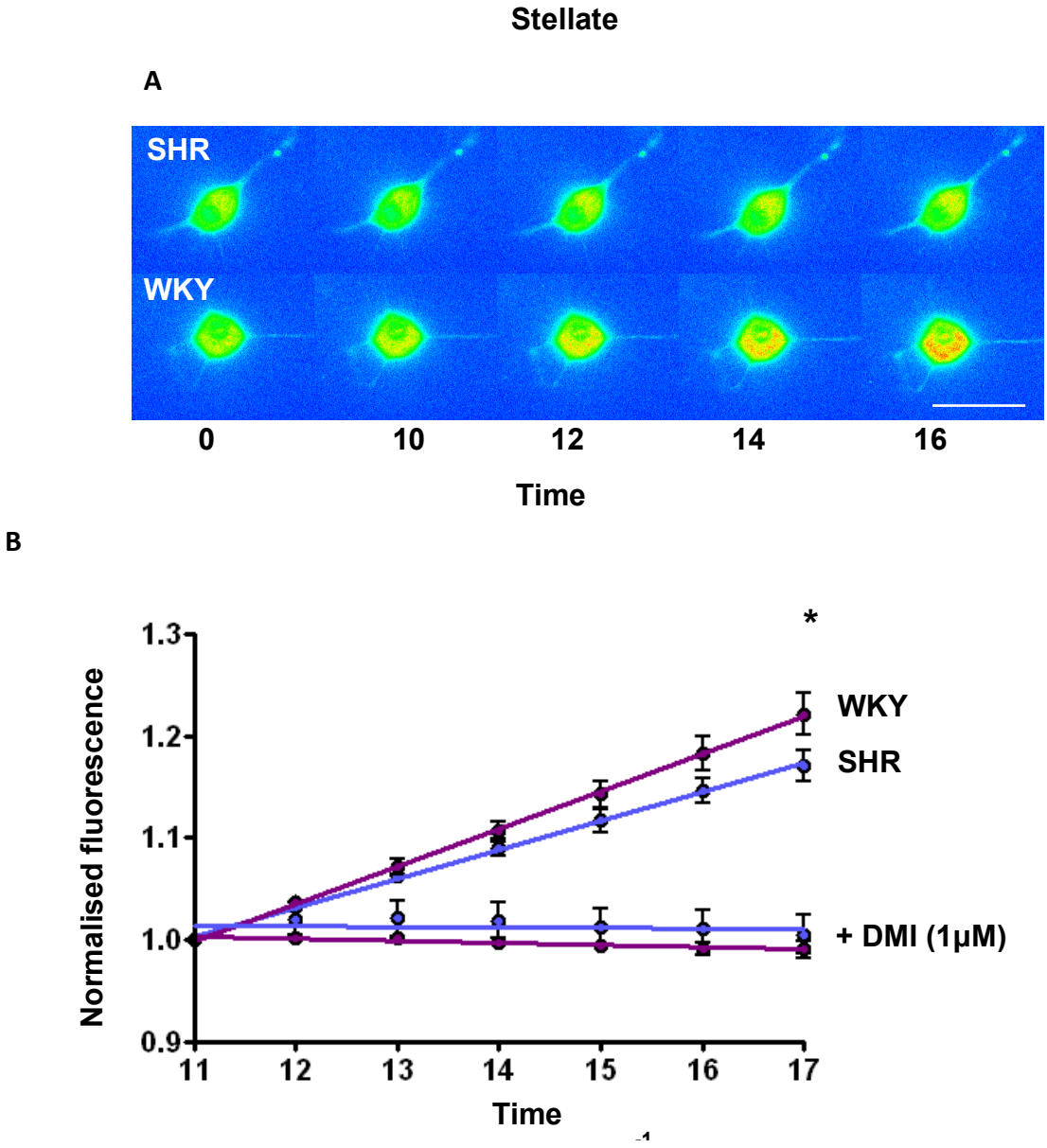

Figure 4.2: Rate of intracellular fluorescence increase is significantly lower in cardiac stellate neurons from the hypertensive 16week SHR. **A,** Representative fluorescent data. **B,** Rate of fluorescence increase (au) over time during NTUA (1:10) hold (SHR n=20, WKY n=19) and in the presence of 1µm DMI. Scale Bar 50µm.

Figure 4.3

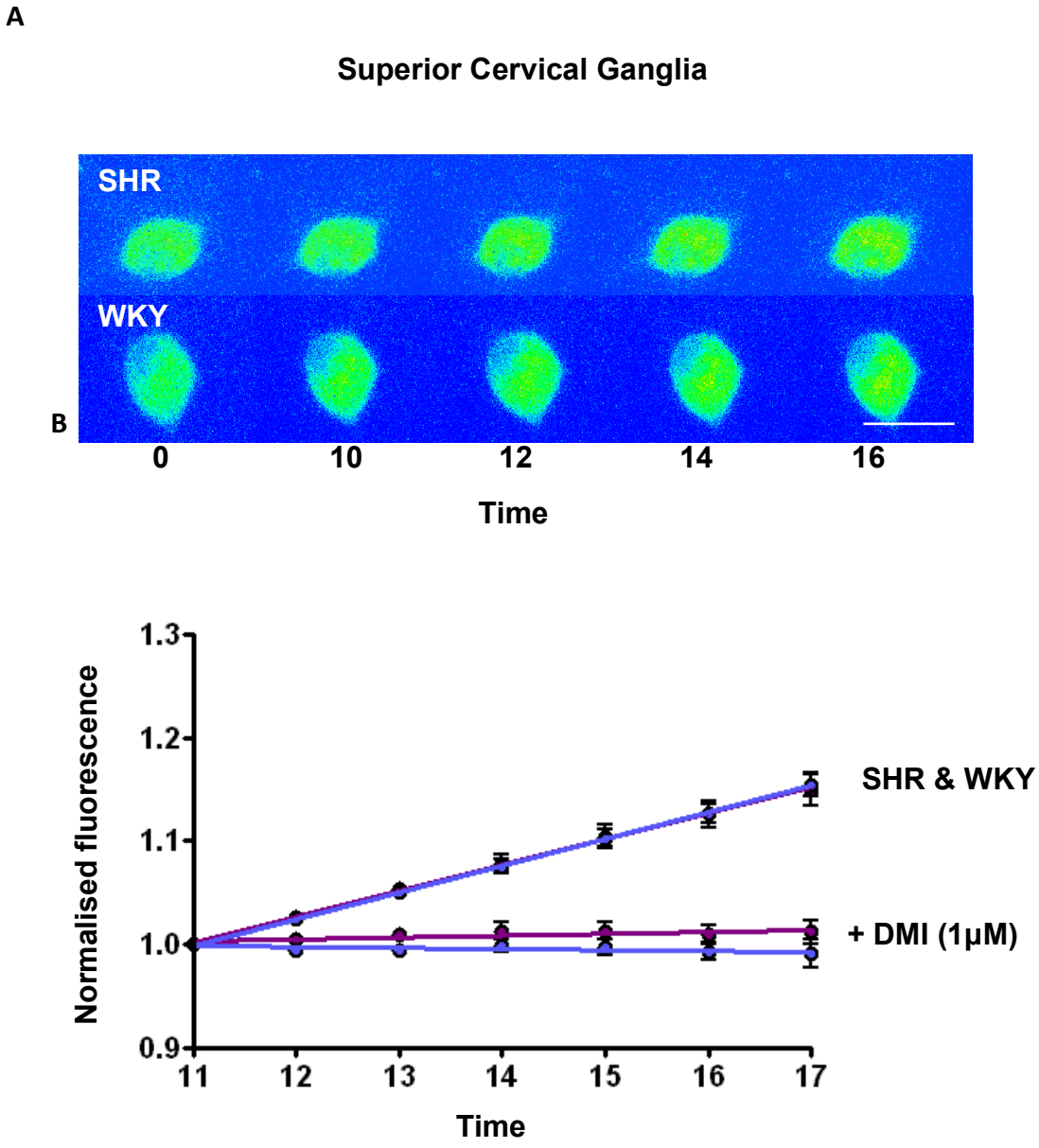

Figure 4.3: A, Representative raw fluorescence data from 16week SCG neuronal cells, in which no difference in the rate of intracellular fluorescence was seen between SHR and WKY cells. **B,** Rate of fluorescence increase (au) over time during NTUA (1:10) hold in isolated SCG neurons (SHR n=24, WKY n=24) and in the presence of 1µm DMI. Scale Bar 50µm.

Figure 4.4

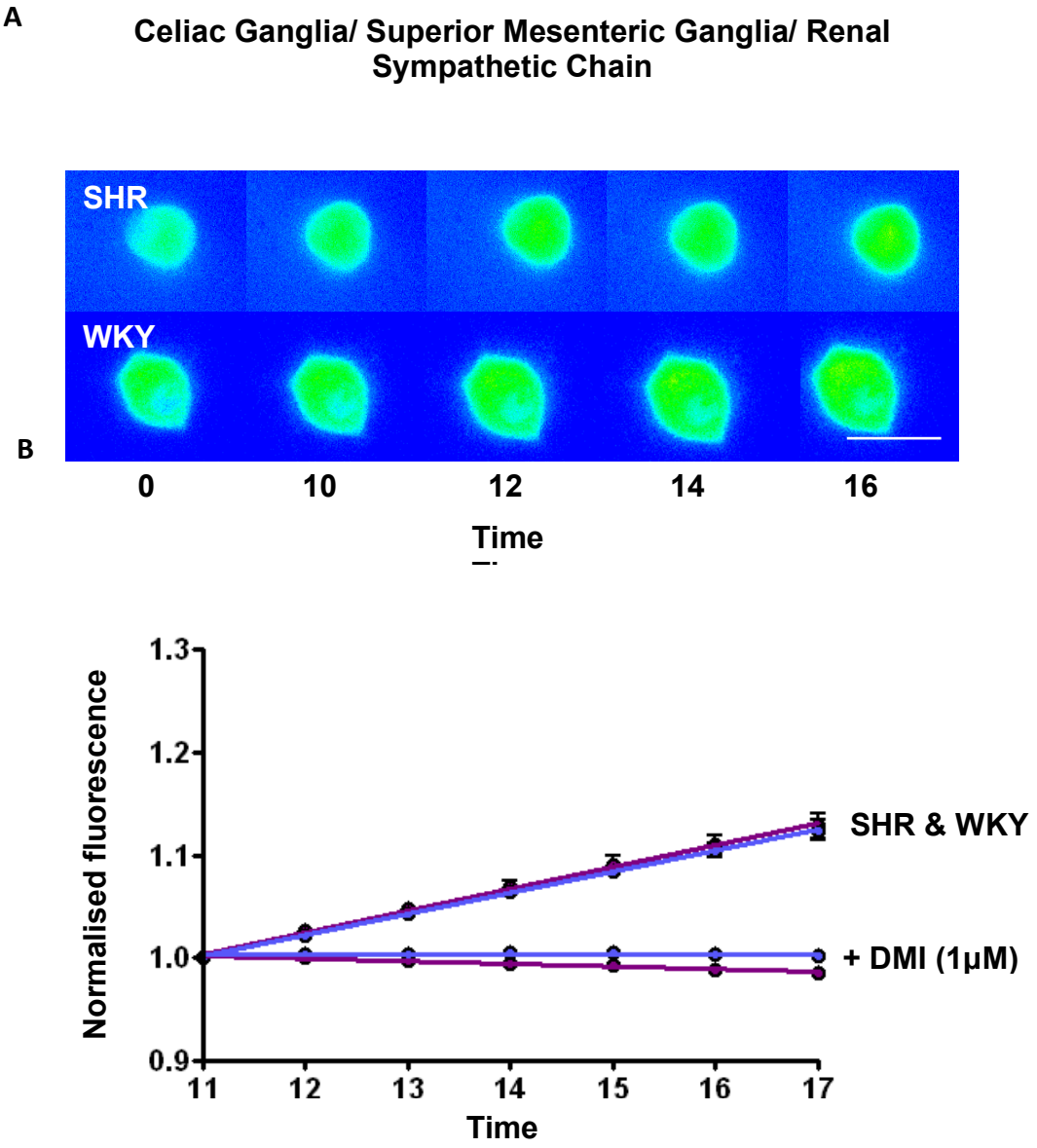

Figure 4.4: A, Representative raw fluorescent data from 16week CG/SMG/RSC neuronal cells, in which no difference in the rate of intracellular fluorescence was seen between SHR and WKY cells. **B,** Rate of fluorescence increase (au) over time during NTUA (1:10) hold in isolated CG/SMG/RSC neurons (SHR n=18, WKY n=23) and in the presence of 1µm DMI. Scale Bar 50µm.

Figure 4.5

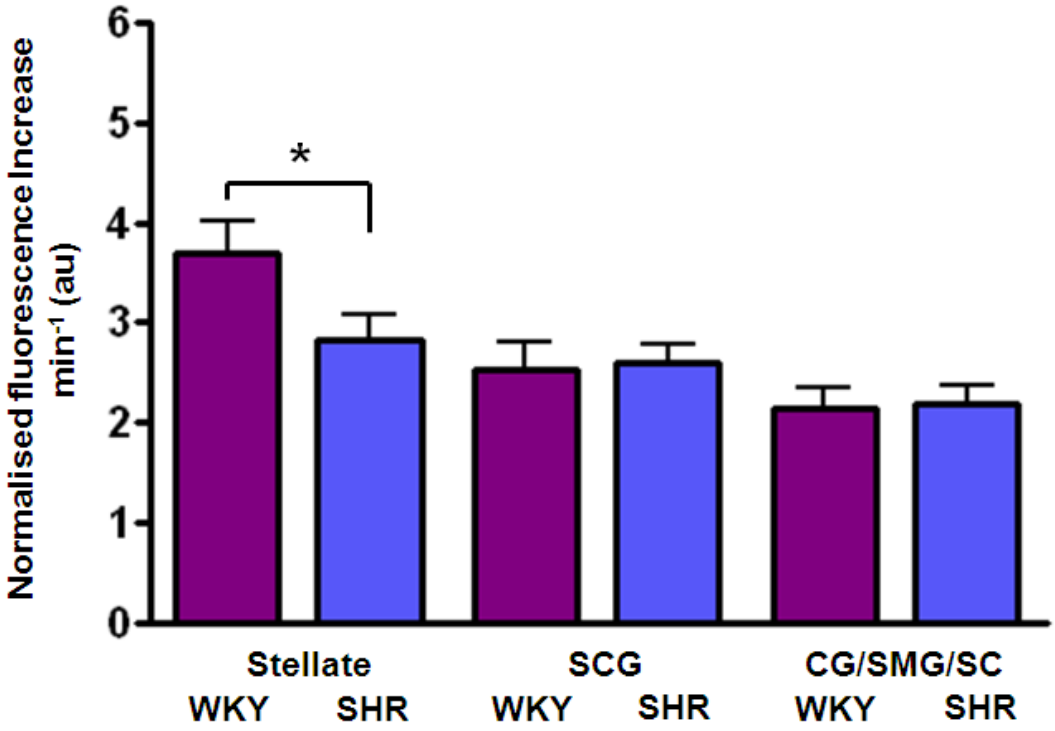

Figure 4.5: Rate of fluorescence increase during NTUA (1:10) hold, plotted as the gradient of the slope derived from y=mx+c. NET action is significantly decreased in the 16week SHR stellate neurons compared to WKY (SHR n=20, WKY n=19) (**p*<0.05, unpaired *t* test). There was no significant difference in uptake rate between SCG (SHR n=24, WKY n=24) cells, nor CG/SMG/RSC cells (SHR n=18, WKY n=23) of the SHR and WKY.

Figure 4.6

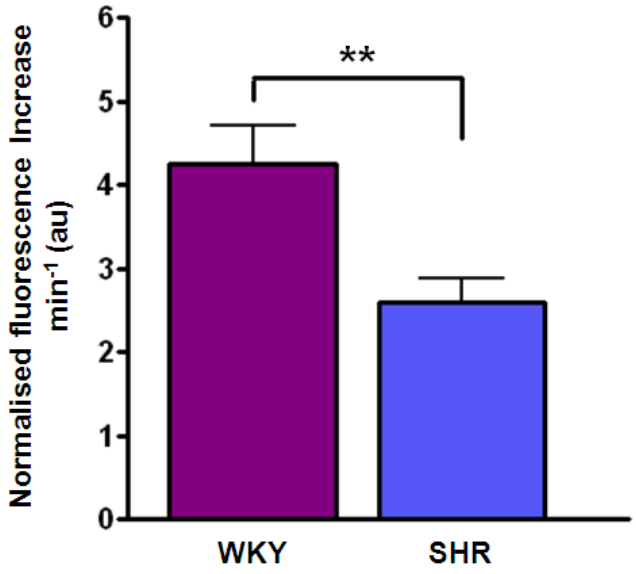

Figure 4.6: Rate of fluorescence increase in stellate neurons during external electrical field stimulation (EFS) (5Hz, 10V, 10ms, 2.5mins). Plotted as the gradient of the slope derived from y=mx+c. EFS exacerbated the difference in NET transporter rate observed between 16week hypertensive SHR and age-matched WKY stellate neurons (SHR n=20, WKY n=19) (***p*<0.01, unpaired *t* test).

4.4. DISCUSSION

The novel findings of this chapter are:

- There was significant impairment (decreased activity) of NET within stellate sympathetic neurons of the SHR.
- Stimulation of stellate sympathetic neurons further potentiates the difference in NET rate between SHR and WKY.
- Decrease in NET transporter activity was not observed in two other major non-cardiac ganglia.

Taken together these results indicate that a reduction in NET activity contributes to the cardiac sympathetic hyperactivity and norepinephrine spillover observed in hypertension, and that NET regulation between different sympathetic ganglia is regionally specific. In addition to the increased intracellular Ca^{2+} transients observed in SHR sympathetic neurons[1], and increased cardiac NE release previously reported[173], the results presented in this chapter provide further evidence for the role of cardiac sympathetic hyperactivity in the SHR and elude to a possible mechanism by which, in part, this may be occurring.

4.4.1. SIGNIFICANT IMPAIRMENT OF NOREPINEPHRINE REUTPAKE TRANSPORTER WITHIN STELLATE SYMPATHETIC NEURONS IS NOT OBSERVED WITHIN OTHER MAJOR SYMPATHETIC GANGLIA IN THE SPONTANEOUSLY HYPERTENSIVE RAT.

The data presented here show a significant reduction in NET activity within stellate sympathetic neurons of the SHR compared to WKY. With no difference being observed in transporter activity between age-matched SHR and WKY neurons

isolated from the superior cervical ganglia, or the celiac ganglia/superior mesenteric ganglia/renal sympathetic chain. These results echo a 1981 study by Rho *et.al.* in which they used a method of sucrose gradient fractionation to identify the synaptosomal ^{3}H-NE from whole homogenised tissue samples[139, 196], where NE tissue accumulation was shown to be either upregulated or downregulated within synaptosomal fractions isolated from different sympathetic tissues of the SHR[139, 196]. Moreover, these current results combined with previous studies indicate that NET regulation is not uniform throughout the sympathetic innervation of the SHR. Therefore, attempting to infer data from different sympathetic beds for a global role of NET in hypertension may explain some disparity within previous studies[3, 195].

The previous studies that have reported no change in NET activity between the SHR and WKY have always used indirect methods of inferring NET function, such as measuring NE overflow[77], or recording atrial parameters [140]. By not assessing NET directly these techniques are open to influence of additional compounding effects from the tissue as well as assessing the sympathetic population of the heart as a whole, rather than studying single cell transporter function. The NTUA assay allows for measuring NET rate within single cells under different physiological and pharmacological conditions. However, this new assay does have its limitations. The chemical compound of the assay has not yet been released, therefore even though it has been tested for specificity to the monoamine transporters, and uptake rate is shown to be inhibited with desipramine, it is unknown which component of the assay produces the fluorescence or how this fluorescence arises within the cell. The NTUA assay has been implicated as a substrate of VMAT[158] (vesicular monoamine

transferase), and appears to be sequested within sympathetic vesicles within the cell. This means fluorescence builds up in the cell; over time repeated stimulations show reduced slope rates when normalised to the starting fluorescence of the slope. This can be normalised by expressing data as an S2/S1 ratio as described in chapter two.

4.4.2. Effect of neuronal activation on stellate sympathetic norepinephrine reutpake transporter activity of the spontainously hypertensive rat.

Increased sympathetic nerve activity[39, 41], and increase NE spillover[3, 201] is associated with clinical hypertension. A number of studies have previously demonstrated that both cell depolarization[116, 202, 203] and synaptic vesicle release[117, 204] increase NET function. The results presented in this chapter show electrical field stimulation induced cell depolarisation to further augment the difference in NET transporter rate between SHR and WKY stellate sympathetic neurons. Moreover, the observed up regulation of NET activity within WKY neurons following neuronal activation consistent with previous studies[116, 202], appears to be absent from the age matched SHR.

The exact mechanism by which depolarisation increases transporter function is unknown. A previous study investigating NET activity in PC12 cells via KCl induced cell depolarisation observed an up regulation in NET activity independent to changes in membrane potential or cell surface expression, but dependent on Ca^{2+} activation of intracellular kinases likely by a CaMKII dependent pathway[116]. Where as, regulation in transporter function by interactions with components of the vesicle release complex has been shown to both increase the surface expression of NET, but

also directly down regulate its catalytic activity by Ca^{2+}/PKC dependent CaMK independent mechanism.

Although with stellate neurons in the presence of desipramine any intracellular uptake of NTUA is thought to be due to the presence of NET. NTUA is a substrate for all monoamine transporters. Therefore, there is clinical significance in using the NTUA assay in monoamine transporter regulation for models of depression and Alzheimer's. The translation implications of this could be transferred to clinical models, as altered NE handling has also been observed in these subjects.

A recently published paper provides evidence for dysregulated intracellular calcium handling in the SHR, leading to greater depolarisation induced calcium transients as measured using fura-2 in the SHR than the WKY[1]. This in combination with reduced NET activity in the SHR observed here would suggest that at least part of the sympathetic hyperactivity observed in SHR is due to increased intracellular calcium transients, resulting in greater NE release, that remains active in the synapse for longer due a reduced activity of NET.

4.4.4 Conclusion

Reduced NET activity within stellate sympathetic neurons of the SHR compared to age matched WKY may contribute to the cardiac sympathetic hyperactivity previously reported in hypertension.

These studies allude to an additional level of complexity in NET regulation within the SHR model of hypertension, revealing a greater degree of heterogeneity in NET function and modulation within different sympathetic tissue populations than ever

previously anticipated. Further reinforcing the principle that care should be taken when inferring data from one sympathetic bed in a role for the global function of NET in hypertension.

4.5. SUMMARY

The role of the norepinephrine re-uptake transporter (NET) in hypertension is controversial. Using a novel fluorescent compound of NET that allows for dynamic monitoring of the transporter kinetics, NET activity was studied within neurons isolated from three major sympathetic beds of the hypertensive SHR compared to age matched WKY. A significant reduction in NET activity was observed within sympathetic stellate SHR neurons (n=20) in comparison to WKY (n=19). This difference was further potentiated with neuronal activation by electrical field stimulation induced cell depolarisation. However, no difference in NET activity was observed between SHR and WKY neurons isolated from the superior cervical ganglia (SHR n=24, WKY n=24) nor the celiac ganglia/superior mesenteric ganglia/renal sympathetic chain (SHR n=18, WKY n=23). These results suggest that defective NET activity within stellate sympathetic neurons of the SHR may be contributing to the increased cardiac sympathetic activity observed in hypertension. Additionally, intracellular modulation of NET varies between different sympathetic beds of the SHR in comparison to its normotensive WKY control, indicating that the dysregulated NET activity observed within the SHR may reside at a number of intracellular sites.

CHAPTER 5:

SITE-SPECIFIC ROLE OF NET IN THE SYMPATHETIC BEDS AS AN EARLY HALLMARK OF HYPERTENSION

5.1. INTRODUCTION

Identifying early hallmarks of hypertension could be clinically useful in facilitating an earlier diagnosis of the disease, identifying potential therapeutic targets, and lead to a greater understanding of the process involved in the development of hypertension. Emerging evidence in isolated sympathetic neurons has shown that depolarisation induced Ca^{2+} transients are already enhanced in young pre-hypertensive SHR compared to normotensive controls similar to the adult animal[1]. Increased intracellular Ca^{2+} transients facilitating neurotransmission may therefore contribute to the development of the hypertensive phenotype of the SHR. Following the observation of NET dysregulation in the adult SHR, increased SHR cardiac sympathetic activity (chapter three) and enhanced Ca^{2+} transients in isolated stellate neurons of the young SHR; I hypothesised that NET may also be dysregulated in the young SHR. The aim of this study was to investigate if deregulation of NET may also be a contributing factor to the early sympathetic hyperactivity observed within the SHR, in a similar fashion to the enhanced intracellular Ca^{2+} transient seen in pre-hypertensive SHR's[1].

5.2. METHODS

5.2.1 ANIMALS

All experiments were performed under British Home Office license requirements (PPL 30/2360) in accordance to the Guide for the Care and Use of Laboratory Animals published by the US National Institutes of Health (NIH Publication No. 85-23, revised 1996) and the Animals (Scientific Procedures) Act 1986 (UK).

Age and weight matched four to five week (90g-120g) pre-hypertensive male SHR[138], and WKY rats were purchased from Harlan (Biscester, UK) and Charles River (Sulzfeld, Germany), and housed under standard laboratory conditions.

5.2.2 ANATOMY

Isolation and preparation of sympathetic post ganglionic neurons

Animals were rendered unconscious using general anaesthesia then humanely killed by an approved Home Office schedule 1 method as previously described. Sympathetic neurons were isolated from three major sympathetic ganglia implied in hypertension[44, 162, 199], the cardiac stellate ganglia, the superior cervical ganglia and the celiac ganglia, superior mesenteric ganglion (CG/SMG) that innervate the kidneys, and other abdominal organs[144, 145]. Isolation and culture of the sympathetic ganglia were carried out using the method previously described[147, 200], and briefly explained within section *4.2.2.* Cells were incubated 37^{o}C 5% CO_2 on Poly-D lysine and laminin coated cover slips (5mm) for 1-2 days before use.

Immunohistochemistry

Cultured cardiac stellate and CG/SMG neurons were fixed with 4% paraformaldehyde and permeabilised with 0.1% Triton X100 and 1% BSA. Cells were then processed for immunoreactivity to the sympathetic marker tyrosine hydroxylase with mouse anti tyrosine hydroxylase (TH), 1:200 (sigma), and Alexa Fluor 647 goat anti-mouse IgG, 1:100-1:200 (invitrogen, A21236).

5.2.3 EXPERIMENTAL PROTOCOL

Measurement of Norepinephrine uptake rate.

Measurement of NET rate was carried out as described in chapters two and four.

Protocol

The protocol for measuring dynamic NET activity using the fluorescent NTUA assay within isolated sympathetic neurons has previously been described within chapter two *(section 2.2.3).* In brief, following a 5-minute control period of Tyrode solution perfusion, perfusion was switched to one containing a 1:10 concentration of NTUA for 5 minute. The perfusion system was then stopped and cells held stationary in the NTUA containing buffer 37±0.5^{o}C for 10 minutes, where the rate of increase in fluorescence within the cell was recorded.

The rate of increase in intracellular fluorescence was recorded by selecting a region of interest (ROI) around the isolated postganglionic cell. Images were acquired every two seconds using a photometrics CoolSNAP HQ^{2} camera, excitation wavelength 440nm, emissions band 535±35nm.

Results are presented as increase in fluorescence over time, normalised to the starting intracellular fluorescence of the cell at t=10 min (when perfusion was stopped).

Inhibition of NET

To confirm that rate of intracellular fluorescence accumulation was specific to NET, the end of each protocol the perfusing solution was switched to one containing

desipramine (DMI 1μM) for 15 minutes followed by a 5 minute perfusion of NTUA (1:10) + DMI (1μM) at 35 minutes, followed by a repeat of the hold protocol at 40-50min. Cells in which DMI failed to inhibited intracellular fluorescence increase were excluded from analysis.

Electrical Field stimulation of isolated sympathetic post ganglionic neurons

Cell depolarisation was induced by electrical field stimulation (EFS) (5Hz, 10V, 10ms) for 2.5min at 17min and 47min (during both the control NTUA (1:10) and NTUA (1:10) + DMI (1μM) holds) by a pair of parallel horizontal platinum electrodes within the perfusion chamber.

5.2.4. Solutions and Drugs

Tyrode solution for isolated postganglionic sympathetic neuron experiments contained (mmol/L NaCl 145, KCl 5, HEPES 10, glucose 10, $CaCl_2$ 2 and $MgCl_2$ 1) (pH 7.38-7.42, 37±0.5^{o}C). NTUA was purchased from MDS Analytical Technologies (catalogue R8173; Wokingham, Berkshire, UK) prepared as described in chapter two. Desipramine (Sigma, UK) was stored as stock solution (1mM in distilled H_2O). Desipramine was made to the desired concentration (1μM) on the day. All drugs under went no more than one freeze thaw cycle.

5.2.5. Statistics

All statistical analysis was carried out using GraphPad Prism (GraphPad Software, San Diego, CA, USA). Data are presented as means±SEM. Analysis was performed using

paired or unpaired Student *t* test as appropriate. For all experiments, statistical significance was accepted at $P<0.05$.

5.3. RESULTS

5.3.1. ISOLATED NEURONS STUDIED ARE SYMPATHETIC.

Cultured cardiac stellate ganglia neurons showed positive immuno-reactivity to sympathetic marker anti-tyrosine hydroxylase in four week SHR and aged matched WKY (figure 5.1.) confirming the cells studied to be sympathetic.

5.3.2. NOREPINEPHRINE UPTAKE WITHIN MAJOR SYMPATHETIC GANGLIA OF THE PRE-HYPERTENSIVE SHR AND WKY.

Norepinephrine re-uptake transporter activity was significantly reduced in cardiac stellate neurons of pre-hypertensive SHR compared to age matched normotensive WKY rats (figure 5.2.)(SHR: 3.21±0.24 au/min, n=24. WKY: 4.21±0.40 au/min, n=21, $P<0.05$, unpaired *t* test; figure 5.5). Moreover no difference in uptake rate was observed between sympathetic neuronal cells of the pre-hypertensive SHR SCG compared to age matched WKY (figure 5.3)(SHR: 4.04±0.13 au/min, n=49. WKY: 4.03±0.15 au/min, n=52; figure 5.5), nor pre-hypertensive SHR CG/SMG neurons compared to age matched WKY (figure 5.4)(SHR: 2.55±0.30 au/min, n=15. WKY: 2.37±0.15 au/min, n=18; figure 5.5). DMI (1μM) blocked the action of the NET fluorescence in all groups.

Figure 5.1

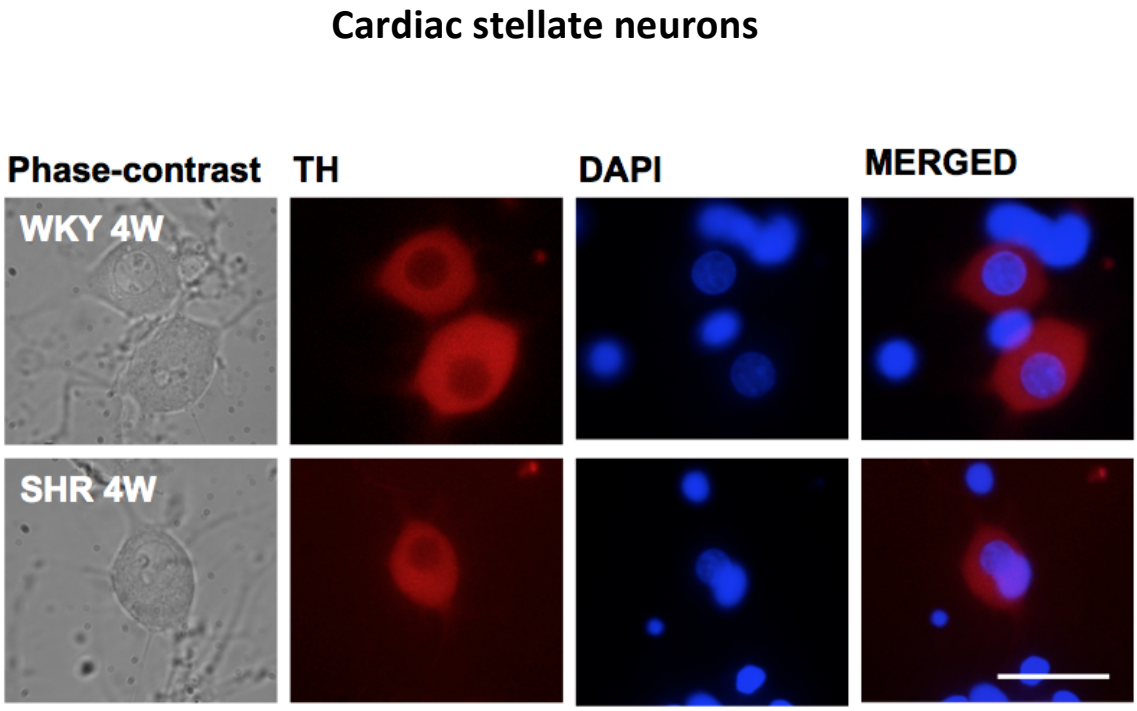

Figure 5.1: Positive immunoreactivity to sympathetic marker tyrosine hydroxylase in four week cardiac stellate neurons. DAPI is a nuclear stain. Scale bar: 50μm.

Figure 5.2

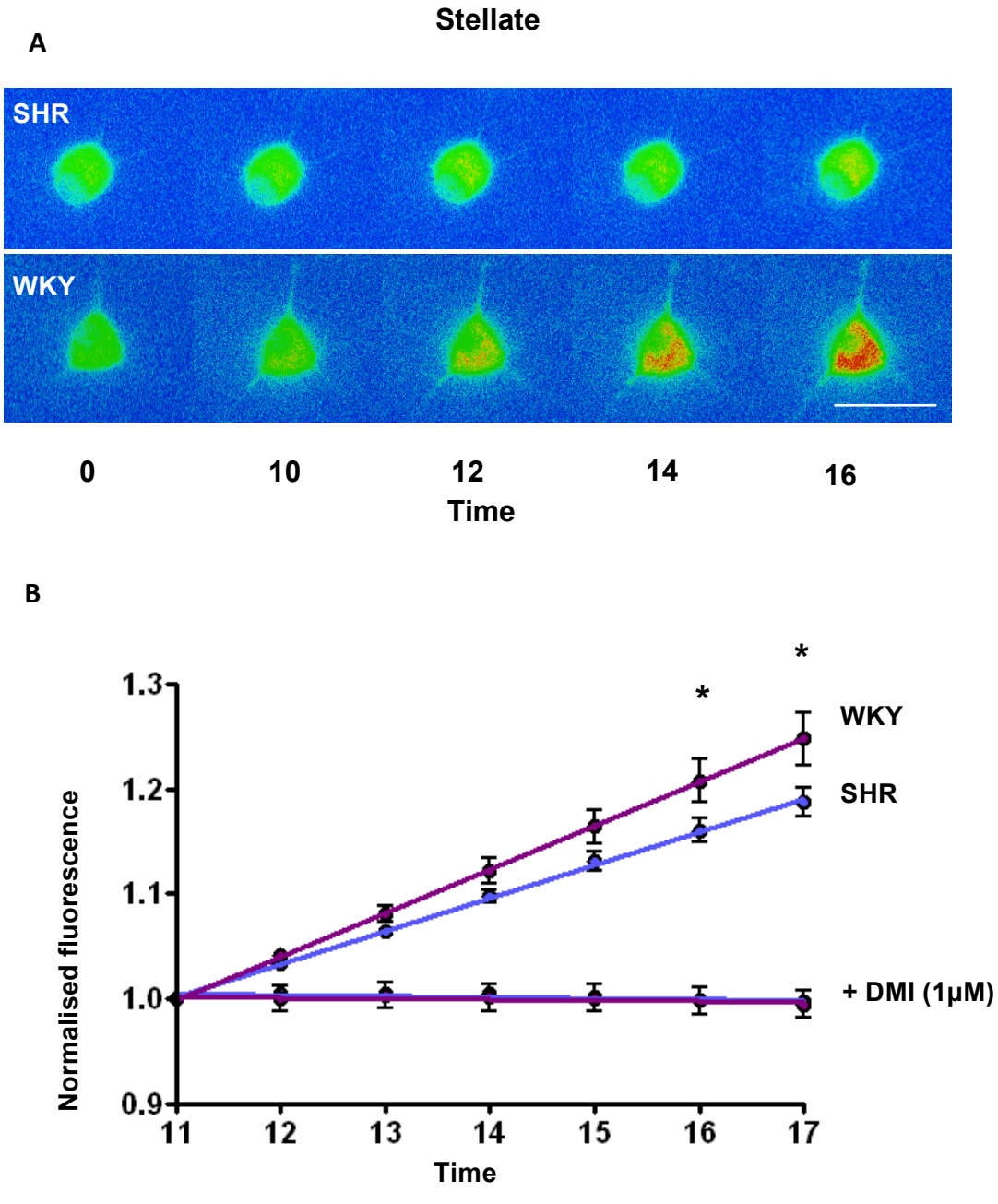

Figure 5.2: Rate of intracellular fluorescence increase is significantly lower in cardiac stellate neurons from the pre-hypertensive four week SHR. **A,** Representative fluorescent data. **B,** Rate of fluorescence increase (au) over time during NTUA (1:10) hold (SHR n=24, WKY n=21) and in the presence of 1µm DMI. Scale Bar 50µm.

Figure 5.3

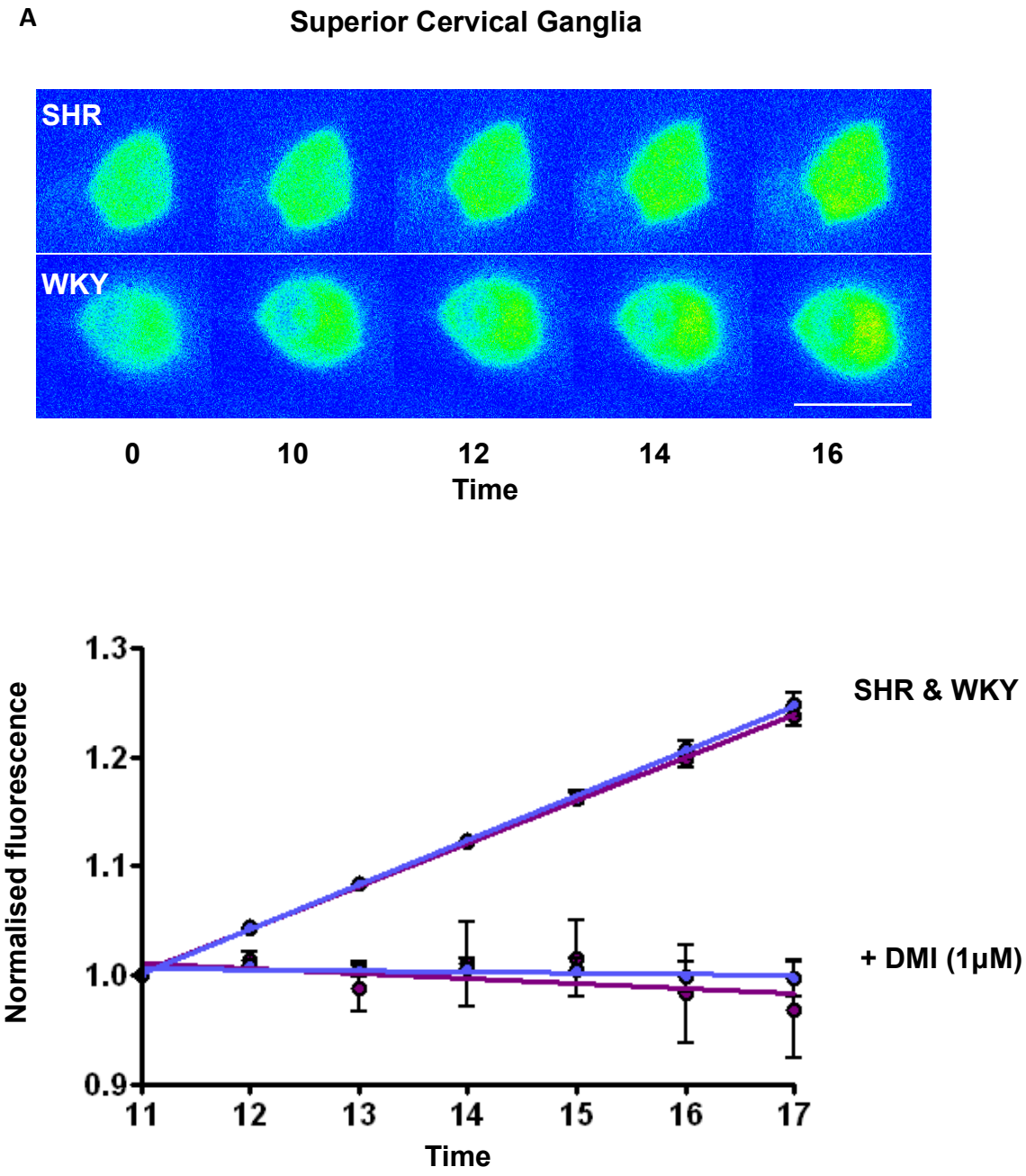

Figure 5.3: **A,** representative raw fluorescent data from four week SCG neuronal cells, in which no difference in the rate of intracellular fluorescence increase was seen between SHR and WKY cells. **B,** Rate of fluorescence increase (au) over time during NTUA (1:10) hold in isolated SCG neurons (SHR n=49, WKY n=54) and in the presence of 1µm DMI. Scale Bar 50µm.

Figure 5.4

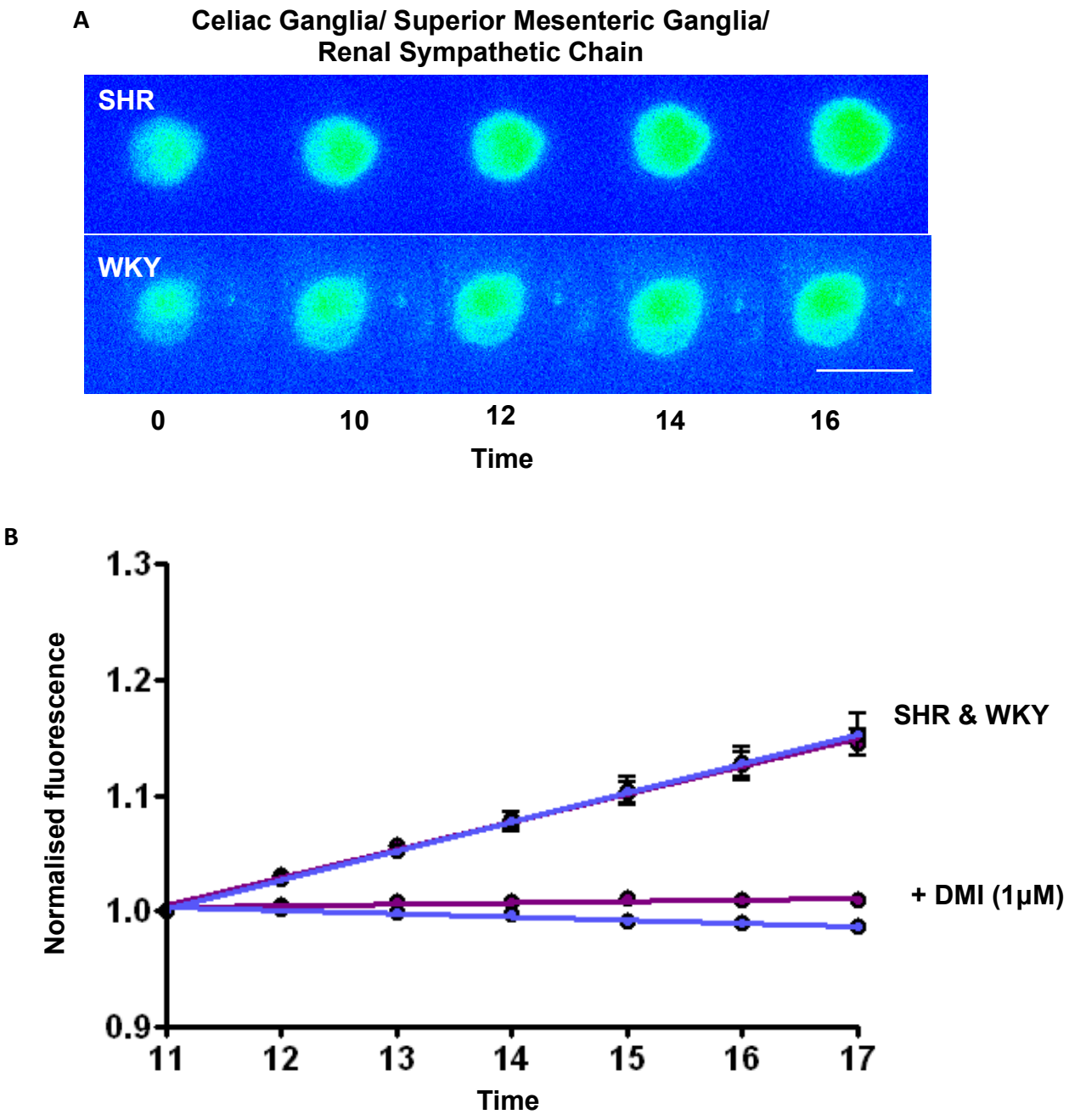

Figure 5.4: A, Representative raw fluorescent data from four week CG/SMG neuronal cells, in which no difference intracellular fluorescence increase was observed between SHR and WKY cells. **B,** Rate of fluorescence increase (au) over time during NTUA (1:10) hold in isolated CG/SMG neurons (SHR n=15, WKY n=18) and in the presence of 1µm DMI. Scale Bar 50µm.

5.3.3. Effect of cell depolarisation on norepinephrine uptake rate within prehypertensive stellate neurons.

To test the effect of neuronal excitability on NET activity between stellate pre-hypertensive SHR verses WKY cells, preparations were depolarised by electrical field stimulation (EFS). Neuronal cell depolarisation potentiated the difference in NET transporter activity between young four week prehypertensive SHR and age matched WKY (SHR: 3.23±0.30 au/min, n=24. WKY: 4.59±0.41 au/min, n=21, $P<0.01$, unpaired *t* test; figure 5.6). The increase in transporter rate observed in young WKY stellate neurons was significantly greater during electrical field stimulation compared to control (WKY n=21, $P<0.05$, paired *t* test). No difference in NET activity was observed with field stimulation in the young pre-hypertensive SHR (SHR n=24, $P=0.87$).

5.4.6 Effect of age on neuronal NE uptake in sympathetic ganglia.

NET rate in cardiac stellate neurons (SHR $P=0.27$, WKY $P=0.33$) and CG/SMG/RSC neurons (SHR $P=0.30$, WKY $P=0.41$) was unaltered between age groups of the same strain (figures 5.7 & 5.9). Although, within superior cervical ganglion neurons increased age was associated with a significant reduction in NET rate in both strains (SHR, $P<0.0001$, unpaired *t* test. WKY, $P<0.0001$, unpaired *t* test, figure 5.8).

Figure 5.5

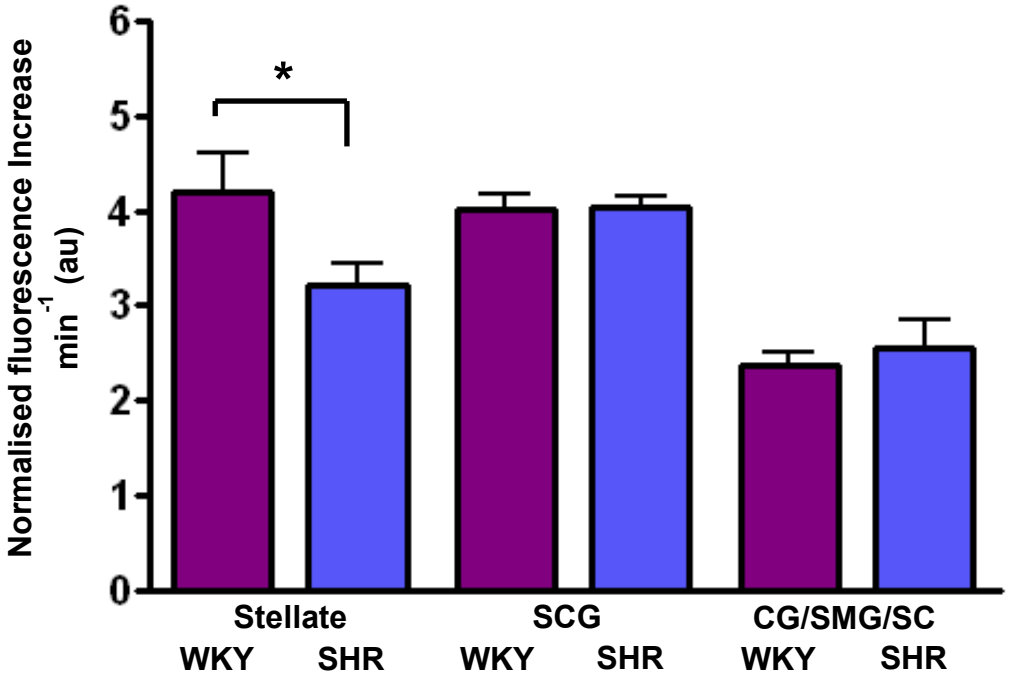

Figure 5.5: Rate of fluorescence increase during NTUA (1:10) hold, plotted as the gradient of the slope derived from y=mx+c. NET action is significantly decreased in the four week SHR stellate neurons compared to WKY (SHR n=24, WKY n=21) (**p*<0.05, unpaired *t* test). There was no significant difference in uptake rate between SCG (SHR n=49, WKY n=54) cells, nor CG/SMG cells of the four week SHR and WKY (SHR n=15, WKY n=18).

Figure 5.6

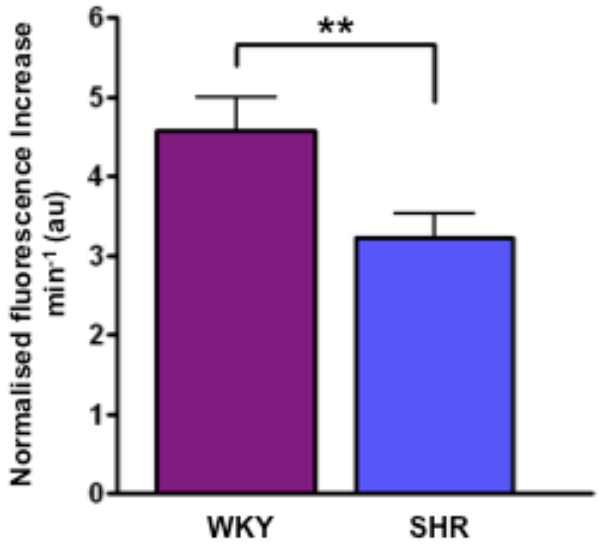

Figure 5.6: Rate of fluorescence increase in four week stellate neurons during external electrical field stimulation (EFS) (5Hz, 10V, 10ms, 2.5mins). Plotted as the gradient of the slope derived from y=mx+c. EFS exacerbated the difference in NET transporter rate between four week pre-hypertensive SHR and age-matched WKY (SHR n=20, WKY n=19) (***p*<0.01, unpaired *t* test).

Figure 5.7

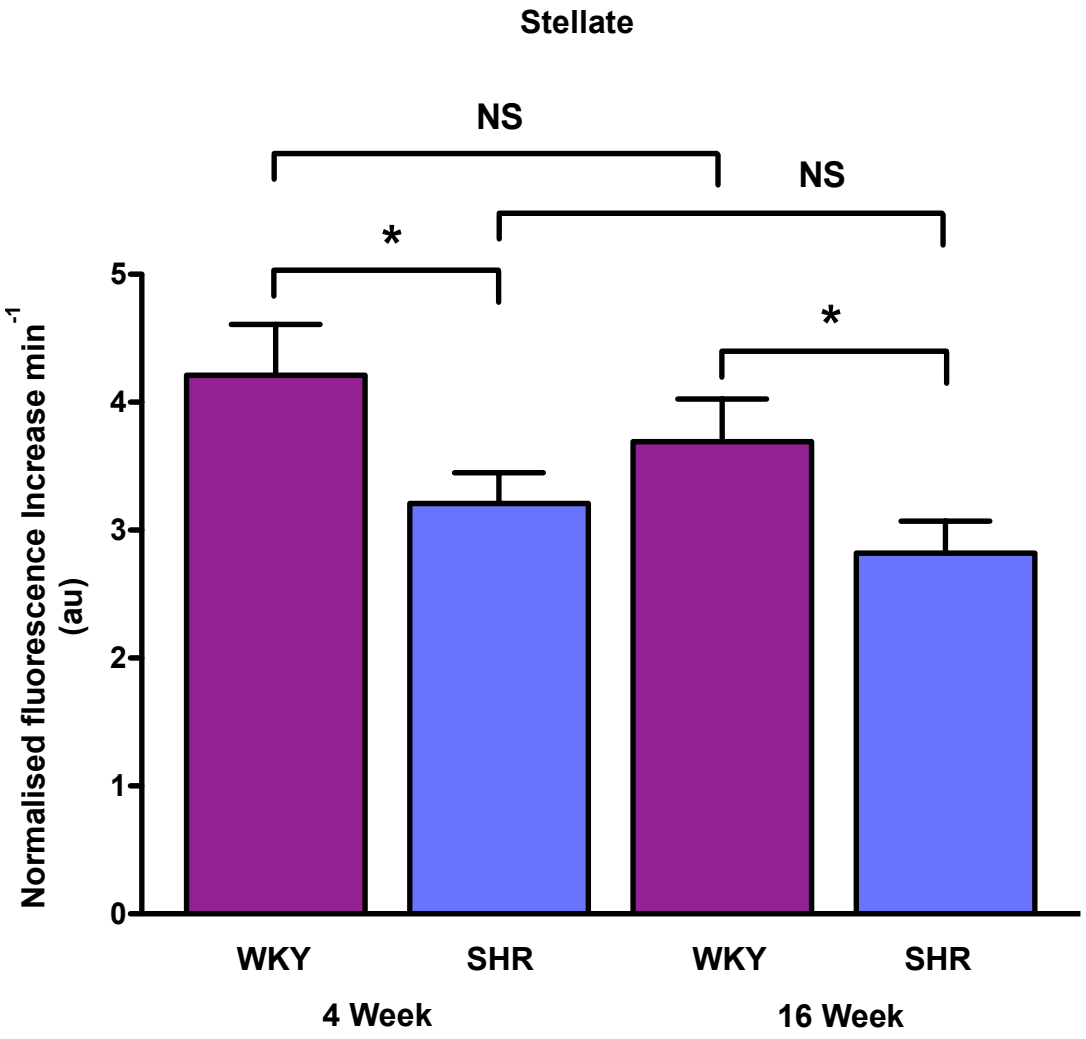

Figure 5.7: Rate of fluorescence increase during NTUA (1:10) hold, plotted as the gradient of the slope derived from y=mx+c. No difference in NET rate between developmental ages of SHR of WKY from stellate neurons.

Figure 5.8

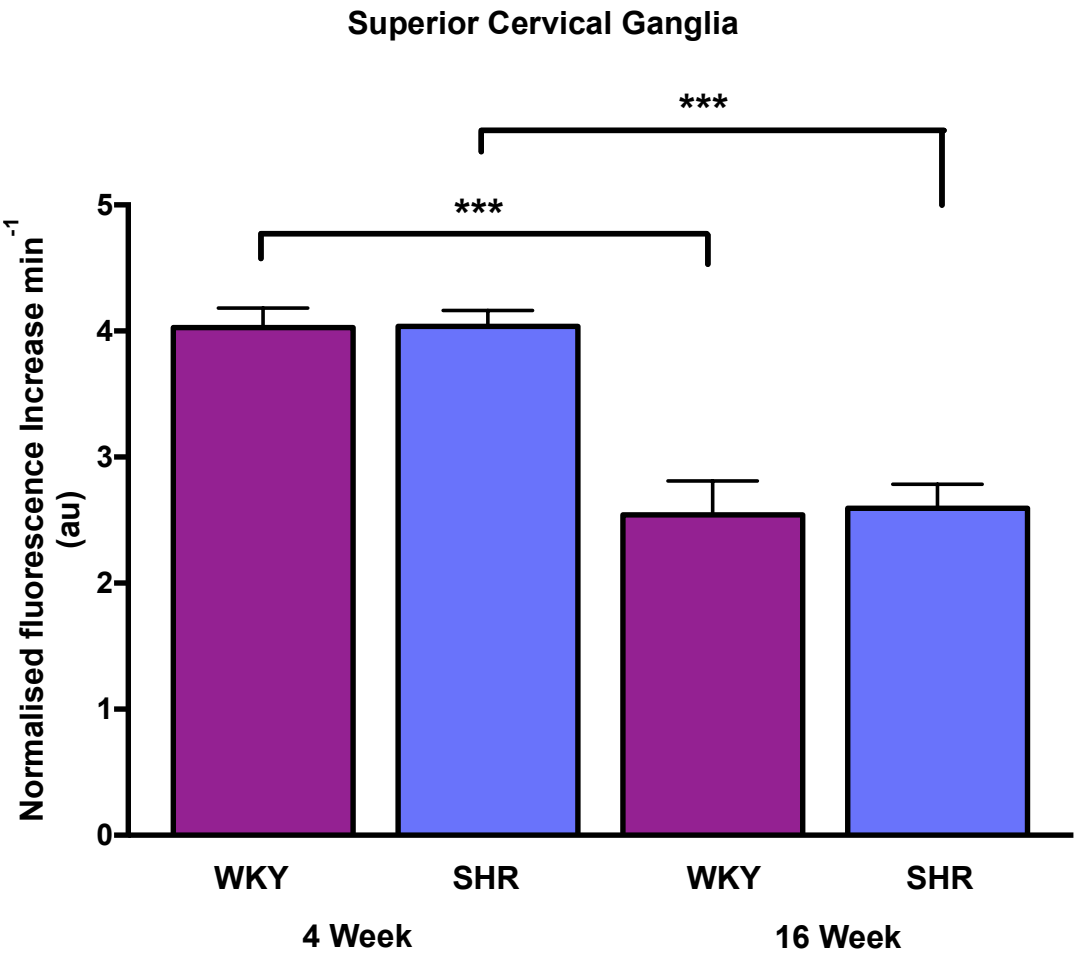

Figure 5.8: Rate of fluorescence increase during NTUA (1:10) hold, plotted as the gradient of the slope derived from y=mx+c. A significant decrease in NET activity with increasing developmental age was observed in both SHR and WKY superior cervical ganglia neurons. (***p<0.001, unpaired t test).

Figure 5.9

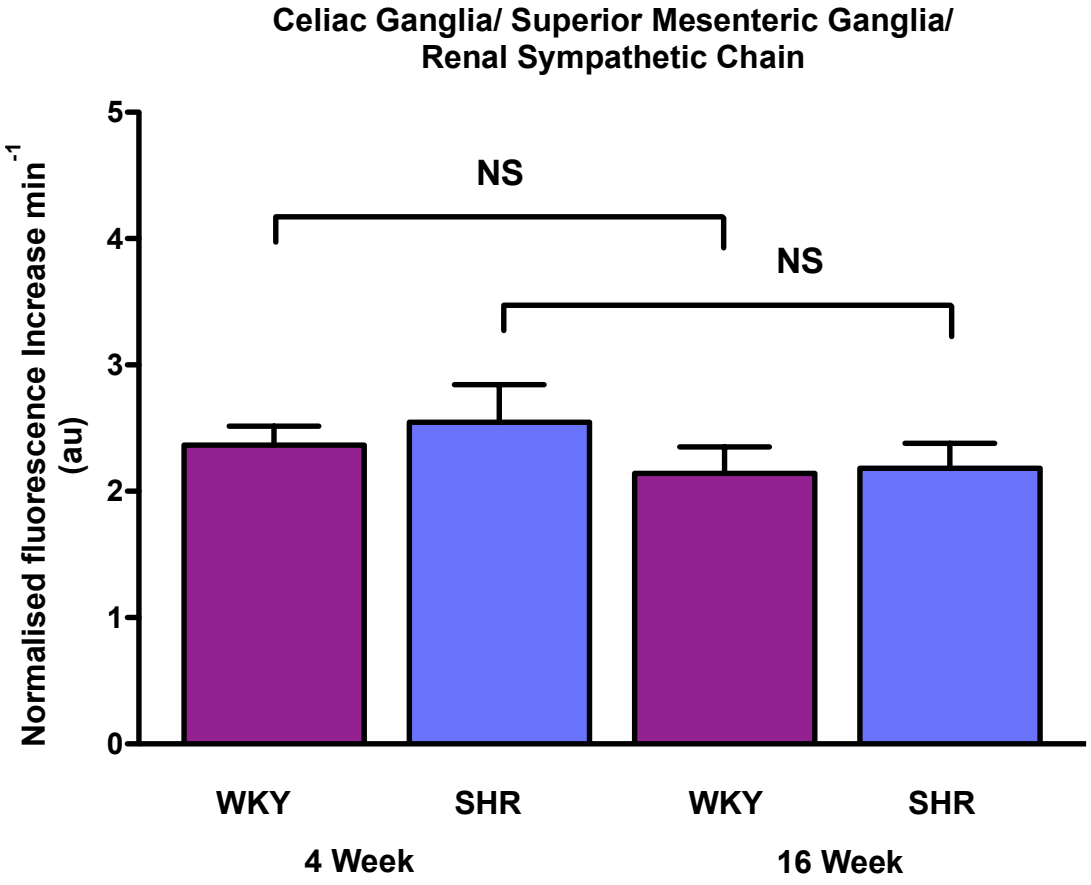

Figure 5.9: Rate of fluorescence increase during NTUA (1:10) hold, plotted as the gradient of the slope derived from y=mx+c. No difference in NET rate between developmental ages of SHR of WKY neurons of the CG/SMG/RSC ganglia.

5.3. DISCUSSION

The novel findings of this chapter are:

- There was a significant impairment of NET within cardiac sympathetic neurons of the young pre-hypertensive SHR, and this defect was not observed in other major sympathetic ganglia.
- Stimulation of cardiac sympathetic neurons further potentiated the difference between the young pre-hypertensive SHR and age matched WKY.
- An age dependent decrease in NET activity was also observed within the superior cervical ganglia, but not other major sympathetic ganglia.

In combination with the results reported in chapter four, the experimental results of this chapter indicate that a reduction in NET activity may contribute to the development, as well as the maintenance of the cardiac sympathetic hyperactivity observed in hypertension. The results in chapters four and five elude to the principle that regulation of NET is regionally specific between different sympathetic beds even at a young pre-hypertensive age.

5.4.1. SIGNIFICANT IMPAIRMENT OF NOREPINEPHRINE RE-UPTAKE TRANSPORTER WITHIN CARDIAC SYMPATHETIC NEURONS OF THE PRE-HYPERTENSIVE SPONTANTOUSLY HYPERTENSIVE RAT IS NOT OBSERVED WITHIN OTHER MAJOR SYMPATHETIC GANGLIA.

Chapter four presented a significant reduction in NET activity within cardiac stellate neurons of the hypertensive SHR in comparison to age matched WKY control. This was not observed in other major sympathetic ganglia that have an established role in hypertension[44, 198]. The results of this chapter show that the reduced NET activity

within the stellate ganglia of the SHR is present at a young pre-hypertensive age. Moreover, this is not observed within other major sympathetic ganglia. These results further indicate heterogeneity in NET regulation between different sympathetic ganglia, which already exists within the SHR at a young age.

5.4.2. Effect of neuronal activation on cardiac sympathetic norepinephrine re-uptake transporter activity of the pre-hypertensive spontantously hypertensive rat.

Cell stimulation within four week cardiac stellate neurons exacerbated the difference in NET activity observed between SHR and WKY at this age, correlating with the results of chapter four in the hypertensive animals. Evidence that neuronal activation increases NET capacity[116, 117, 202-204] may in wild type, normotensive individuals act as a compensatory mechanism to maintain appropriate junctional NE concentrations during neurotransmitter release, facilitating rapid clearance of released NE from the synapse. The increased sympathetic nerve activity associated with hypertension[39, 41] and reduced NET activity of the SHR during neuronal depolarisation would exacerbate the action of NE release and contribute to the sympathetic hyperactivity observed in the SHR.

Interactions of the transporter with components of the vesicle release complex, predominantly syntaxin 1A, facilitates the localisation of NET to the site of neurotransmitter release. Syntaxin 1A/NET interactions are Ca^{2+} dependent[116-118], and PKC independent[116, 118], requiring a direct interaction between the synaptic vesicle and NET as the response is blocked by treatment of both antisense oligonucleotide syntaxin 1A and botulinum toxin[117, 118]. Lack of modulation of SHR

stellate NET activity in response to neuronal depolarisation within this study suggests a potential failure of NET to interact with syntaxin 1A, reducing insertion into the plasma membrane within the SHR.

5.4.3. Significant reduction in norepinephrine re-uptake transporter activity with age in superior cervical ganglia neurons is not observed within other major sympathetic ganglia.

An Increase sympathetic activity has been reported with age in patients with hypertension, and rodent models[195, 205-208]. A reduction in NET transport capacity with age has also previously been implied in both human[205, 206, 209] and animal[195, 207] studies. Although no difference in basal NET activity was observed between age-matched SHR and WKY SCG neurons, a significant reduction in activity was observed with age between ganglia of the same strain. This suggests that ageing itself may contribute to the sympathetic phenotype observed in hypertension. Moreover, the reduction in NET activity observed within the SCG was not observed within neurons isolated from either the stellate or the CG/SMG/RSC ganglia. Providing further evidence for the heterogeneity of NET regulation between different sympathetic beds. The reduction in SCG NET activity is interesting, because this ganglia predominately innervates vascular tissue and it is well established that vasoconstriction and vascular stiffness increase with age.

5.4.4 Conclusion

Reduced cardiac NET activity within the pre-hypertensive SHR compared to age matched WKY may be a contributing factor to the development of the sympathetic

hyperactivity observed in established hypertension. Moreover, reduced NET activity within SCG neurons with age may further potentiate the development of the phenotype. These results further contribute to the conclusions previously drawn that NET regulation is not uniform between different sympathetic beds and that care should be taken when inferring results from one bed into a global role for the norepinephrine re-uptake transporter in disease. Identification of NET dysregulation as an early hallmark in hypertensions may open potential new therapeutic targets for hypertension.

5.5. SUMMARY

Evidence for dysregulation of the norepinephrine re-uptake transporter (NET) in the development of hypertension has previously been inconclusive. Using a novel fluorescent indicator designed to measure dynamic NET activity, NET was studied within neuronal cells isolated from three major sympathetic ganglia of the young pre-hypertensive SHR and age matched WKY controls. A significant reduction in NET activity was observed within sympathetic cardiac stellate SHR neurons (n=24) in comparison to WKY (n=21). This difference was further potentiated with neuronal activation by cell electrical field stimulation induced cell depolarisation. However, no difference in NET activity was observed between SHR and WKY neurons isolated from the superior cervical ganglia (SHR n=49, WKY n=54) nor the celiac ganglia/superior mesenteric ganglia (SHR n=15, WKY n=18). These results indicate that there is a site specific defective intracellular modulation of the norepinephrine

re-uptake transporter within sympathetic neurons of the SHR. This may be an early hallmark of the neural dysfunction that precedes hypertension itsself.

CHAPTER 6:

PHARMACOLOGICAL MODULATION OF THE NOREPINEPHRINE RE-UPTAKE TRANSPORTER IN THE WISTAR KYOTO AND SPONTANEOUSLY HYPERTENSIVE RAT SYMPATHETIC NEURONS

6.1 INTRODUCTION

The norepinephrine re-uptake transporter (NET) protein was considered inert for many years, contributing to the termination of action of released NE within the synapse. However, a number of studies into the function of NET in the 1980's revealed that several intracellular and extracellular signalling molecules regulate NET, and that phosphorylation of NET is a major pathway regulating its cell surface expression, and therefore its function. NET is also the target of action of a number of clinical therapeutic[82, 210, 211] and recreational drugs[212, 213], therefore its modulation has been of great scientific interest.

Previous studies into the role of NET in the aetiology and development of hypertension, alongside other cardiovascular diseases, have only investigated changes in global NET function. However, the identification that synapses can modulate NET capacity in responses to changes in neurotransmission[117], opens the possibility that pathophysiological changes in the cardiac neural axis previously identified in disease states, may partially arise via modulation of NET dynamics. Numerous consensus sites for protein kinases, phosphatases and glycosylation have been identified within the NET transporter gene sequence. Previous studies looking at global dynamics of NET have not been able to study the effect of NET regulation by different modulators directly. Using the NTUA assay I aimed to assess the modulation in activity of NET upon exposure to a number of molecules implicated in cardiac diseases and neuromodulation. In particular, brain natriuretic peptide (BNP)[214-217], nitric oxide (NO)[218, 219], and protein kinase c (PKC)[220, 221] have all been shown to regulate intracellular Ca^{2+} signals and exocytosis.

6.1.1 NATRIURETIC PEPTIDES IN CARDIOVASCULAR DISEASES.

Natriuretic peptide hormones were identified in the 1980's as a family of vasoactive peptides with actions on the kidney[222], vasculature[223] and cardiac system[224]. Administration of natriuretic peptides relaxes vascular smooth muscle reducing ventricular preload and lowering blood pressure[225]. Atrial natriuretic peptide (ANP) and brain natriuretic peptide (BNP) are released in response to ventricular myocte stretch[214, 226]. C-type natriuretic peptide (CNP) is structurally different from ANP and BNP, and predominantly has action within the CNS and vascular system rather than the heart[227]. BNP is used as a clinical marker for a number of cardio-vascular diseases including, aortic stenosis, hypertrophic cardiomyopathy, restricted cardiomyopathy, left ventricular dysfunction and heart failure[214-217, 228]. Moreover, plasma levels of BNP as a disease biomarker can predict disease state and prognosis much better than plasma levels of ANP[229-231].

BNP and ANP are thought to have both central and peripheral sympatho-inhibitory effects, reducing the level of sympathetic control at the junction [232, 233]. However, exogenous applied BNP augments vagal neurotransmission in a response that is blocked by NPR antagonists[234]. BNP binds to the NPR-A receptor on the neuronal surface membrane signalling via particulate guanylyl cyclase (pGC). Although raised BNP concentrations have been observed to increase vagal neurotransmission, the exact mechanisms behind their sympathoinhbitory mechanisms are not yet fully understood. Therefore, due to the high presence of BNP as an indicator of cardiovascular disease progression I used the NTUA assay to test if a component of

the cardio protective role attributed to BNP was due to BNP modulation of NET and how this modulation may vary between age matched SHR and WKY.

6.1.2. Neuronal nitric oxide synthase in cardio vascular disease.

In 1998, Furchgott, Ignarro and Murad were awarded the Nobel Prize for physiology or medicine for their discovery of nitric oxide (NO) as a signalling molecule of the cardiovascular system. Since then the role of NO signalling within cardiac, vascular and neuronal tissues has been extensively studied. Neuronal nitric oxide synthase is an intrinsic neuromodulator within both cardiac stellate and sympathetic neurons. It acts via soluble guanylyl cyclase (sGC) to generate cGMP. In cholinergic neurons nitric oxide increases Ca^{2+} transients and acetylcholine release[34, 235], whereas, within sympathetic neurons it acts to reduce Ca^{2+} influx and norepinephrine release[236]. Disruption to the nNOS/cGMP pathways has previously been identified in sympathetic neurons of the SHR. Viral transfer of the nNOS gene via a PRS sympathetic specific promoter into cardiac sympathetic neurons of the SHR has been shown to rescue the sympathetic hyperactivity observed in this model[36, 237]. Disruption of the NO pathway in the SHR could conceivably also affect other intracellular signalling mechanisms such as NET given its action on calcium handling proteins, therefore the effect of up regulating NO in stellate neurons of the SHR was studied.

6.1.3 Intracellular activation of cGMP

Brain natriuretic peptide and nitric oxide both activate intracellular signalling pathways that generate the second messenger cGMP. BNP binds to surface NPR-A

receptors that are coupled to pGC at the cell membrane. Where as, NO diffuses intracellularly and activates sGC within the cells cytoplasm[238]. Both GC'c produce the second messenger cGMP from GTP, however the spatial restriction of the cGMP and therefore the area in which it is active may vary between the two neuromodulators. cGMP bind to the regulatory sites of protein kinase G (PKG) activating it. As mentioned a number of phosphorylation sites have been identified within the NET gene sequence, opening a potential route for how BNP and NO, may modulate NET via a GC, cGMP, PKG pathway (figure 6.2)

6.1.4 Protein kinase C (PKC) in cardio vascular disease

As mentioned in chapter one, the NET protein gene sequence contains a number of well defined PKC phosphorylation sites[100]. Protein kinase C mediated phosphorylation of NET facilitates receptor internalisation, therefore reducing transport capacity [103-106]. Modulation of PKC activity as a potential therapeutic target for treatment of a number of cardio vascular diseases including atherosclerosis, ischaemic heart disease, cardiac hypertrophy, heart failure, and hypertension has previously been studied[239]. However previous reports have predominantly focused on the effects of PKC within the cardiomyoctyes of the atria and ventricle. Due to the extensive evidence for PKC modulation of NET, and the potential role as a therapeutic target in cardiovascular disease, use of NTUA has allowed me to directly monitor NET activity in response to PKC inhibition in SHR and WKY isolated sympathetic neurons.

6.2 METHODS

6.2.1 ANIMALS

All experiments were performed under British Home Office license requirements (PPL 30/2360) in accordance to the Guide for the Care and Use of Laboratory Animals published by the US National Institutes of Health (NIH Publication No. 85-23, revised 1996) and the Animals (Scientific Procedures) Act 1986 (UK).

Age and weight matched 4-6 week (90-110g) male SHR and WKY rats were purchased from Harlan (Biscester, UK) and housed under standard laboratory conditions.

6.2.2 ANATOMY

Isolation and preparation of sympathetic post ganglionic neurons

Stellate sympathetic neurons were isolated and plated by the method previously described in chapters three and four.

6.2.3 EXPERIMENTAL PROTOCOL

Assay preparation

See chapter two.

Protocol

Prior to the start of the experiment cells were pre-incubated in a low 1:100 concentration of the assay in cell plating medium for 20 min, 37^{o}C, 5% CO_2. See chapter two.

A control period of 5 minutes in Tyrode solution was followed by a 5 minute perfusion with buffer containing 1:10 concentration of the NTUA assay (consistent with concentrations used in previous studies[158]). The cells were held stationary in the NTUA containing buffer 37±0.5^{o}C for 10 minutes, where the rate of increase in fluorescence within the cell was recorded (S1). Following this the perfusing tyrodes was changed to one containing the drug of choice for an appropriate incubation time, based on previous studies. Followed by a second application of NTUA 1:10 + the chosen drug and a second hold in perfusion in which NET rate in the presence of chosen drug was recorded (S2).

Brain natriuretic peptide (BNP)

Brain natriuretic peptide was stored as a stock solution at 100µM, and diluted to a concentration of 250nM on the day of use. This high dose of BNP was used as any effect on NET was expected to be minimal therefore a concentration that would be more likely to produce results rather than increasing concentrations was used to prevent experimental and animal wastage. BNP was added to the perfusing Tyrode for 15 minutes prior to the S2 hold. The concentration and time of incubation used for BNP are consistent with previous studies.

Sodium nitroprusside (SNP- NO donor)

The NO donor SNP was used to study the effect of NO on NET activity in isolated sympathetic neurons. SNP (100µM) was made up on the day of use to avoid any degradation of the drug that can happen when stored. SNP was added to the perfusing system for 20 minutes prior to the S2 hold based on previous studies. Due

to the light sensitive nature of SNP, during these experiments the imaging time was set to one image every 180s during the SNP perfusion and increased back to one image every 2 seconds during the S2 hold.

8-bromo cGMP (activates cGMP dependent kinases)

8-bromo cyclic GMP (8-Br-cGMP) is a cell permeable cGMP analogue that possesses a greater resistance to hydrolysis by phosphatases than cGMP; activating cGMP dependent kinases. To observe any change in NET rate due to direct action of guanylyl cyclase experiments were performed using 8-Br-cGMP. The 8-Br-cGMP results combined with those of SNP and BNP may help establish the level of the GC signalling pathway in which NET activity of the SHR and WKY may be modulated. 8-Br-cGMP directly activates cGMP dependent kinases[240], therefore bypasses the need for cGMP synthesis by the GC activation pathway (figure 6.2).

Calphostin C (PKC inhibitor)

Protein kinase C has been shown to reduce transporter activity by sequestration of NET from the extracellular membrane. Whether, inhibiting PKC can result in greater transport capacity within resting sympathetic neurons is currently unknown. Inhibition of PKC is predicted to result in an increase in NET activity due to up regulation of NET to the extracellular membrane, therefore potentially rescuing the reduced NET observed in the SHR. The PKC inhibitor, calphostin C (0.1μM)[241] was used to assess if PKC modulation of NET could be used to a potentially therapeutic advantage in the SHR.

Calphostin C (Cal C) was stored as a stock solution of 1μM and made up to a concentration of 0.1μM on the day. Cal C was added to the perfusing Tyrode for 30 minute based on methods previously described[241]. Due to the light sensitive nature of Cal C the time base of the imaging was reduced to one image every 180s during the hold.

6.2.4. Solutions and Drugs

Tyrode solution for isolated postganglionic sympathetic neuron experiments contained mmol/L NaCl 145, KCl 5, HEPES 10, glucose 10, $CaCl_2$ 2 and $MgCl_2$ 1 (pH 7.38-7.42, 37±0.5^{o}C). NTUA was purchased from MDS Analytical Technologies (catalogue R8173; Wokingham, Berkshire, UK) prepared as described in chapter two. BNP, 8-BcGMP and Cal C (Sigma, UK) were stored as stock solutions (in distilled H_2O), and made to the desired concentration (1μM) on the day. SNP was made up on the day to the desired concentration within Tyrode solution. All drugs under went no more than one freeze thaw cycle.

6.2.5. Statistics

All statistical analysis was carried out using GraphPad Prism (GraphPad Software, San Diego, CA, USA). Comparison of S1 (control) to S2 (drug treated) slopes was carried out by creating an S2/S1 ratio of the normalised slope rates for all experiments. This S2/S1 ratio with drug treatment was then compared to an S2/S1 ratio for time alone (figure 6.1).

Figure 6.1

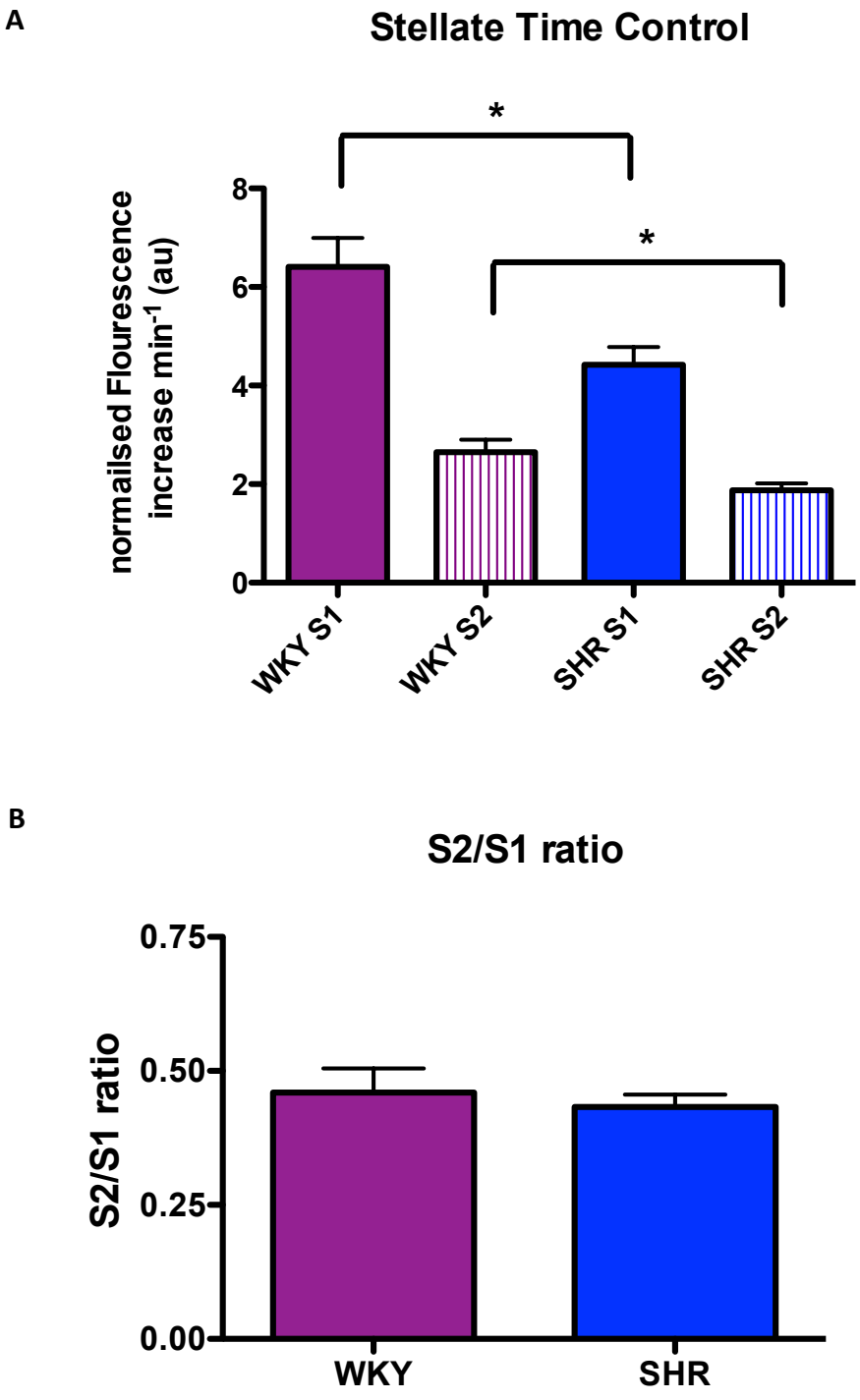

Figure 6.1: Rate of fluorescence increase in stellate neurons. Plotted as the gradient of the slope derived from y=mx+c. **A,** a reduction in uptake rate was observed with time in both cell types (WKY n=18, SHR n=11) **B,** S2/S1 ratio for paired results WKY and SHR (WKY n=18, SHR n=11). S2/S1 ratio normalises the difference in uptake rate observed between the SHR and WKY however does allow for a comparison of time alone with drug treatment over time. (*p<0.05).

Figure 6.2

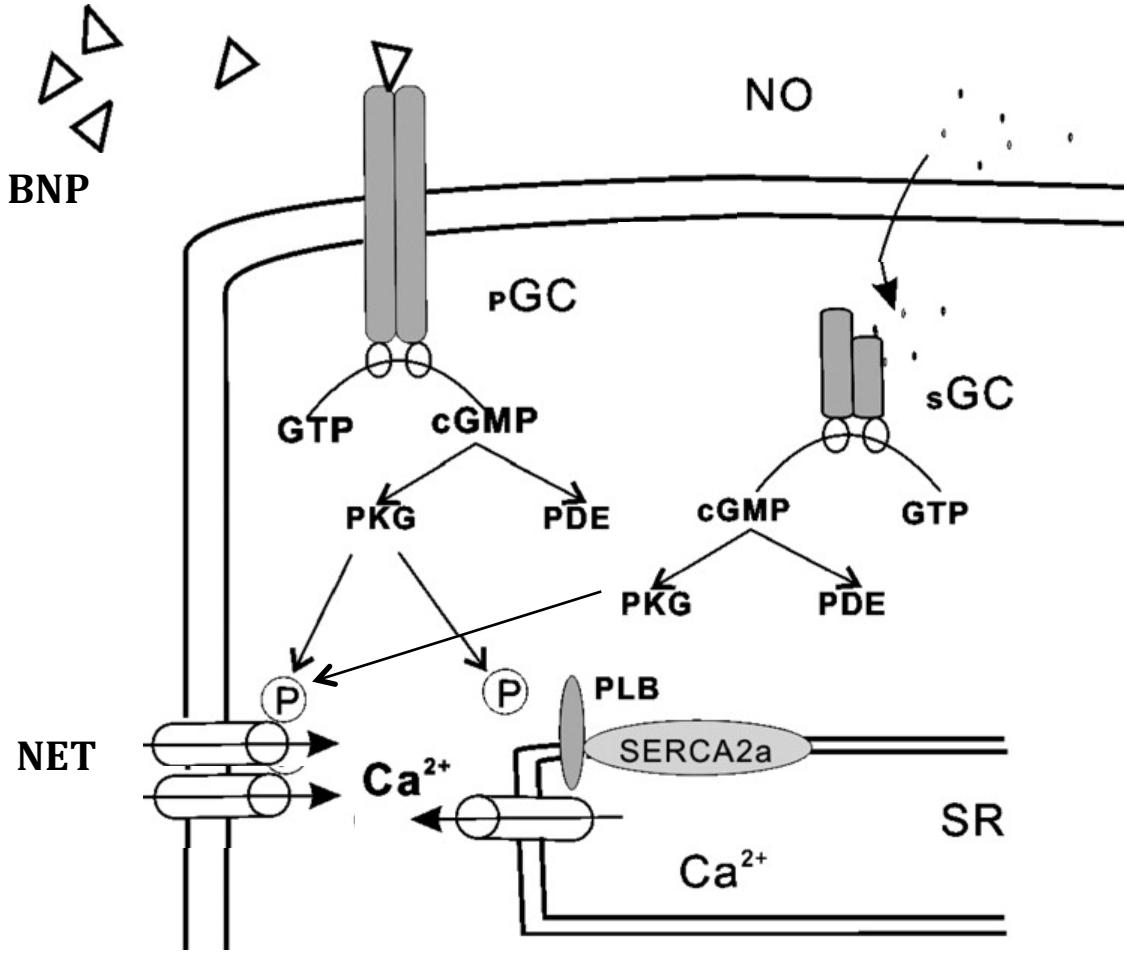

Figure 6.2. Schematic of the different routes of activation of cGMP via NO-sGC and BNP-pGC pathways. BNP binds to the membrane bound NPR-A receptor which is coupled to pGC. Where as NO diffuses into the cell and activate sGC. The activation of both GC's leads to the conversion of GTP to cGMP. cGMP is involved in the regulation of a number of intracellular functions, and signaling cascades including the activation of protein kinase G (PKG), which in turn can activate a number of protein kinases, and directly phosphorylate target proteins its self.

Unsurprisingly due to the nature of the experiment, with all slopes normalised to their starting fluorescence, a reduction in uptake rate between S1 and S2 was observed in both species. S1: WKY: 6.66 ± 0.58 au/min^{-1}, SHR: 4.43 ± 0.35 au/min^{-1}; S2: WKY: 2.65 ± 0.25 au/min^{-1}, SHR: 1.09 ± 2.18 au/min^{-1}; WKY n=18, SHR n=11. Uptake rate was significantly lower in the SHR compared to the WKY at both time points. However, calculating S2/S1 ratio for time alone normalised these results (figure 6.1).

Data are presented as means±SEM. Analysis was performed using unpaired Student *t* test between the S2/S1 ratio of a drug treatment and S2/S1 ratio for time control within the age-matched strains. Unpaired Student *t* test after confirming both sets of data followed a normal distribution using the D'Agostino and Pearson omnibus normality test. Where n≤5, normal distribution of data could not be verified, therefore data was compared using the nonparametric Mann Whitney test. For all experiments, statistical significance was accepted at $P<0.05$.

6.3 Results

6.3.1. Brain natriuretic peptide decreases norepinephrine re-uptake transporter activity within the Wistar Kyoto rat, with no difference observed in the spontaneously hypertensive rat.

Brain natriuretic peptide signals via membrane bound receptors to stimulate particular GC. BNP (250nM) significantly reduced NET transporter activity in cardiac stellate neurons of four week WKY rats compared to control (WKY BNP: 25.2±2.2 % S2/S1, n=24. Control: 48.0±4.3 % S2/S1, n=17, $P<0.05$, unpaired *t* test; figure 6.3).

However, no difference in uptake rate was observed between BNP treated stellate sympathetic neuronal cells of the pre-hypertensive SHR compared to control (SHR BNP: 52.4±5.5 % S2/S1, n=18. SHR control: 43.3±2.3 % S2/S1, n=11; figure 6.3). norepinephrine

6.3.2. Sodium nitroprusside decreases norepinephrine re-uptake transporter activity within the Wistar Kyoto rat, with no difference observed in the spontaneously hypertensive rat.

SNP is a nitric oxide donor, providing NO for the activation of soluble GC. SNP (100µM) significantly reduced NET transporter activity in cardiac stellate neurons of four week WKY rats compared to control (WKY SNP: 31.4±3.3 % S2/S1, n=18. Control: 48.0±4.3 % S2/S1, n=17, $P<0.05$, unpaired *t* test; figure 6.4). However, no difference in uptake rate was observed between SNP treated stellate neurons of the pre-hypertensive SHR compared to control (SHR SNP: 35.3±8.5 % S2/S1, n=8. SHR control: 43.3±2.3 % S2/S1, n=11; figure 6.4).

6.3.3. 8-BcGMP decreases norepinephrine re-uptake transporter activity within the Wistar Kyoto rat, with no difference observed in the spontaneously hypertensive rat.

8-BrcGMP (100µM) activates cGMP dependent kinases, removing the need for cGMP to be activated by GC. 8-Br-cGMP significantly reduced NET transporter activity in cardiac stellate neurons of four week WKY rats compared to control (WKY 8-BcGMP: 25.5±3.3 % S2/S1, n=13. Control: 48.0±4.3 % S2/S1, n=17, $P<0.05$, unpaired *t* test; figure 6.5). Again no difference in uptake rate was observed between 8-BcGMP treated stellate sympathetic neuronal cells of the pre-hypertensive SHR compared to control (SHR 8-BcGMP: 42.9±10.0 % S2/S1, n=15. SHR control: 43.3±2.3 % S2/S1,

Figure 6.3

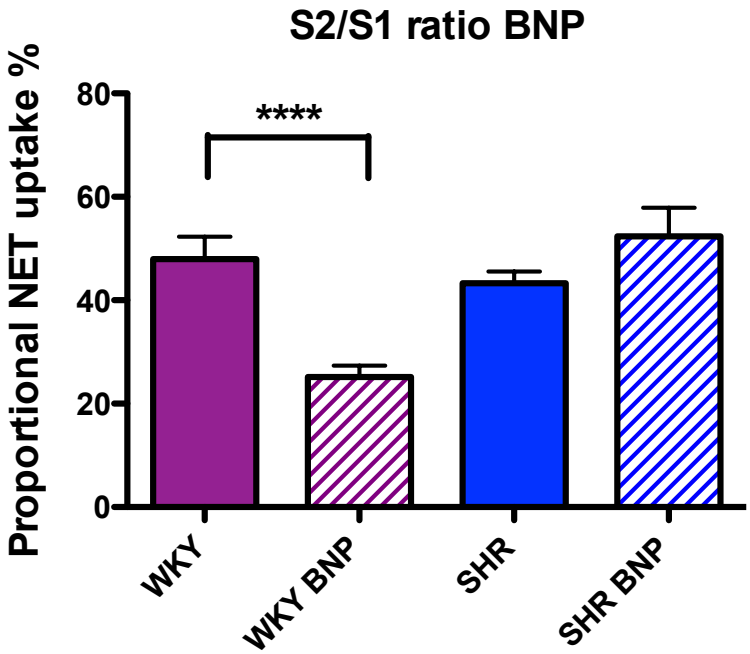

Figure 6.3: Rate of fluorescence increase during NTUA (1:10) hold, plotted as the S2/S1 ratio of the gradient of the slopes derived from y=mx+c. BNP (250nM) significantly decreased NET action in four week WKY stellate neurons (****p<0.001 *t* test) with no change in NET rate observed within stellate neurons of the pre-hypertensive SHR. (WKY, n=17, SHR n=11, WKY BNP n=24. SHR BNP n=18).

Figure 6.4

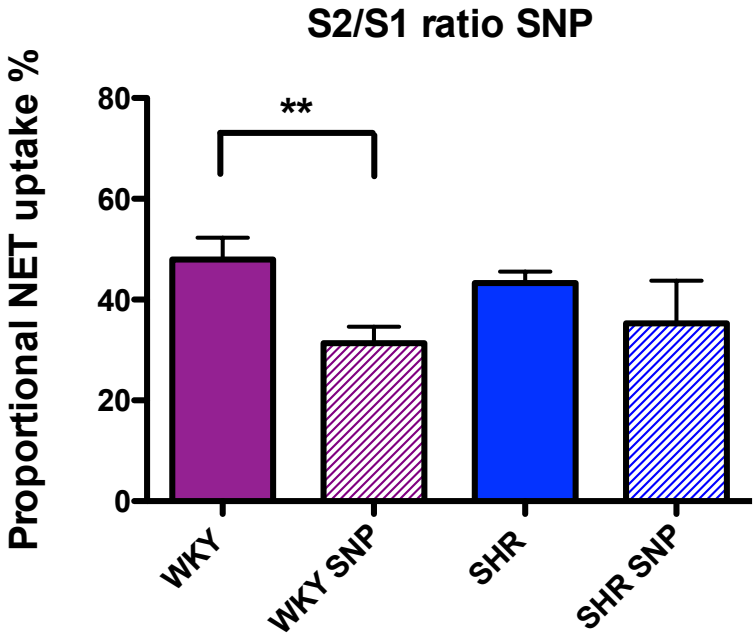

Figure 6.4: Rate of fluorescence increase during NTUA (1:10) hold, plotted as the S2/S1 ratio of the gradient of the slopes derived from y=mx+c. SNP (100µM) significantly decreased NET action in four week WKY stellate neurons (**p<0.01 *t* test) with no change in NET rate observed within stellate neurons of the pre-hypertensive SHR. (WKY, n=17, SHR n=11, WKY SNP n=18. SHR SNP n=8).

Figure 6.5

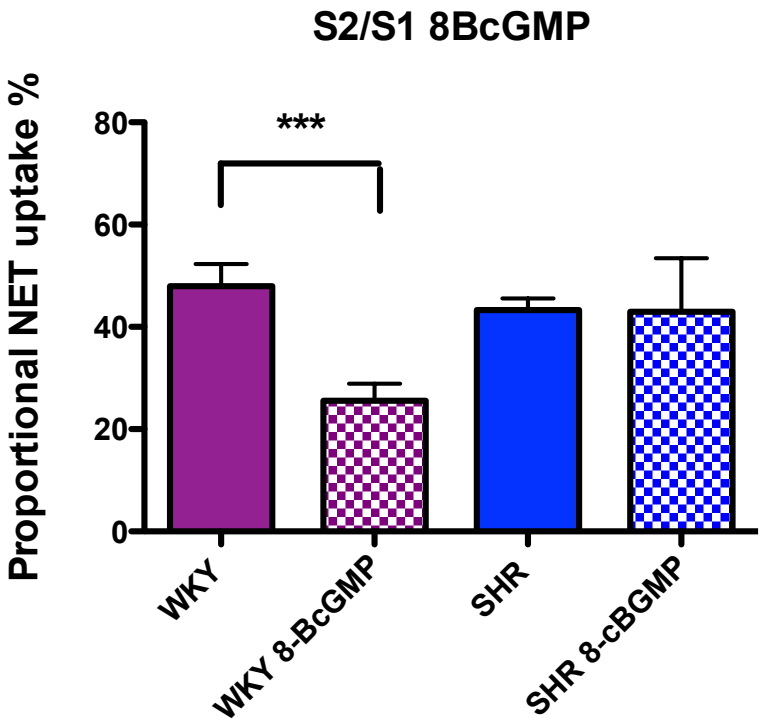

Figure 6.5: Rate of fluorescence increase during NTUA (1:10) hold, plotted as the S2/S1 ratio of the gradient of the slopes derived from y=mx+c. 8-Br-cGMP (100µM) significantly decreased NET action in four week WKY stellate neurons (***p<0.005 *t* test) with no change in NET rate observed within stellate neurons of the pre-hypertensive SHR. (WKY, n=17, SHR n=11, WKY 8-Br-cGMP n=13. SHR 8-Br-cGMP n=15).

n=11; figure 6.5). These results indicate that the intracellular signalling level of BNP and SNP induced NET regulation that is faulty in the SHR is below the level of guanylate cyclase.

6.3.4. Protein kinase C inhibition by calphostin C, increases norepinephrine re-uptake transporter activity in both pre-hypertensive spontaneously hypertensive rat and Wistar Kyoto rat sympathetic neurons.

Calphostin C (0.1μM) significantly increased NET transport capacity compared to control in both WKY and SHR stellate neurons, although the increase in the WKY was greater (figure 6.6). Stellate (WKY Cal C: 84.3±7.9 % S2/S1, n=13. WKY Control: 48.0±4.3 % S2/S1, n=17, SHR Cal C: 67.4±10.0 % S2/S1, n=15. SHR control: 43.3±2.3 % S2/S1, n=11; $P<0.05$, unpaired *t* test and Mann Whitney test; figure 6.6).

Calphostin C (0.1μM) produced a significant increase in NET transport capacity compared to control (figure 6.6). In isolated stellate neurons the increase in cellular fluorescence over time in the presence of Cal C, appears more sigmoidal than the traditional linear NTUA induced fluorescent increase observed in all other studies (figure 6.6.A). Cal C is light sensitive so this phenomenon may be due to toxic actions of the dye. Alternatively inhibition of PKC encourages receptor translocation to the membrane, therefore the slowing phase of the curve may be due to exhaustion of intracellular receptors, meaning few receptors are being translocated to the membrane in the late phase as the fluorescence appears to increase more slowly.

Figure 6.6

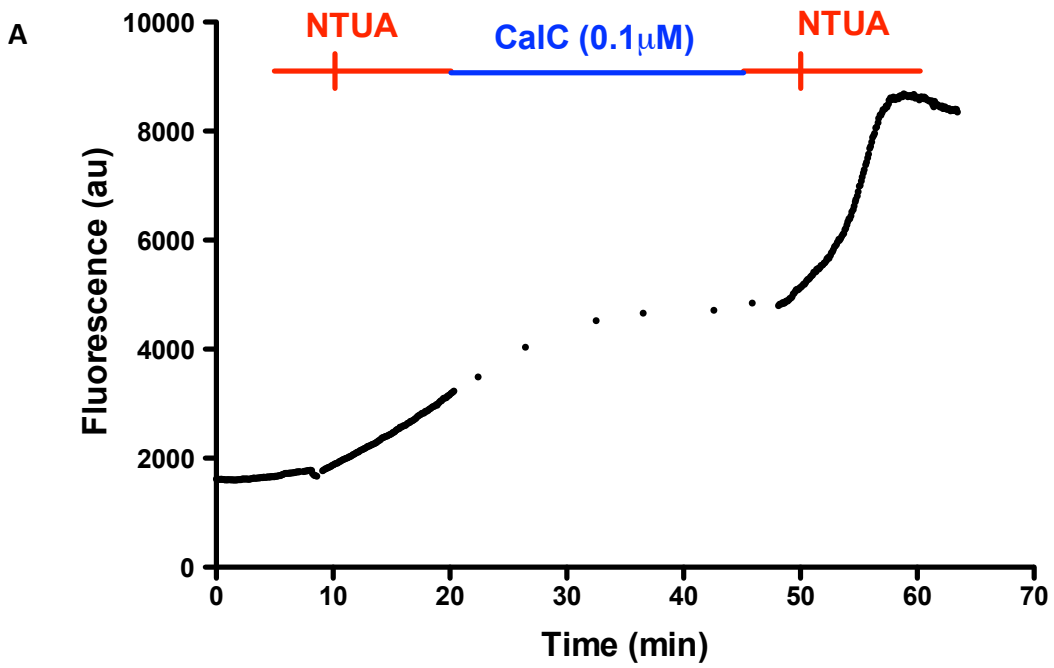

Figure 6.6: A, Raw data trace from an example experiment with the addition of calphostin C (0.1μM) to the perfusing tyrodes before S2 stimulation. As can be seen during the S1 stimulation intracellular fluorescence increases linearly with time as has previously been reported. Although within the presence of Cal C, the intracellular fluorescence increase in S2 appears to be less linear and by eye more sigmoidal. This was not observed with any other drug treatment.

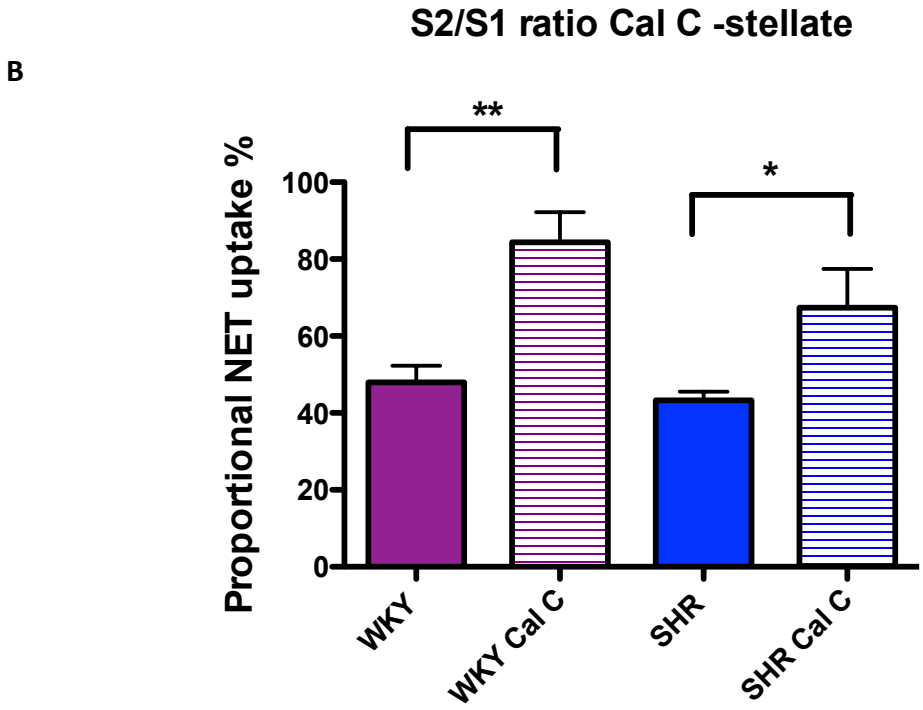

Figure 6.6: B, Rate of fluorescence increase during NTUA (1:10) hold, plotted as the S2/S1 ratio of the gradient of the slopes derived from y=mx+c. Cal C (0.1μM) significantly increased NET action in both WKY (**p<0.01, Mann Whitney test) and SHR stellate neurons (*p<0.05 t test) (WKY, n=17, SHR n=11, WKY Cal C n=5. SHR Cal C n=12).

6.4 DISCUSSION

The novel finding of this chapter are:

- Sodium nitroprusside, brain natriuretic peptide and 8-Br-cGMP all reduced NET activity in WKY stellate neurons.
- Sodium nitroprusside, brain natriuretic peptide and 8-Br-cGMP had no effect on NET uptake in the SHR stellate neurons.
- Protein kinase C inhibition increased NET uptake rate in both SHR and WKY stellate neurons.

Pharmacological modulation of NET can be visualised using the NTUA assay. An up-regulation of NET transport occurs in both SHR and WKY stellate neurons treated with Cal C. Whereas, WKY NET activity is reduced by activators of cGMP; BNP, SNP and 8-Br-cGMP, although no effect on NET is observed in the SHR (summary figure 6.7).

Data within this chapter has been analysed by comparing the calculated ratio of S2/S1 for each drug treatment compared to that ratio calculated over the same time period minus any drug – as described in 6.2.5. This method was used as it allows all slope values to be normalised to their initial fluorescence, normalising the effect of different NET receptor surface expression between cells, and allows for each drug treatment on a cell to be compared to its internal control. This method however involves a lot of post experiment analysis; the chance to reduce this may help prevent the possibility of additional errors being added in the analysis stage. This

could be achieved by comparing the normalised gradients of the S2 slopes for drug and time alone, without the additional analysis step to the internal control.

6.4.1. Reduction of norepinephrine re-uptake transporter transport capacity via stimulation of the cGMP pathway by brain natriuretic peptide, Sodium nitroprusside or 8-cBGMP.

Brain natriuretic peptide, sodium nitroprusside and 8-Br-cGMP all act through different upstream pathways, however all three result in activation of intracellular cGMP dependent protein kinases. Norepinephrine re-uptake transporter activity is reduced in WKY stellate neurons upon treatment of BNP, SNP and 8-Br-cGMP suggesting that NET may be modulated by cGMP. This may not be the only action each drug is having on NET activity. However, the consistency between the results suggest, that at least in part, these three drugs may all share a common mechanism.

No effect on NET activity is observed in stellate neurons of the SHR with addition of BNP, SNP, or 8-Br-cGMP. Indicating that the NET protein of the SHR has different or faulty regulation compared to that of the WKY, and that in part this difference in regulation occurs down stream of cGMP in BNP or SNP activated pathways.

In the WKY neurons the dual action of cGMP on reducing intracellular calcium transients and NET activity would have a balancing effect of pairing the reduced neurotransmitter release with slower re-uptake.

Figure 6.7

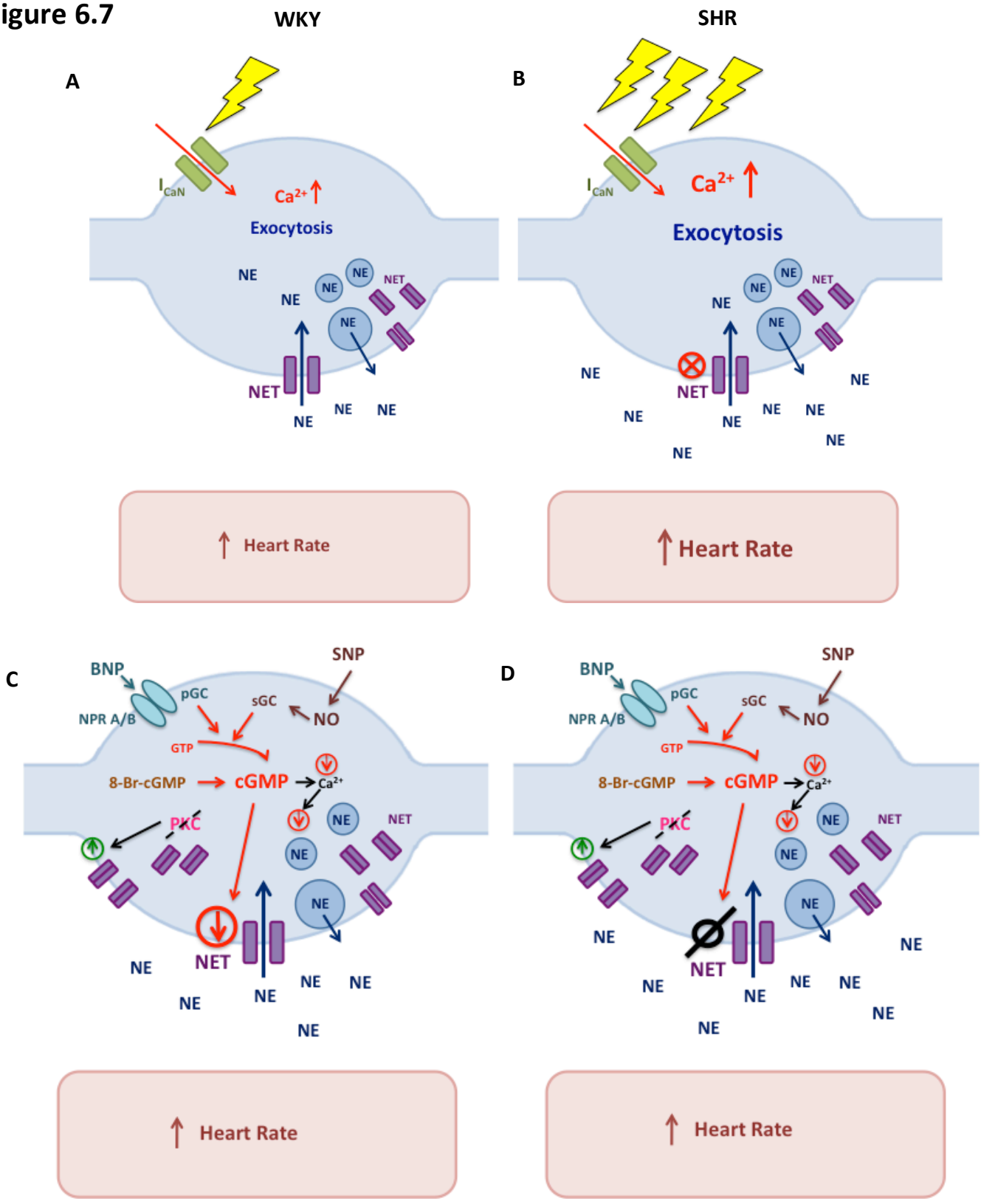

Figure 6.7. Schematic representation of the intracellular modulation of NET in stellate neurons of the pre-hypertensive SHR and WKY. **A,** and **B,** baseline regulation of NET in SHR and WKY cells as identified in chapters 3 and 4. **C,** and **D,** schematic representation of NET modulation following BNP, SNP and 8-br-cGMP signalling. The modulation pathways marked on the schematic are only those that have been studied in this thesis. Further modulatory pathways of NET are likely to exist. This schematic displays the complex regulation of the NET transporter within sympathetic nerve terminals.

Enhanced Reduced Un-changed

Within the SHR cGMP also reduces intracellular calcium but has no effect on NET this may lead to an overall reduction in synaptic NE concentrations and NE release would be reduced but NET activity would be working at the same (all be it lower than the WKY) rate it was originally working at.

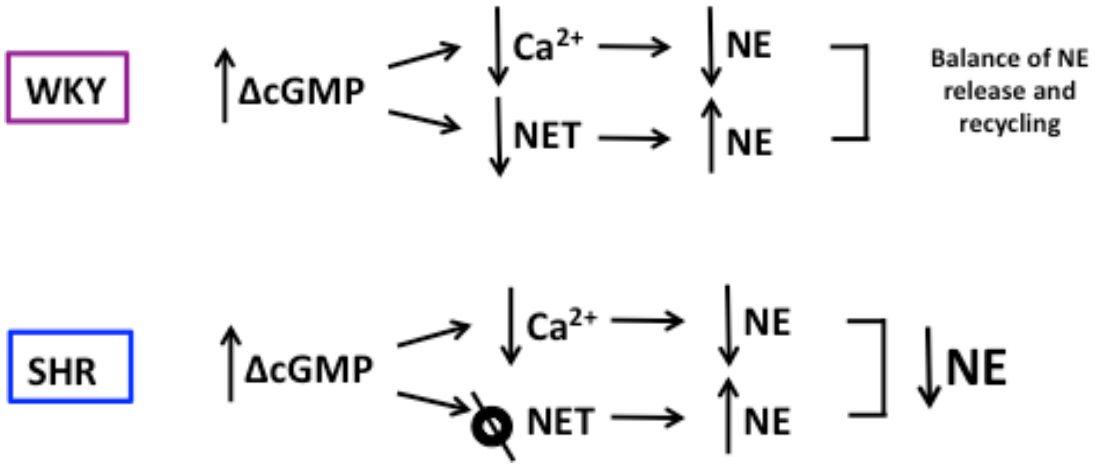

6.4.2 Influence on norepinephrine re-uptake transporter activity of protein kinase C inhibition by calphostin C.

Protein kinase C has previously been shown to facilitate NET receptor internalisation[103-106]. A cytoplasmic pool of transporters ready for membrane insertion has also previously been postulated. With the hypothesis that the cytoplasmic pool of NET receptors may be regulated by PKC, I tested to see the effect of Cal C on the basal activity of NET within stellate neurons. Calphostin C up-regulated NET transport capacity in both SHR and WKY neurons. One of the major limitations of the NTUA assay is the inability to ascertain the difference between increase in kinetics of an individual NET, or an increase in NET surface expression. However, the fluorescent increase observed in this study was dramatic and unlikely

to occur via increase of uptake rate capacity of individual transporters alone. To assess changes in NET surface density radio ligand binding assays of high affinity NET selective ligands can be used based on methods previously described[119].

Regulation of NET function by components of the vesicle SNARE complex have previously been described by Sung *et.al.*[117, 118], acting to up regulate the surface trafficking of NET, while also directly limiting NET catalytic function[117, 118]. This occurs via a Ca^{2+} dependent, PKC mediated pathway[116]. It seems the role for Ca^{2+} in the SNARE complex mediated modulation of NET is predominantly due to the need for cell depolarisation and Ca^{2+} entry for vesicle release. Sung demonstrated that when the syntaxin 1A/NET interaction is blocked PKC induced regulation of NET is abolished. This suggests that it is the pool of NET transporters in the membrane that are most sensitive to kinase interaction not the cytoplasmic pool[117, 118].

An observational result of the Cal C studies was that NTUA fluorescent increase over time in response to Cal C appeared to occur in a sigmoidal fashion, not linear as observed in all other experiments[35, 158]. This could be due to a number of mechanisms and would require further investigation. Increased NET protein membrane trafficking could result in the slowing phase observed due to exhaustion of intracellular NET, therefore no additional transporters can be inserted into the membrane and norepinephrine uptake is at a maximum. Alternatively, although all care was taken to limit the phototoxic nature of Cal C the 'abnormal' fluorescence increase may be due to damage to the cell, although visually the cells looked similar at the end of the experiment compared to other experiments previously. The

sigmoidal fluorescence increase may also be due to overloading of the cell. Any cell in which the fluorescence began to saturate was excluded from analysis.

6.4.3 Conclusion

This study has identified differences in NET regulation between the SHR and WKY. A fault exists in the regulation of NET through a cGMP signalling pathway within SHR stellate neurons. Whether the activity of individual transporters, or the surface expression of NET is being affected by the pharmacological manipulations within this chapter is unknown. Overall, this may have a small beneficial compensatory effect to cGMP stimulation.

6.5 Summary

The norepinephrine re-uptake transport is known to be highly modulated, the action of which has been utilised in a number of clinical and recreational drugs. Using the NTUA assay the data within this chapter has identified how NET activity can be modulated in a single cell pharmacologically. Within stellate sympathetic neurons of the WKY NET can reduced by modulators of cGMP activity SNP, BNP and 8-Br-cGMP, and up regulated by inhibition of constitutively active PKC, whereas, SHR stellate neuron NET activity can be up regulated by PKC inhibition. However inhibition of cGMP signalling has no effect on NET in the SHR. This indicates that there may be a difference in intracellular regulation of NET between the SHR and WKY which contributes to the lower resting NET activity observed in the SHR in chapters four and five.

CHAPTER 7:
CONCLUDING DISCUSSION

7.1 Main findings of this thesis

1. Cardiac sympathetic activity is increased in the young four week SHR, although it is still normotensive compared to its age matched genetic control, the WKY.
2. Norepinephrine re-uptake transporter activity is reduced in isolated stellate (cardiac) ganglion neurons within SHR rats at both developmental ages studied compared to their age matched WKY controls.
3. Norepinephrine re-uptake activity is unchanged in isolated sympathetic cells of the superior cervical ganglia (vascular), superior mesenteric ganglia (renal) and celiac ganglia of the SHR compared to their age matched WKY at both four weeks and 16 weeks of age.
4. The rate of norepinephrine re-uptake transporter activity within isolated sympathetic cells can be enhanced by cell depolarisation, decreased by pharmacological activators of cGMP, BNP, SNP and 8-Br-cGMP in the WKY but not the SHR. Whereas, PKC inhibition increases NET activity within both cell types.

Increased sympathetic activity and reduced vagal tone are well established contributing factors to the pathophysiology of human hypertension. Dysregulation within multiple levels of the cardiac neural axis during hypertension has previously been extensively studied[242-245]. However, emerging evidence has also identified dysregulation in cardiac neural signalling at the end organ level.

Although the precise mechanisms underlying dysregulation in cardiac neural signalling at the end organ level are unknown, many have been postulated; such as, increased neurotransmitter release, altered intracellular Ca^{2+} handling, reduced α_2 adrenoceptor activity and altered postsynaptic β_1 receptor signalling. Previously studied, but with conflicting results, the contribution of the norepinephrine re-uptake transporter to increase sympathetic signalling and NE spill over in hypertension has been unknown. The combined effect of these factors, plus additional influences are likely to contribute to the sympathetic hyperactivity in the SHR.

This thesis provides evidence that at the single neuron level cardiac NET activity of the SHR is decreased and has reduced regulation by cGMP compared to WKY. The age of development of disease at which the cardiac sympathetic hyperactivity arises has also previously been unknown. Within this thesis I show that many cardiac parameters are already altered at four weeks of age in the SHR when the animals are still normotensive. This suggests that the increase in cardiac sympathetic activity may pre-dispose or prelude the development of hypertension itself.

7.2 Role of cardiac sympathetic hyperactivity in the young spontaneously hypertensive rat

7.2.1 Absence of physiological indicators of hypertension

The four-week-old SHR showed no elevation in blood pressure compared to age matched WKY. Although previous studies have suggested that there may be a slight elevation in blood pressure at five weeks of age[246], within this paper animals were restrained in a tail cuff therefore it is likely that the blood pressure may be artificially

elevated as there would be an unusually high level of sympathetic drive. It is also worth noting that the SHR is often used as a model of attention deficit hyperactivity disorders, which may complicate these measurements. There are multiple methods of measuring blood pressure in rats of this age including tail cuff, radio-telemetry, and implanted devices with most previous studies investigating the four week old SHR consistently finding them to be normotensive [184, 247, 248]. Most blood pressure measurements are also taken after the animals have been conditioned to the recording protocol (such as with tail cuff) or the animal has undergone a recovery period after surgery. Therefore this thesis confirms what is seen as the most consistent finding of blood pressure in the four-week-old SHR to be normotensive at rest under highly controlled conditions (2% isoflurane) with a large sample number (n=18 SHR, n=20 WKY)[249].

7.2.2 Increased heart rate in four week spontaneously hypertensive rat

Although the SHR may not be tachycardic when compared to other rat strains [250], it has been shown to be consistently tachycardic when compared to its genetically matched normotensive control the WKY. We and others [184] observe no change in intrinsic heart rate of the isolated heart but a slightly higher resting heart rate *in vivo* at four weeks of age compared to the WKY, but even under carefully controlled conditions, readings of up to 38 animals (n=18 SHR, n=20 WKY) are required to demonstrate a statistical significance and many studies in this area are likely to be underpowered. A radio telemetry study of freely moving SHR's and WKY's at four weeks of age has also revealed a small tachycardia [184].

7.2.3 Increased sympathetic neurotransmitter release in the spontaneously hypertensive rat.

The increased cardiac sympathetic activity is coupled with increase muscle sympathetic nerve activity[48] (MSNA) and neurotransmitter release. Chapters three and five, combined with data previously reported[1] confirm that the increased sympathetic activity is observed in the young SHR. Evidence for increased intracellular Ca^{2+} transients[1], reduced norepinephrine re-uptake[35], increased cardiac neurotransmitter release[249] and enhanced heart rate response to sympathetic stimulation have all now been demonstrated with the pre-hypertensive SHR[249]. Using this knowledge and utilizing a number of techniques described in this thesis will allow for further study into the difference in sympathetic activity and regulation between the young SHR and WKY. BNP, nicotine and other neuromodulators could also be used in conjunction with the carbon fibre probes to measure the effect of paracrine factors on NE secretion in the SHR.

7.2.4 Cardiac sympathetic impairment: pathogenesis or epiphenomenon

A question remains as to whether the cardiac sympathetic hyperactivity that has now been identified in the pre-hypertensive and hypertensive SHR is linked to the pathogenesis of disease, or is it just an epiphenomenon of hypertension within the SHR?

Evidence pointing towards abnormal autonomic control in hypertension was reported as early as the 1970's[251]. Further research has identified sympathetic hyperactivity as a key feature of essential hypertension[40, 41, 43, 177]. Increased cardiac sympathetic activity has been established in the adult SHR, that results in significant

changes in cardiac function that is not observed in the WKY, including increased heart rate, neurotransmitter release and left ventricular hypertrophy[1, 34]. Suggesting, that altered cardiac autonomic function may in part contribute to the hypertensive phenotype of the SHR.

To identify if the increased cardiac activity observed in the SHR is an epiphenomenon of the phenotype, other rat models of hypertension such as the two-kidney, 1 clip model of hypertension[252, 253] or the Dhal salt sensitive rat[254, 255] would need to be characterised to see if all hypertensive animals carried the same autonomic cardio-vascular phenotype.

There is evidence-linking impairment of the kidney, vasculature and the autonomic nervous system to the aetiology of many patients with high blood pressure that we define as being hypertensive. In addition clinically severe hypertension also results in renal and vascular end organ damage thereby exacerbating the condition. Increased sympathetic activity and reduced vagal tone are now well established as major contributing factors to the pathophysiology of human hypertension [32, 40, 129, 150, 256], and that observed in the SHR[12, 18, 36, 45, 257]. Hypertension is associated with increased muscle sympathetic nerve activity[10, 40], increased levels of plasma NE [2, 11], and increased renal NE spillover [11, 258], Evidence for sympathetic hyperactivity has also been inferred from spectral analysis of heart rate variability in borderline and hypertensive patients where a linear correlation with blood pressure has been demonstrated[5]. Increased muscle sympathetic nerve activity in response to mental stress has also been documented within normotensive offspring from families with a history of hypertension[9]. This suggests that sympathetic activation may be an early

marker of hypertension in those who are genetically predisposed to the disease, potentially providing novel therapeutic targets for treatment. Currently used therapeutic treatments for hypertension target the sympatho-adrenal axis and renin-angiotensin pathways treating the end organ after symptoms of the disease have developed. Greater identification of early hallmarks of the disease may help develop therapies that prevent the progression of hypertension if sympathetic hyperactivity can be targeted.

7.3 Role of the norepinephrine re-uptake transporter in cardiac sympathetic hyperactivity of the spontaneously hypertensive rat

7.3.1 Baseline norepinephrine re-uptake transporter activity

Previous studies into the role of NET in hypertension have often produced inconclusive or conflicting results[3, 43, 77, 139, 140, 182, 259] By measuring NET transport capacity within single isolated sympathetic ganglion neurons I have limited the variables that occur by measuring NE run off from an intact tissue. Utilising the NTUA assay within isolated neurons has allowed me to monitor NET activity on the single cellular level. From this I have identified that within stellate neurons there is a significant decrease in NET transport capacity within both four week SHR and 16 week SHR compared to age matched WKY. However, no difference in NET rate is observed from cells isolated from the SCG or celiac, superior mesenteric ganglia[35].

The results in the older animals reinforce those previously reported in the Esler group, demonstrating reduced NET rate with hypertension[3] and with age[260]. The significance of this result reinforces the principle that conclusions can only be drawn for the tissue population studied, and that looking into one cell type cannot be used

to draw global predictions for that disease. This may explain some of the disparity into the role of NET in hypertension previously reported[3, 195].

Further study into action of NET with NTUA and functional studies within hypertensive and other cardiac models from neurons at different locations, will be essential in studying the multifactorial nature of the development and maintenance of disease.

7.3.2 Molecular modulation of NET

The importance of NET in regulating neurotransmission has lead to studies revealing the dynamic nature of the transporter. NET has the ability to adapt transport capacity and cell surface expression in response to different stimuli[114, 117].

Cell depolarisation and Ca^{2+} dependence via PKC

Cell depolarisation has previously been shown to increase NE re-uptake within PC12 cells[116]. Within chapters four and five, I demonstrated that within stellate neurons electrical field stimulation (EFS) of the neuron in the presence of the NTUA assay resulted in an increase in transporter action within the WKY. However, little difference in the rate of NET activity between the SHR at basal and EFS rates were observed[35].

Extensive study into PKC in NET regulation has described its ability to facilitate NET receptor internalisation via phosphorylation sites described within the NET gene sequence[100]. Increased NET activity observed in chapter six may be due to an up regulation in NET protein surface membrane expression, as on previously described[114], although this can not be isolated from a possible up regulation of the

individual transports function within this study. These results suggest that PKC inhibition can up regulate transporter activity in a similar way to cell depolarisation.

The role for Ca^{2+} in the syntaxin 1A/NET interaction and PKC inhibition both appear to facilitate the movement of transporters to the site of release[117, 118]. These results, particularly in relation to cell depolarisation may potentiate the increased sympathetic hyperactivity observed within the SHR[237]. Without the ability of NET to respond to increased levels of cell stimulation, altered intracellular Ca^{2+} handling[1] and neurotransmitter release[237] observed in the SHR, NET may not compensate for the increase in neurotransmission as it appears to in the WKY.

cGMP signalling

Previous studies into SNP modulation of NET have only been carried out within analogues of sympathetic cell types. Kaye *et.al.* within PC12 cells and SCG neurons observed a reduction in NET activity in a non-cGMP dependent manner, likely by S-nitrosylation of a regulatory site[120, 121, 123]. Others have observed no effect for SNP on NE uptake in SK-N-SH cells[119]. Within chapter six I observed a reduction in NET activity within isolated stellate ganglia of the WKY but not the SHR, when stimulating the cGMP signalling pathway with SNP, BNP or 8-Br-cGMP.

This suggests that although the SNP may be acting through S-nitrosylation of the NET protein to some degree, the comparative results observed from SNP, BNP and 8-Br-cGMP indicate that NET is regulated by cGMP, the end factor in all these signaling cascades. Moreover using the data presented here, the faulty NET regulation in the SHR is in part due to impaired cGMP regulation of NET. Further study using the NET

assay and other techniques including measuring protein expression levels and protein pull down experiments would provide further information behind the intracellular signalling pathways that control NET regulation.

Clinical significance/potential therapeutic target.

Although the act of pharmacologically slowing NET down within the SHR would not be clinically useful, these results do allude to faulty handling of NET modulation in the SHR stellate ganglion. By utilising the NTUA assay on single cells along side other techniques, potential pharmacological targets to up regulate NET activity or surface trafficking of NET in the SHR may be found. Altering the observed reduction in NET activity at both developmental ages in the SHR would also be beneficial combined with the increase neurotransmitter release observe in this model. As the greater the NE releases the faster it will need to be cleared from the synapse to maintain balance.

Highly modulated transporter systems should remain an active focus of research into autonomic modulation as a preventative measure against hypertension and other CV and CNS diseases.

7.4. CONCLUSIONS

This thesis works supports the idea that cardiac autonomic impairment via dysregulation of NET may be important in the development and maintenance of hypertension. Whether NET is a critical component in the aetiology of hypertension

remains to be determined. Nevertheless, results from this thesis would suggest that targeted modulation of cardiac NET could be therapeutically viable and beneficial.

Figure: 7.1 **Summary of NET modulation results**

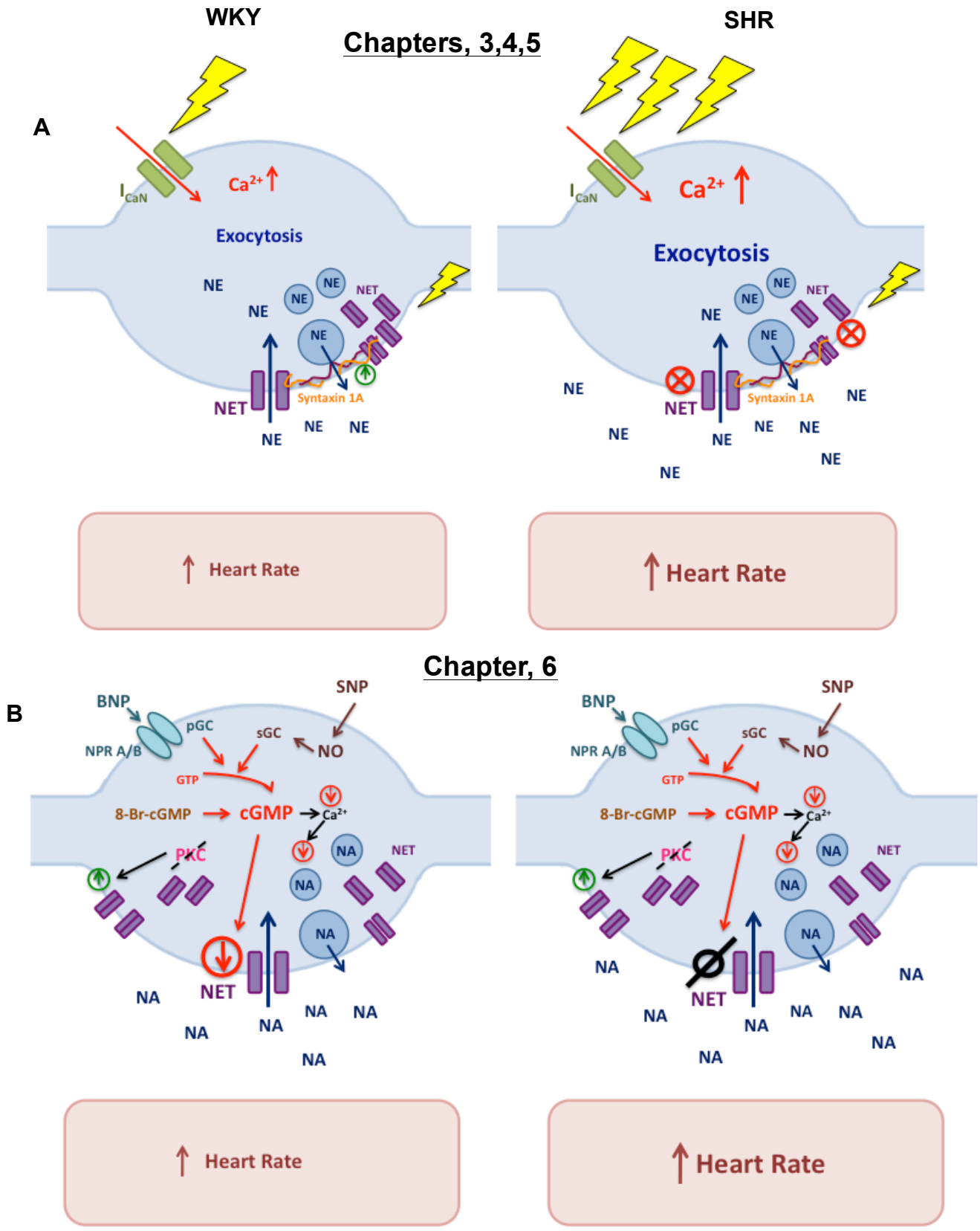

Figure 7.1: Schematic representations of the effect on NET modulation determined in chapters 3-6. **A,** NET modulation is reduced in the SHR compared to age matched WKY. Field stimulation has no effect on NET rate in the SHR however it does increase NET activity in the WKY, this may be due to a synataxin 1A interaction. Greater NA release in the SHR leads to greater heart rate response of the end organ. **B,** NET activity is reduced in WKY neurons in response to cGMP modulators BNP,SNP and 8-Br-cGMP, where as there are no effects in the SHR. Inhibition of protein kinase C increases NET rate in both the SHR and WKY.

Enhanced Reduced Un-changed

References

1. Li D, Lee CW, Buckler KJ, Parekh A, Herring N, Paterson DJ. Abnormal intracellular calcium homeostasis in sympathetic neurons from young prehypertensive rats. *Hypertension*. 2012;59:642-649
2. Esler M, Jennings G, Biviano B, Lambert G, Hasking G. Mechanism of elevated plasma noradrenaline in the course of essential hypertension. *Journal of Cardiovascular Pharmacology*. 1986;8 Suppl 5:S39-43
3. Rumantir MS, Kaye DM, Jennings GL, Vaz M, Hastings JA, Esler MD. Phenotypic evidence of faulty neuronal norepinephrine reuptake in essential hypertension. *Hypertension*. 2000;36:824-829
4. Opie LH, Clusin WT. Cellular mechanism for ischemic ventricular arrhythmias. *Annual Review Medicine*. 1990;41:231-238
5. Lubbe WF, Podzuweit T, Opie LH. Potential arrhythmogenic role of cyclic adenosine monophosphate (amp) and cytosolic calcium overload: Implications for prophylactic effects of beta-blockers in myocardial infarction and proarrhythmic effects of phosphodiesterase inhibitors. *Journal of the American College of Cardiology*. 1992;19:1622-1633
6. Kleiger RE, Miller JP, Bigger JT, Jr., Moss AJ. Decreased heart rate variability and its association with increased mortality after acute myocardial infarction. *The American Journal of Cardiology*. 1987;59:256-262
7. La Rovere MT, Bigger JT, Jr., Marcus FI, Mortara A, Schwartz PJ. Baroreflex sensitivity and heart-rate variability in prediction of total cardiac mortality after myocardial infarction. Atrami (autonomic tone and reflexes after myocardial infarction) investigators. *Lancet*. 1998;351:478-484

8. Cohn PF. When is concern about silent myocardial ischemia justified? *Annals of Internal Medicine*. 1984;100:597-599

9. Nolan J, Batin PD, Andrews R, Lindsay SJ, Brooksby P, Mullen M, Baig W, Flapan AD, Cowley A, Prescott RJ, Neilson JM, Fox KA. Prospective study of heart rate variability and mortality in chronic heart failure: Results of the united kingdom heart failure evaluation and assessment of risk trial (uk-heart). *Circulation*. 1998;98:1510-1516

10. Grassi G. Assessment of sympathetic cardiovascular drive in human hypertension: Achievements and perspectives. *Hypertension*. 2009;54:690-697

11. Schlaich MP, Kaye DM, Lambert E, Sommerville M, Socratous F, Esler MD. Relation between cardiac sympathetic activity and hypertensive left ventricular hypertrophy. *Circulation*. 2003;108:560-565

12. Levy D, Garrison RJ, Savage DD, Kannel WB, Castelli WP. Prognostic implications of echocardiographically determined left ventricular mass in the Framingham heart study. *The New England Journal of Medicine*. 1990;322:1561-1566

13. Ng GA, Brack KE, Patel VH, Coote JH. Autonomic modulation of electrical restitution, alternans and ventricular fibrillation initiation in the isolated heart. *Cardiovascular Research*. 2007;73:750-760

14. Danson EJ, Paterson DJ. Enhanced neuronal nitric oxide synthase expression is central to cardiac vagal phenotype in exercise-trained mice. *The Journal of Physiology*. 2003;546:225-232

15. Dawson TA, Li D, Woodward T, Barber Z, Wang L, Paterson DJ. Cardiac cholinergic no-cgmp signaling following acute myocardial infarction and nnos gene transfer. *American journal of physiology. Heart and circulatory physiology*. 2008;295:H990-H998

16. Mohan RM, Heaton DA, Danson EJ, Krishnan SP, Cai S, Channon KM, Paterson DJ. Neuronal nitric oxide synthase gene transfer promotes cardiac vagal gain of function. *Circulation Research*. 2002;91:1089-1091

17. Cole CR, Blackstone EH, Pashkow FJ, Snader CE, Lauer MS. Heart-rate recovery immediately after exercise as a predictor of mortality. *New England Journal of Medicine*. 1999;341:1351-1357

18. Langewitz W, Ruddel H, Schachinger H. Reduced parasympathetic cardiac control in patients with hypertension at rest and under mental stress. *American Heart Journal*. 1994;127:122-128

19. Randomised trial of intravenous atenolol among 16 027 cases of suspected acute myocardial infarction: Isis-1. First international study of infarct survival collaborative group. *Lancet*. 1986;2:57-66

20. The cardiac insufficiency bisoprolol study ii (cibis-ii): A randomised trial. *Lancet*. 1999;353:9-13

21. Effects of enalapril on mortality in severe congestive heart failure. Results of the cooperative north scandinavian enalapril survival study (consensus). The consensus trial study group. *The New England journal of medicine*. 1987;316:1429-1435

22. Pfeffer MA, Braunwald E, Moye LA, Basta L, Brown EJ, Jr., Cuddy TE, Davis BR, Geltman EM, Goldman S, Flaker GC, et al. Effect of captopril on mortality and morbidity in patients with left ventricular dysfunction after myocardial infarction. Results of the survival and ventricular enlargement trial. The save investigators. *The New England journal of medicine*. 1992;327:669-677

23. Esler MD, Krum H, Sobotka PA, Schlaich MP, Schmieder RE, Bohm M. Renal sympathetic denervation in patients with treatment-resistant hypertension (the symplicity htn-2 trial): A randomised controlled trial. *Lancet*. 2010;376:1903-1909

24. Schlaich MP, Sobotka PA, Krum H, Lambert E, Esler MD. Renal sympathetic-nerve ablation for uncontrolled hypertension. *The New England Journal of Medicine*. 2009;361:932-934

25. Abdala AP, McBryde FD, Marina N, Hendy EB, Engelman ZJ, Fudim M, Sobotka PA, Gourine AV, Paton JF. Hypertension is critically dependent on the carotid body input in the spontaneously hypertensive rat. *The Journal of physiology*. 2012;590:4269-4277

26. Paton JF, Sobotka PA, Fudim M, Engleman ZJ, Hart EC, McBryde FD, Abdala AP, Marina N, Gourine AV, Lobo M, Patel N, Burchell A, Ratcliffe L, Nightingale A. The carotid body as a therapeutic target for the treatment of sympathetically mediated diseases. *Hypertension*. 2013;61:5-13

27. Jordan J, Heusser K, Brinkmann J, Tank J. Electrical carotid sinus stimulation in treatment resistant arterial hypertension. *Autonomic Neuroscience: Basic and Clinical*. 2012;172:31-36

28. Armour JA. Potential clinical relevance of the 'little brain' on the mammalian heart. *Experimental Physiology*. 2008;93:165-176

29. Malliani A, Schwartz PJ, Zanchetti A. A sympathetic reflex elicited by experimental coronary occlusion. *American Journal of Physiology*. 1969;217:703-709

30. Malliani A, Pagani M, Bergamaschi M. Positive feedback sympathetic reflexes and hypertension. *The American Journal of Cardiology*. 1979;44:860-865

31. Salo LM, Campos RR, McAllen RM. Differential control of cardiac functions by the brain. *Clinical and Experimental Pharmacology and Physiology*. 2006;33:1255-1258

32. Fisher JP, Paton JF. The sympathetic nervous system and blood pressure in humans: Implications for hypertension. *Journal of Human Hypertension*. 2012;26:463-475

33. Zucker IH, Schultz HD, Li YF, Wang Y, Wang W, Patel KP. The origin of sympathetic outflow in heart failure: The roles of angiotensin ii and nitric oxide. *Progress in Biophysics and Molecular Biology*. 2004;84:217-232

34. Heaton DA, Li D, Almond SC, Dawson TA, Wang L, Channon KM, Paterson DJ. Gene transfer of neuronal nitric oxide synthase into intracardiac ganglia reverses vagal impairment in hypertensive rats. *Hypertension*. 2007;49:380-388

35. Shanks J, Mane S, Ryan R, Paterson DJ. Ganglion-specific impairment of the norepinephrine transporter in the hypertensive rat. *Hypertension*. 2013;61:187-193

36. Li D, Nikiforova N, Lu CJ, Wannop K, McMenamin M, Lee CW, Buckler KJ, Paterson DJ. Targeted neuronal nitric oxide synthase transgene delivery into stellate neurons reverses impaired intracellular calcium transients in prehypertensive rats. *Hypertension*. 2013;61:202-207

37. Li D, Wang L, Lee C-W, Dawson TA, Paterson DJ. Noradrenergic cell specific gene transfer with neuronal nitric oxide synthase reduces cardiac sympathetic neurotransmission in hypertensive rats. *Hypertension*. 2007;50:1-6

38. Lee RMKW, Triggle CR, Cheung DWT, Coughlin MD. Structural and functional consequences of neonatal sympathectomy on the blood vessels of spontaneously hypertensive rats. *Hypertension*. 1987;10:328-338

39. Sendeski MM, Consolim-Colombo FM, Leite CC, Rubira MC, Lessa P, Krieger EM. Increased sympathetic nerve activity correlates with neurovascular compression at the rostral ventrolateral medulla. *Hypertension*. 2006;47:988-995

40. Anderson EA, Sinkey CA, Lawton WJ, Mark AL. Elevated sympathetic nerve activity in borderline hypertensive humans: Evidence from direct intraneural recordings. *Hypertension*. 1989;14:177-183

41. Greenwood JP, Stoker JB, Mary DASG. Single-unit sympathetic discharge: Quantitative assesment in human hypertensive disease. *Circulation Research*. 1999;100:1305-1310

42. Davrath LR, Goren Y, Pinhas E, Toledo E, Akselrod S. American journal of physiology. Heart and circulatory physiology. *American Journal of Physiology - Heart and Circulatory Physiology*. 2003;285:1697-1704

43. Schlaich MP, Lambert E, Kaye DM, Krozowski Z, Campbell DJ, Lambert G, Hastings JA, Aggarwal A, Esler MD. Sympathetic augmentation in hypertension: Role of nerve firing, norepinephrine reuptake, and angiotensin neuromodulation. *Hypertension*. 2004;43:169-175

44. Flaa A, Mundal HH, Eide I, Kjeldsen S, Rostrup M. Sympathetic activity and cardiovascular risk factors in young men in the low, normal, and high blood pressure ranges. *Hypertension*. 2006;47:396-402

45. Cassis LA, Stitzel RE, Head RJ. Hypernoradrenergic innervation of the caudal artery of the spontaneously hypertensive rat: An influence upon neuoeffector mechanisms. *Pharmacology and Experimental Therapeutics*. 1985;234:792-803

46. Esler M, Jennings G, Korner P, Blombery P, Sacharias N, Leonard P. Measurement of total and organ-specific norepinephrine kinetics in humans. *American Journal of Physiology*. 1984;247:E21-28

47. Lucini D, Mela GS, Malliani A, Pagani M. Impairment in cardiac autonomic regulation preceding arterial hypertension in humans: Insights from spectral analysis of beat-by-beat cardiovascular variability. *Circulation*. 2002;106:2673-2679

48. Noll G, Wenzel RR, Schneider M, Oesch V, Binggeli C, Shaw S, Weidmann P, Luscher TF. Increased activation of sympathetic nervous system and endothelin by mental stress in normotensive offspring of hypertensive parents. *Circulation*. 1996;93:866-869

49. Reuter H. Localization of beta adrenergic receptors, and effects of noradrenaline and cyclic nucleotides on action potentials, ionic currents and tension in mammalian cardiac muscle. *The Journal of physiology*. 1974;242:429-451

50. McGregor DD. The effect of sympathetic nerve stimulation of vasoconstrictor responses in perfused mesenteric blood vessels of the rat. *The Journal of physiology*. 1965;177:21-30

51. Dunlap K, Luebke JI, Turner TJ. Exocytotic Ca^{2+} channels in mammalian central neurons. *Trends in Neuroscience*. 1995;18:89-98

52. Nowycky MC, Fox AP, Tsien RW. Three types of neuronal calcium channel with different calcium agonist sensitivity. *Nature*. 1985;316:440-443

53. Jackson VM, Trout SJ, Brain KL, Cunnane TC. Characterization of action potential-evoked calcium transients in mouse postganglionic sympathetic axon bundles. *The Journal of physiology*. 2001;537:3-16

54. Smith SJ, Augustine GJ. Calcium ions, active zones and synaptic transmitter release. *Trends in Neuroscience*. 1988;11:458-464

55. Llinas R, Sugimori M, Silver RB. Microdomains of high calcium concentration in a presynaptic terminal. *Science*. 1992;256:677-679

56. Bennett MK, Calakos N, Scheller RH. Syntaxin: A synaptic protein implicated in docking of synaptic vesicles at presynaptic active zones. *Science*. 1992;257:255-259

57. Sheng ZH, Rettig J, Cook T, Catterall WA. Calcium-dependent interaction of n-type calcium channels with the synaptic core complex. *Nature*. 1996;379:451-454

58. Mochida S, Sheng ZH, Baker C, Kobayashi H, Catterall WA. Inhibition of neurotransmission by peptides containing the synaptic protein interaction site of n-type Ca^{2+} channels. *Neuron*. 1996;17:781-788

59. Stanley EF, Mirotznik RR. Cleavage of syntaxin prevents g-protein regulation of presynaptic calcium channels. *Nature*. 1997;385:340-343

60. Elliott TR. Antiperistalsis and other muscular activities of the colon. *The Journal of physiology*. 1904;31:272-304

61. Elliott TR. On the innervation of the ileo-colic sphincter. *The Journal of physiology*. 1904;31:157-168

62. Wightman RM, Troyer KP, Mundorf ML, Catahan R. The association of vesicular contents and its effects on release. *Annals of the New York Academy of Sciences*. 2002;971:620-626

63. Albillos A, Dernick G, Horstmann H, Almers W, Alvarez de Toledo G, Lindau M. The exocytotic event in chromaffin cells revealed by patch amperometry. *Nature*. 1997;389:509-512

64. Travis ER, Wightman RM. Spatio-temporal resolution of exocytosis from individual cells. *The Annual Review of Biophysics and Biomolecular Structure*. 1998;27:77-103

65. Zhou Z, Misler S, Chow RH. Rapid fluctuations in transmitter release from single vesicles in bovine adrenal chromaffin cells. *Biophysical Journal*. 1996;70:1543-1552

66. Link E, Edelmann L, Chou JH, Binz T, Yamasaki S, Eisel U, Baumert M, Sudhof TC, Niemann H, Jahn R. Tetanus toxin action: Inhibition of neurotransmitter release linked to synaptobrevin proteolysis. *Biochemical and biophysical research communications*. 1992;189:1017-1023

67. Schiavo G, Benfenati F, Poulain B, Rossetto O, Polverino de Laureto P, DasGupta BR, Montecucco C. Tetanus and botulinum-b neurotoxins block neurotransmitter release by proteolytic cleavage of synaptobrevin. *Nature*. 1992;359:832-835

68. Blasi J, Chapman ER, Link E, Binz T, Yamasaki S, De Camilli P, Sudhof TC, Niemann H, Jahn R. Botulinum neurotoxin a selectively cleaves the synaptic protein snap-25. *Nature*. 1993;365:160-163

69. Blasi J, Chapman ER, Yamasaki S, Binz T, Niemann H, Jahn R. Botulinum neurotoxin c1 blocks neurotransmitter release by means of cleaving hpc-1/syntaxin. *Embo Journal*. 1993;12:4821-4828

70. Sudhof TC, Rizo J. Synaptic vesicle exocytosis. *Cold Spring Harbour Perspectives in Biology*. 2011;3: 1-14

71. Dulubova I, Khvotchev M, Liu S, Huryeva I, Sudhof TC, Rizo J. Munc18-1 binds directly to the neuronal snare complex. *Proceedings of the National Academy of Sciences U S A*. 2007;104:2697-2702

72. Khvotchev M, Dulubova I, Sun J, Dai H, Rizo J, Sudhof TC. Dual modes of munc18-1/snare interactions are coupled by functionally critical binding to syntaxin-1 n terminus. *The Journal of neuroscience : the official journal of the Society for Neuroscience*. 2007;27:12147-12155

73. Dai H, Shen N, Arac D, Rizo J. A quaternary snare-synaptotagmin-c Ca^{2+}-phospholipid complex in neurotransmitter release. *Journal of Molecular Biology*. 2007;367:848-863

74. Brown GL, Gillespie JS. The output of sympathetic transmitter from the spleen of the cat. *The Journal of physiology*. 1957;138:81-102

75. Langer SZ. The metabolism of (3H)noradrenaline released by electrical stimulation from the isolated nictitating membrane of the cat and from the vas deferens of the rat. *The Journal of physiology*. 1970;208:515-546

76. Schwartz DD. Activation of alpha-2 adrenergic receptors inhibits norepinephrine release by a pertussis toxin-insensitive pathway independent of changes in cytosolic calcium in cultured rat sympathetic neurons. *The Journal of Pharmacology and Experimental Therapeutics*. 1997;282:248-255

77. Zugck C, Lossnitzer D, Backs J, Kristen A, Kinscherf R, Haass M. Increased cardiac norepinephrine release in spontaneously hypertensive rats: Role of presynaptic alpha-2_a adrenoceptors. *Hypertension*. 2003;21:1363-1369

78. Saura J, Kettler R, Da Prada M, Richards JG. Quantitative enzyme radioautography with 3h-ro 41-1049 and 3h-ro 19-6327 in vitro: Localization and abundance of MAO-a and mao-b in rat cns, peripheral organs, and human brain. *The Journal of neuroscience : the official journal of the Society for Neuroscience*. 1992;12:1977-1999

79. Xu F, Gainetdinov RR, Wetsel WC, Jones SR, Bohn LM, Miller GW, Wang YM, Caron MG. Mice lacking the norepinephrine transporter are supersensitive to psychostimulants. *Nature Neuroscience*. 2000;3:465-471

80. Fowler CJ, Ross SB. Selective inhibitors of monoamine oxidase a and b: Biochemical, pharmacological, and clinical properties. *Medicine Research Reviews*. 1984;4:323-358

81. Labrosse EH, Axelrod J, Kety SS. O-methylation, the principal route of metabolism of epinephrine in man. *Science*. 1958;128:593-594

82. Axelrod J, Whitby LG, Hertting G. Effect of psychotropic drugs on the uptake of h3-norepinephrine by tissues. *Science*. 1961;133:383-384

83. Hammer W, Sjoqvist F. Plasma levels of monomethylated tricyclic antidepressants during treatment with imipramine-like compounds. *Life sciences*. 1967;6:1895-1903

84. Partilla JS, Dempsey AG, Nagpal AS, Blough BE, Baumann MH, Rothman RB. Interaction of amphetamines and related compounds at the vesicular monoamine transporter. *The Journal of Pharmacology and Experimental Therapeutics*. 2006;319:237-246

85. Bonisch H, Bruss M. The noradrenaline transporter of the neuronal plasma membrane. *Annals of the New York Academy of Sciences*. 1994;733:193-202

86. Zahniser NR, Doolen S. Chronic and acute regulation of Na^+/Cl^- -dependent neurotransmitter transporters: Drugs, substrates, presynaptic receptors, and signaling systems. *Pharmacology and Therapeutics*. 2001;92:21-55

87. Trendelenburg U. The tips lecture: Functional aspects of the neuronal uptake of noradrenaline. *Trends in Pharmacological Sciences*. 1991;12:334-337

88. Gu JG, Albuquerque C, Lee CJ, MacDermott AB. Synaptic strengthening through activation of Ca^{2+}-permeable ampa receptors. *Nature*. 1996;381:793-796

89. Pacholczyk T, Blakely RD, Amara SG. Expression cloning of a cocaine- and antidepressant-sensitive human noradrenaline transporter. *Nature*. 1991;350:350-354

90. Bruss M, Kunz J, Lingen B, Bonisch H. Chromosomal mapping of the human gene for the tricyclic antidepressant-sensitive noradrenaline transporter. *Human Genetics*. 1993;91:278-280

91. Gelernter J, Kruger S, Pakstis AJ, Pacholczyk T, Sparkes RS, Kidd KK, Amara S. Assignment of the norepinephrine transporter protein (net1) locus to chromosome 16. *Genomics*. 1993;18:690-692

92. Giros B, Wang YM, Suter S, McLeskey SB, Pifl C, Caron MG. Delineation of discrete domains for substrate, cocaine, and tricyclic antidepressant interactions using chimeric dopamine-norepinephrine transporters. *The Journal of Biological Chemistry*. 1994;269:15985-15988

93. Kitayama S, Morita K, Dohi T. Functional characterization of the splicing variants of human norepinephrine transporter. *Neuroscience Letters*. 2001;312:108-112

94. Meyer J, Wiedemann P, Okladnova O, Bruss M, Staab T, Stober G, Riederer P, Bonisch H, Lesch KP. Cloning and functional characterization of the human norepinephrine transporter gene promoter. *Journal of Neural Transmission*. 1998;105:1341-1350

95. Schwartz JW, Blakely RD, DeFelice LJ. Binding and transport in norepinephrine transporters. Real-time, spatially resolved analysis in single cells using a fluorescent substrate. *The Journal of Biological Chemistry*. 2003;278:9768-9777

96. Sammet S, Graefe KH. Kinetic analysis of the interaction between noradrenaline and na+ in neuronal uptake: Kinetic evidence for co-transport. *Naunyn-Schmiedeberg's Archives of Pharmacology*. 1979;309:99-107

97. Bonisch H, Harder R. Binding of 3h-desipramine to the neuronal noradrenaline carrier of rat phaeochromocytoma cells (pc-12 cells). *Naunyn-Schmiedeberg's Archives of Pharmacology*. 1986;334:403-411

98. Schomig E, Trendelenburg U, Azevedo I, Moura D. The steady-state concentration gradient for 3h-noradrenaline generated by uptake1 in the extracellular space of the rat vas deferens incubated with this amine. *Naunyn-Schmiedeberg's Archives of Pharmacology*. 1991;344:41-46

99. Sung U, Jennings JL, Link AJ, Blakely RD. Proteomic analysis of human norepinephrine transporter complexes reveals associations with protein phosphatase 2a anchoring subunit and 14-3-3 proteins. *Biochemical and biophysical research communications*. 2005;333:671-678

100. Jayanthi LD, Annamalai B, Samuvel DJ, Gether U, Ramamoorthy S. Phosphorylation of the norepinephrine transporter at threonine 258 and srine 259 is linked to protein kinase c-mediated transporter internalization. *The Journal of Biological Chemistry*. 2006;281:23326-23340

101. Melikian HE, Ramamoorthy S, Tate CG, Blakely RD. Inability to n-glycosylate the human norepinephrine transporter reduces protein stability, surface trafficking, and transport activity but not ligand recognition. *Molecular pharmacology*. 1996;50:266-276

102. Nguyen TT, Amara SG. N-linked oligosaccharides are required for cell surface expression of the norepinephrine transporter but do not influence substrate or inhibitor recognition. *Journal of neurochemistry*. 1996;67:645-655

103. Apparsundaram S, Schroeter S, Giovanetti E, Blakely RD. Acute regulation of norepinephrine transport: Ii. Pkc-modulated surface expression of human norepinephrine transporter proteins. *Journal of Pharmacology and Experimental Therapeutics*. 1998;287:744-751

104. Apparsundaram S, Sung U, Price RD, Blakely RD. Trafficking-dependent and -independent pathways of neurotransmitter transporter regulation differentially involving p38 mitogen-activated protein kinase revealed in studies of insulin modulation of norepinephrine transport in sk-n-sh cells. *The Journal of Pharmacology and Experimental Therapeutics*. 2001;299:666-677

105. Jayanthi LD, Annamalai B, Samuvel DJ, Gether U, Ramamoorthy S. Phosphorylation of the norepinephrine transporter at threonine 258 and serine 259 is linked to protein kinase c-mediated transporter internalization. *Journal of Biological Chemistry*. 2006;281:23326-23340

106. Apparsundaram S, Galli A, DeFelice LJ, Hartzell HC, Blakely RD. Acute regulation of norepinephrine transport: I. Protein kinase c-linked muscarinic receptors influence transport capacity and transporter density in sk-n-sh cells. *The Journal of Pharmacology and Experimental Therapeutics*. 1998;287:733-743

107. Bhagat B, Burke WJ, Dhalla NS. Insulin-induced enhancement of uptake of noradrenaline in atrial strips. *British Journal of Pharmacology*. 1981;74:325-332

108. Mandela P, Ordway GA. The norepinephrine transporter and its regulation. *Journal of neurochemistry*. 2006;97:310-333

109. James S, Patel NJ, Thomas PK, Burnstock G. Immunocytochemical localisation of insulin receptors on rat superior cervical ganglion neurons in dissociated cell culture. *Journal of Anatomy*. 1993;182 (Pt 1):95-100

110. Karagiannis SN, King RH, Thomas PK. Colocalisation of insulin and igf-1 receptors in cultured rat sensory and sympathetic ganglion cells. *Journal of Anatomy*. 1997;191 (Pt 3):431-440

111. Figlewicz DP, Bentson K, Ocrant I. The effect of insulin on norepinephrine uptake by pc12 cells. *Brain Research Bullitin*. 1993;32:425-431

112. Figlewicz DP, Szot P, Israel PA, Payne C, Dorsa DM. Insulin reduces norepinephrine transporter mrna in vivo in rat locus coeruleus. *Brain research*. 1993;602:161-164

113. Zhu CB, Hewlett WA, Feoktistov I, Biaggioni I, Blakely RD. Adenosine receptor, protein kinase g, and p38 mitogen-activated protein kinase-dependent up-regulation of serotonin transporters involves both transporter trafficking and activation. *Molecular pharmacology*. 2004;65:1462-1474

114. Apparsundaram S, Sung U, Price RD, Blakely RD. Trafficking-dependent and -independent pathways of neurotransmitter transporter regulation differentially involving p38 mitogen-activated protein kinase revealed in studies of insulin modulation of norepinephrine transport in sk-n-sh cells. *Journal of Pharmacology and Experimental Therapeutics*. 2001;299:666-677

115. Landsberg L. Insulin-mediated sympathetic stimulation: Role in the pathogenesis of obesity-related hypertension (or, how insulin affects blood pressure, and why). *Journal of Hypertension*. 2001;19:523-528

116. Mandela P, Ordway GA. Kcl stimulation increases norepinephrine transporter function in pc12 cells. *Journal of neurochemistry*. 2006;98:1521-1530

117. Sung U, Apparsundaram S, Galli A, Kahlig KM, Savchenko V, Schroeter S, Quick MW, Blakely RD. A regulated interaction of syntaxin 1a with the antidepressant-sensitive

norepinephrine transporter establishes catecholamine clearance capacity. *Journal of Neuroscience*. 2003;23:1697-1709

118. Sung U, Blakely RD. Calcium-dependent interactions of the human norepinephrine transporter with syntaxin 1a. *Mol Cell Neurosci*. 2007;34:251-260

119. Aparsundaram S, Galli A, Defelice LJ, Hartzell HC, Blakely RD. Acute regulation of norepinephrine transport: 1. Protein kinase c- linked muscarinic receptors influence transport capacity and transport density in sk-n-sh cells. *Journal of Pharmacology and Experimental Therapeutics*. 1998;287:733-743

120. Kaye DM, Wiviott SD, Kobzik L, Kelly RA, Smith TW. S-nitrosothiols inhibit neuronal norepinephrine transport. *American Journal of Physiology*. 1997;272:H875-883

121. Kaye DM, Gruskin S, Smith AI, Esler MD. Nitric oxide mediated modulation of norepinephrine transport: Identification of a potential target for s-nitrosylation. *British Journal of Pharmacology*. 2000;130:1060-1064

122. Vatta MS, Presas M, Bianciotti LG, Zarrabeitia V, Fernandez BE. B and c types natriuretic peptides modulate norepinephrine uptake and release in the rat hypothalamus. *Regulatory Peptides*. 1996;65:175-184

123. Stamler JS, Toone EJ, Lipton SA, Sucher NJ. (s)no signals: Translocation, regulation, and a consensus motif. *Neuron*. 1997;18:691-696

124. Ansorge MS, Zhou M, Lira A, Hen R, Gingrich JA. Early-life blockade of the 5-ht transporter alters emotional behavior in adult mice. *Science*. 2004;306:879-881

125. Caspi A, Sugden K, Moffitt TE, Taylor A, Craig IW, Harrington H, McClay J, Mill J, Martin J, Braithwaite A, Poulton R. Influence of life stress on depression: Moderation by a polymorphism in the 5-htt gene. *Science*. 2003;301:386-389

126. Sjogren B, Hamblin MW, Svenningsson P. Cholesterol depletion reduces serotonin binding and signaling via human 5-ht(7(a)) receptors. *European Journal of Pharmacology*. 2006;552:1-10

127. Inoue K, Itoh K, Yoshida K, Shimizu T, Suzuki T. Positive association between t-182c polymorphism in the norepinephrine transporter gene and susceptibility to major depressive disorder in a japanese population. *Neuropsychobiology*. 2004;50:301-304

128. Ryu SH, Lee SH, Lee HJ, Cha JH, Ham BJ, Han CS, Choi MJ, Lee MS. Association between norepinephrine transporter gene polymorphism and major depression. *Neuropsychobiology*. 2004;49:174-177

129. Schlaich MP, Lambert E, Kaye DM, Krozowski Z, Campbell DJ, Lambert G, Hastings J, Aggarwal A, Esler MD. Sympathetic augmentation in hypertension: Role of nerve firing, norepinephrine reuptake, and angiotensin neuromodulation. *Hypertension*. 2004;43:169-175

130. Meredith IT, Eisenhofer G, Lambert GW, Dewar EM, Jennings GL, Esler MD. Cardiac sympathetic nervous activity in congestive heart failure. Evidence for increased neuronal norepinephrine release and preserved neuronal uptake. *Circulation*. 1993;88:136-145

131. Bottalico B, Larsson I, Brodszki J, Hernandez-Andrade E, Casslen B, Marsal K, Hansson SR. Norepinephrine transporter (net), serotonin transporter (sert), vesicular monoamine transporter (vmat2) and organic cation transporters (oct1, 2 and emt) in human placenta from pre-eclamptic and normotensive pregnancies. *Placenta*. 2004;25:518-529

132. Shannon JR, Flattem NL, Jordan J, Jacob G, Black BK, Biaggioni I, Blakely RD, Robertson D. Orthostatic intolerance and tachycardia associated with norepinephrine-transporter deficiency. *The New England journal of medicine*. 2000;342:541-549

133. Garland EM, Robertson D. Chiari i malformation as a cause of orthostatic intolerance symptoms: A media myth? *Am J Med*. 2001;111:546-552

134. Hahn MK, Blakely RD. Monoamine transporter gene structure and polymorphisms in relation to psychiatric and other complex disorders. *Pharmacogenomics Journal*. 2002;2:217-235

135. Guyton AC, Coleman TG. Quantitative analysis of the pathophysiology of hypertension. 1969. *Journal of the American Society of Nephrology : JASN*. 1999;10:2248-2258

136. Jouven X, Empana JP, Schwartz PJ, Desnos M, Courbon D, Ducimetiere P. Heart-rate profile during exercise as a predictor of sudden death. *The New England journal of medicine*. 2005;352:1951-1958

137. Keller NR, Diedrich A, Appalsamy M, Tuntrakool S, Lonce S, Finney C, Caron MG, Robertson D. Norepinephrine transporter-deficient mice exhibit excessive tachycardia and elevated blood pressure with wakefulness and activity. *Circulation*. 2004;110:1191-1196

138. Okamoto K, Aoki K. Development of a strain of spontaneously hypertensive rats. *Japanese circulation journal*. 1963;27:282-293

139. Rho JH, Newman B, Alexander N. Altered in vitro uptake of norepinephrine by cardiovascular tissues of spontaneously hypertensive rats: Part 2. Portal-mesenteric veins and atria. *Hypertension*. 1981;3:710-717

140. Dyke AC, Angus JA, Korner PI. A functional study of the development of the cardiac sympathetic neuroeffector junction in the shr. *Hypertension*. 1989;7:345-353

141. Hahn MK, Robertson D, Blakely RD. A mutation in the human norepinephrine transporter gene (slc6a2) associated with orthostatic intolerance disrupts surface expression of mutant and wild-type transporters. *The Journal of neuroscience : the official journal of the Society for Neuroscience*. 2003;23:4470-4478

142. Pardini BJ, Lund DD, Schmid PG. Innervation patterns of the middle cervical--stellate ganglion complex in the rat. *Neuroscience Letters*. 1990;117:300-306

143. Bowers CW, Zigmond RE. Localization of neurons in the rat superior cervical ganglion that project into different postganglionic trunks. *The Journal of Comparative Neurology*. 1979;185:381-391

144. Hamer DW, Santer RM. Anatomy and blood supply of the coeliac-superior mesenteric ganglion complex of the rat. *Anatomy and Embryology*. 1981;162:353-362

145. Berthoud HR, Powley TL. Characterization of vagal innervation to the rat celiac, suprarenal and mesenteric ganglia. *Journal of the Autonomic Nervous System*. 1993;42:153-169

146. Orike N, Thrasivoulou C, Cowen T. Serum-free culture of dissociated, purified adult and aged sympathetic neurons and quantitative assays of growth and survival. *Journal of Neuroscience Methods*. 2001;106:153-160

147. He Y, Baas PW. Growing and working with peripheral neurons. *Methods Cell Biology*. 2003;71:17-35

148. Mayer AF, Schroeder C, Heusser K, Tank J, Diedrich A, Schmieder RE, Luft FC, Jordan J. Influences of norepinephrine transporter function on the distribution of sympathetic activity in humans. *Hypertension*. 2006;48:120-126

149. Whitby LG, Hertting G, Axelrod J. Effect of cocaine on the disposition of noradrenaline labelled with tritium. *Nature*. 1960;187:604-605

150. Schwaiger M, Kalff V, Rosenspire K, Haka MS, Molina E, Hutchins GD, Deeb M, Wolfe E, Jr., Wieland DM. Noninvasive evaluation of sympathetic nervous system in human heart by positron emission tomography. *Circulation*. 1990;82:457-464

151. Kummer W, Habeck JO. Chemoreceptor a-fibres in the human carotid body contain tyrosine hydroxylase and neurofilament immunoreactivity. *Neuroscience*. 1992;47:713-725

152. Cannon B, Nedergaard J, Lundberg JM, Hokfelt T, Terenius L, Goldstein M. 'Neuropeptide tyrosine' (npy) is co-stored with noradrenaline in vascular but not in parenchymal sympathetic nerves of brown adipose tissue. *Experimental Cell Research*. 1986;164:546-550

153. Dahlstrom A, Fuxe K. Localization of monoamines in the lower brain stem. *Experientia*. 1964;20:398-399

154. Brain KL, Cunnane TC. Bretylium abolishes neurotransmitter release without necessarily abolishing the nerve terminal action potential in sympathetic terminals. *British Journal of Pharmacology*. 2008;153:831-839

155. Esler MD, Lambert GW, Ferrier C, Kaye DM, Wallin BG, Kalff V, Kelly MJ, Jennings GL. Central nervous system noradrenergic control of sympathetic outflow in normotensive and hypertensive humans. *Clinical and Experimental Hypertension*. 1995;17:409-423

156. Haunso A, Buchanan D. Pharmacological characterization of a fluorescent uptake assay for the noradrenaline transporter. *Journal of Biomolecular Screening*. 2007;12:378-384

157. Jorgensen S, Nielsen EO, Peters D, Dyhring T. Validation of a fluorescence-based high-throughput assay for the measurement of neurotransmitter transporter uptake activity. *Journal of Neuroscience Methods*. 2008;169:168-176

158. Parker LK, Shanks JA, Kennard JAG, Brain KL. Dynamic monitoring of net activity in mature murine sympathetic terminals using a fluorescent substrate. *British Journal of Pharmacology*. 2010;159:797-807

159. Nishimura M, Sato K, Shimada S, Tohyama M. Expression of norepinephrine and serotonin transporter mrnas in the rat superior cervical ganglion. *Brain Research Molecular Brain Research*. 1999;67:82-86

160. Oancea E, Teruel MN, Quest AF, Meyer T. Green fluorescent protein (gfp)-tagged cysteine-rich domains from protein kinase c as fluorescent indicators for diacylglycerol signaling in living cells. *The Journal of cell biology*. 1998;140:485-498

161. Thomas D, Tovey SC, Collins TJ, Bootman MD, Berridge MJ, Lipp P. A comparison of fluorescent ca2+ indicator properties and their use in measuring elementary and global ca2+ signals. *Cell Calcium*. 2000;28:213-223

162. Herring N, Lee CW, Sunderland N, Wright K, Paterson DJ. Pravastatin normalises peripheral cardiac sympathetic hyperactivity in the spontaneously hypertensive rat. *Journal of Molecular and Cellular Cardiology*. 2011;50:99-106

163. Teschemacher AG, Seward EP. Bidirectional modulation of exocytosis by angiotensin ii involves multiple g-protein-regulated transduction pathways in chromaffin cells. *The Journal of neuroscience : the official journal of the Society for Neuroscience*. 2000;20:4776-4785

164. Gillis KD. Single-channel recording. In: Sakman B, Neher, E., ed. *Techniques for membrane capacitance measurements*. Plenum; 1995:55–198.

165. Schroeder TJ, Jankowski JA, Senyshyn J, Holz RW, Wightman RM. Zones of exocytotic release on bovine adrenal medullary cells in culture. *The Journal of Biological Chemistry*. 1994;269:17215-17220

166. Adams RN. In vivo electrochemical measurements in the cns. *Progress in Neurobiology*. 1990;35:297-311

167. Angleson JK, Betz WJ. Monitoring secretion in real time: Capacitance, amperometry and fluorescence compared. *Trends in Neuroscience*. 1997;20:281-287

168. Zhou Z, Misler S. Amperometric detection of stimulus-induced quantal release of catecholamines from cultured superior cervical ganglion neurons. *Proceedings of the National Academy of Sciences*. 1995;92:6938-6942

169. Chiti Z, Teschemacher AG. Exocytosis of norepinephrine at axon varicosities and neuronal cell bodies in the rat brain. *FASEB Journal*. 2007;21:2540-2550

170. Wightman RM, Schroeder TJ, Finnegan JM, Ciolkowski EL, Pihel K. Time course of release of catecholamines from individual vesicles during exocytosis at adrenal medullary cells. *Biophysical Journal*. 1995;68:383-390

171. Schulte A, Chow RH. A simple method for insulating carbon-fiber microelectrodes using anodic electrophoretic deposition of paint. *Analytical chemistry*. 1996;68:3054-3058

172. Elhamdani A, Zhou Z, Artalejo CR. Timing of dense-core vesicle exocytosis depends on the facilitation l-type ca channel in adrenal chromaffin cells. *The Journal of neuroscience : the official journal of the Society for Neuroscience*. 1998;18:6230-6240

173. Lee CW, Li D, Channon KM, Paterson DJ. L-arginine supplementation reduces cardiac noradrenergic neurotransmission in spontaneously hypertensive rats. *Journal of Molecular and Cellular Cardiology*. 2009;47:149-155

174. Feng M, Whitesall S, Zhang Y, Beibel M, D'Alecy L, DiPetrillo K. Validation of volume-pressure recording tail-cuff blood pressure measurements. *American Journal of hypertension*. 2008;21:1288-1291

175. Bunag RD. Validation in awake rats of a tail-cuff method for measuring systolic pressure. *Journal of Applied Physiology*. 1973;34:279-282

176. Mohan RM, Golding S, Paterson DJ. Intermittent hypoxia modulates nnos expression and heart rate response to sympathetic nerve stimulation. *American Journal of Physiology - Heart and Circulatory Physiology*. 2001;281:132-138

177. Davrath LR, Goren Y, Pinhas E, Toledo E, Akselrod S. Early automoic malfunction in normotensive inidividuals with a genetic predisposition to essential hypertension.

American Journal of Physiology - Heart and Circulatory Physiology. 2003;285:1697-1704

178. Kondo M, Fujiwara T, Tabei R. Noradrenergic hyperinnervation in the heart of stroke-prone spontaneously hypertensive rats (SHRSP). *Hypertension Research*. 1996;19:69-73

179. Ganau A, Devereux RB, Roman MJ, de Simone G, Pickering TG, Saba PS, Vargiu P, Simongini I, Laragh JH. Patterns of left ventricular hypertrophy and geometric remodeling in essential hypertension. *Journal of the American College of Cardiology*. 1992;19:1550-1558

180. Devereux RB, Savage DD, Sachs I, Laragh JH. Relation of hemodynamic load to left ventricular hypertrophy and performance in hypertension. *The American Journal of Cardiology*. 1983;51:171-176

181. Sen S, Tarazi RC, Khairallah PA, Bumpus FM. Cardiac hypertrophy in spontaneously hypertensive rats. *Circulation Research*. 1974;35:775-781

182. Stephens N, Bund SJ, Jagger C, Heagerty AM. Arterial neuroeffector responses in early and mature spontaneously hypertensive rats. *Hypertension*. 1991;18:674-682

183. Carlson DE, Gann DS. Alpha-adrenergic input in the locus coeruleus modulates plasma adrenocorticotropin in cats. *Endocrinology*. 1992;130:2795-2803

184. Komolova M, Friberg P, Adams MA. Altered vascular resistance properties and acute pressure-natriuresis mechanism in neonatal and weaning spontaneously hypertensive rats. *Hypertension*. 2012;59:979-984

185. Minami N, Head GA. Cardiac vagal responsiveness during development in spontaneously hypertensive rats. *Autonomic Neuroscience*. 2000;82:115-122

186. Lockinger A, Koberle D, Konig PS, Saria A, Herold M, Cornelissen G, Halberg F. Neuropeptide chronomics in clinically healthy young adults: Circaoctohoran and circadian patterns. *Peptides*. 2004;25:533-542

187. Kondo K, Matsubara T, Nakamura J, Hotta N. Characteristic patterns of circadian variation in plasma catecholamine levels, blood pressure and heart rate variability in type 2 diabetic patients. *Diabetic Medicine*. 2002;19:359-365

188. Cuculi F, Herring N, De Caterina AR, Banning AP, Prendergast BD, Forfar JC, Choudhury RP, Channon KM, Kharbanda RK. Relationship of plasma neuropeptide y with angiographic, electrocardiographic and coronary physiology indices of reperfusion during st elevation myocardial infarction. *Heart*. 2013;99:1198-1203

189. Herring N, Cranley J, Lokale MN, Li D, Shanks J, Alston EN, Girard BM, Carter E, Parsons RL, Habecker BA, Paterson DJ. The cardiac sympathetic co-transmitter galanin reduces acetylcholine release and vagal bradycardia: Implications for neural control of cardiac excitability. *Journal of Molecular and Cellular Cardiology*. 2012;52:667-676

190. Herring N, Lokale MN, Danson EJ, Heaton DA, Paterson DJ. Neuropeptide Y reduces acetylcholine release and vagal bradycardia via a Y2 receptor-mediated, protein kinase c-dependent pathway. *Journal of Molecular and Cellular Cardiology*. 2008;44:477-485

191. Judy WV, Farrell SK. Arterial baroreceptor reflex control of sympathetic nerve activity in the spontaneously hypertensive rat. *Hypertension*. 1979;1:605-614

192. Head GA, Adams MA. Characterization of the baroreceptor heart rate reflex during development in spontaneously hypertensive rats. *Clinical and Experimental Pharmacology and Physiology*. 1992;19:587-597

193. Esler M, Jackman G, Bobik A, Leonard P, Kelleher D, Skews H, Jennings G, Korner P. Norepinephrine kinetics in essential hypertension. Defective neuronal uptake of norepinephrine in some patients. *Hypertension*. 1981;3:149-156

194. Kimura S, Miura Y, Adachi M, Nezu M, Toriyabe S, Sugawara T, Ishizuka Y, Noshiro T, Takahashi M. The effect of sodium depletion on plasma norepinephrine kinetics in

patients with essential hypertension. *Japanese Circulation Journal*. 1983;47:1232-1241

195. Cabassi A, Vinci S, Quartieri F, Moschini L, Borghetti A. Norepinephrine reuptake is impaired in skeletal muscle of hypertensive rats in vivo. *Hypertension*. 2001;37:698-702

196. Rho JH, Newman B, Alexander N. Altered in vitro uptake of norepinephrine by cardiovascular tissues of spontaneously hypertensive rats. Part 1. Mesenteric artery. *Hypertension*. 1981;3:704-709

197. Rho JH, Newman B, Alexander N. Altered in vitro uptake of norepinephrine by cardiovascular tissues of spontaneously hypertensive rats. Part 2. Portal-mesenteric veins and atria. *Hypertension*. 1981;3:710-717

198. Varagic J, Frohlich ED. Local cardiac renin-angiotensin system: Hypertension and cardiac failure. *Journal of Molecular and Cellular Cardiology*. 2002;34:1435-1442

199. B S, Hegde AH, K CR, J S. Exploring the binding mechanism of ondansetron hydrochloride to serum albumins: Spectroscopic approach. *Spectrochimica Acta Part A: Molecular and Biomolecular Spectroscopy*. 2012;86:410-416

200. Fanou-Fogny N, N JS, Koreissi Y, R AMD, Melse-Boonstra A, I DB. Weight status and iron deficiency among urban malian women of reproductive age. *British Journal of Nutrition*. 2011;105:574-579

201. Leineweber K, Wangemann T, Giessler C, Bruck H, Dhein S, Kostelka M, Mohr FW, Silber RE, Brodde OE. Age-dependent changes of cardiac neuronal noradrenaline reuptake transporter (uptake1) in the human heart. *Journal of American College of Cardiology*. 2002;40:1459

202. Savchenko V, Sung U, Blakely RD. Cell surface trafficking of the antidepressant-sensitive norepinephrine transporter revealed with an ectodomain antibody. *Molecular and Cellular Neurosciences*. 2003;24:1131-1150

203. Galli A, Blakely RD, DeFelice LJ. Patch-clamp and amperometric recordings from norepinephrine transporters: Channel activity and voltage-dependent uptake. *Proceeding of the National Academy of Sciences U S A*. 1998;95:13260-13265

204. Schroeter S, Apparsundaram S, Wiley RG, Miner LH, Sesack SR, Blakely RD. Immunolocalization of the cocaine- and antidepressant-sensitive l-norepinephrine transporter. *The Journal of comparative neurology*. 2000;420:211-232

205. Morrow LA, Linares OA, Hill TJ, Sanfield JA, Supiano MA, Rosen SG, Halter JB. Age differences in the plasma clearance mechanisms for epinephrine and norepinephrine in humans. *The Journal of Clinical Endocrinology and Metabolism*. 1987;65:508-511

206. Veith RC, Featherstone JA, Linares OA, Halter JB. Age differences in plasma norepinephrine kinetics in humans. *The Journal of Gerontology*. 1986;41:319-324

207. Borton M, Dochery JR. The effects of ageing on neuronal uptake of noradrenaline in the rat. *Naunyn-Schmiedeberg's Archives of Pharmacology*. 1989;340:139-143

208. Hoffman WE, Seals C, Miletich DJ, Albrecht RF. Plasma and myocardial catecholamine levels in young and aged rats during halothane anesthesia. *Neurobiology of Aging*. 1985;6:117-120

209. Esler M, Skews H, Leonard P, Jackman G, Bobik A, Korner P. Age-dependence of noradrenaline kinetics in normal subjects. *Clinical Science (London)*. 1981;60:217-219

210. Wong EH, Sonders MS, Amara SG, Tinholt PM, Piercey MF, Hoffmann WP, Hyslop DK, Franklin S, Porsolt RD, Bonsignori A, Carfagna N, McArthur RA. Reboxetine: A pharmacologically potent, selective, and specific norepinephrine reuptake inhibitor. *Biological Psychiatry*. 2000;47:818-829

211. Frazer A. Norepinephrine involvement in antidepressant action. *Journal of Clinical Psychiatry*. 2000;61 Suppl 10:25-30

212. Vongpatanasin W, Mansour Y, Chavoshan B, Arbique D, Victor RG. Cocaine stimulates the human cardiovascular system via a central mechanism of action. *Circulation*. 1999;100:497-502

213. Tatsumi M, Groshan K, Blakely RD, Richelson E. Pharmacological profile of antidepressants and related compounds at human monoamine transporters. *European Journal of Pharmacology*. 1997;340:249-258

214. Mizuno Y, Yoshimura M, Harada E, Nakayama M, Sakamoto T, Shimasaki Y, Ogawa H, Kugiyama K, Saito Y, Nakao K, Yasue H. Plasma levels of a- and b-type natriuretic peptides in patients with hypertrophic cardiomyopathy or idiopathic dilated cardiomyopathy. *The American Journal of Cardiology*. 2000;86:1036-1040, A1011

215. Qi W, Mathisen P, Kjekshus J, Simonsen S, Bjornerheim R, Endresen K, Hall C. Natriuretic peptides in patients with aortic stenosis. *American Heart Journal*. 2001;142:725-732

216. Berger R, Huelsman M, Strecker K, Bojic A, Moser P, Stanek B, Pacher R. B-type natriuretic peptide predicts sudden death in patients with chronic heart failure. *Circulation*. 2002;105:2392-2397

217. Sagnella GA. Measurement and significance of circulating natriuretic peptides in cardiovascular disease. *Clinical science*. 1998;95:519-529

218. Takimoto Y, Aoyama T, Tanaka K, Keyamura R, Yui Y, Sasayama S. Augmented expression of neuronal nitric oxide synthase in the atria parasympathetically decreases heart rate during acute myocardial infarction in rats. *Circulation*. 2002;105:490-496

219. Saraiva RM, Minhas KM, Zheng M, Pitz E, Treuer A, Gonzalez D, Schuleri KH, Vandegaer KM, Barouch LA, Hare JM. Reduced neuronal nitric oxide synthase expression contributes to cardiac oxidative stress and nitroso-redox imbalance in

ob/ob mice. *Nitric oxide : biology and chemistry / official journal of the Nitric Oxide Society*. 2007;16:331-338

220. Force T, Pombo CM, Avruch JA, Bonventre JV, Kyriakis JM. Stress-activated protein kinases in cardiovascular disease. *Circulation Research*. 1996;78:947-953

221. Bowling N, Walsh RA, Song G, Estridge T, Sandusky GE, Fouts RL, Mintze K, Pickard T, Roden R, Bristow MR, Sabbah HN, Mizrahi JL, Gromo G, King GL, Vlahos CJ. Increased protein kinase c activity and expression of ca2+-sensitive isoforms in the failing human heart. *Circulation*. 1999;99:384-391

222. Ballermann BJ, Brenner BM. Atrial natriuretic peptide and the kidney. *American Journal of Kidney Disease*. 1987;10:7-12

223. Rautureau Y, Baxter GF. Acute actions of natriuretic peptides in coronary vasculature and ischaemic myocardium. *Current Pharmaceutical Design*. 2004;10:2477-2482

224. Bonow RO. New insights into the cardiac natriuretic peptides. *Circulation*. 1996;93:1946-1950

225. Tonolo G, Richards AM, Manunta P, Troffa C, Pazzola A, Madeddu P, Towrie A, Fraser R, Glorioso N. Low-dose infusion of atrial natriuretic factor in mild essential hypertension. *Circulation*. 1989;80:893-902

226. Edwards BS, Zimmerman RS, Schwab TR, Heublein DM, Burnett JC, Jr. Atrial stretch, not pressure, is the principal determinant controlling the acute release of atrial natriuretic factor. *Circulation Research*. 1988;62:191-195

227. Minamino N, Makino Y, Tateyama H, Kangawa K, Matsuo H. Characterization of immunoreactive human c-type natriuretic peptide in brain and heart. *Biochemical and biophysical research communications*. 1991;179:535-542

228. Takemura G, Takatsu Y, Doyama K, Itoh H, Saito Y, Koshiji M, Ando F, Fujiwara T, Nakao K, Fujiwara H. Expression of atrial and brain natriuretic peptides and their

genes in hearts of patients with cardiac amyloidosis. *Journal of the American College of Cardiology*. 1998;31:754-765

229. Cowie MR, Struthers AD, Wood DA, Coats AJ, Thompson SG, Poole-Wilson PA, Sutton GC. Value of natriuretic peptides in assessment of patients with possible new heart failure in primary care. *Lancet*. 1997;350:1349-1353

230. Yamamoto K, Burnett JC, Jr., Jougasaki M, Nishimura RA, Bailey KR, Saito Y, Nakao K, Redfield MM. Superiority of brain natriuretic peptide as a hormonal marker of ventricular systolic and diastolic dysfunction and ventricular hypertrophy. *Hypertension*. 1996;28:988-994

231. Omland T, Aakvaag A, Bonarjee VV, Caidahl K, Lie RT, Nilsen DW, Sundsfjord JA, Dickstein K. Plasma brain natriuretic peptide as an indicator of left ventricular systolic function and long-term survival after acute myocardial infarction. Comparison with plasma atrial natriuretic peptide and n-terminal proatrial natriuretic peptide. *Circulation*. 1996;93:1963-1969

232. Floras JS. Sympathoinhibitory effects of atrial natriuretic factor in normal humans. *Circulation*. 1990;81:1860-1873

233. Brunner-La Rocca HP, Kaye DM, Woods RL, Hastings J, Esler MD. Effects of intravenous brain natriuretic peptide on regional sympathetic activity in patients with chronic heart failure as compared with healthy control subjects. *Journal of the American College of Cardiology*. 2001;37:1221-1227

234. Herring N, Paterson DJ. Letter by herring and paterson regarding article, "common nos1ap variants are associated with a prolonged qtc interval in the rotterdam study". *Circulation*. 2007;116:e564

235. Herring N, Paterson DJ. Nitric oxide-cgmp pathway facilitates acetylcholine release and bradycardia during vagal nerve stimulation in the guinea-pig *in vitro*. *Journal of Physiology*. 2001;535:507-518

236. Wang L, Li D, Dawson TA, Paterson DJ. Long-term effect of neuronal nitric oxide synthase over-expression on cardiac neurotransmission mediated by a lentiviral vector. *The Journal of Physiology*. 2009;587:3629-3637

237. Danson EJ, Li D, Wang L, Dawson TA, Paterson DJ. Targeting cardiac sympatho-vagal imbalance using gene transfer of nitric oxide synthase. *Journal of Molecular and Cellular Cardiology*. 2009;46:482-489

238. Lucas KA, Pitari GM, Kazerounian S, Ruiz-Stewart I, Park J, Schulz S, Chepenik KP, Waldman SA. Guanylyl cyclases and signaling by cyclic gmp. *Pharmacological Review*. 2000;52:375-414

239. Murphy S, Frishman WH. Protein kinase c in cardiac disease and as a potential therapeutic target. *Cardiology in Review*. 2005;13:3-12

240. Smolenski A, Burkhardt AM, Eigenthaler M, Butt E, Gambaryan S, Lohmann SM, Walter U. Functional analysis of cgmp-dependent protein kinases i and ii as mediators of no/cgmp effects. *Naunyn-Schmiedeberg's Archives of Pharmacology*. 1998;358:134-139

241. Bruns RF, Miller FD, Merriman RL, Howbert JJ, Heath WF, Kobayashi E, Takahashi I, Tamaoki T, Nakano H. Inhibition of protein kinase c by calphostin c is light-dependent. *Biochemical and biophysical research communications*. 1991;176:288-293

242. Sakai K, Hirooka Y, Matsuo I, Eshima K, Shigematsu H, Shimokawa H, Takeshita A. Overexpression of enos in nts causes hypotension and bradycardia in vivo. *Hypertension*. 2000;36:1023-1028

243. Li Q, Dale WE, Hasser EM, Blaine EH. Acute and chronic angiotensin hypertension: Neural and nonneural components, time course, and dose dependency. *American Journal of Physiology*. 1996;271:R200-207

244. Somers VK, Anderson EA, Mark AL. Sympathetic neural mechanisms in human hypertension. *Current Opinion in Nephrology and Hypertension*. 1993;2:96-105

245. Korner PI. *Essential hypertension and its causes : Neural and non-neural mechanisms*. Oxford: Oxford University Press; 2007.

246. Dickhout JG, Lee RM. Blood pressure and heart rate development in young spontaneously hypertensive rats. *American Journal of Physiology*. 1998;274:H794-800

247. Kokubo M, Uemura A, Matsubara T, Murohara T. Noninvasive evaluation of the time course of change in cardiac function in spontaneously hypertensive rats by echocardiography. *Hypertension research : official journal of the Japanese Society of Hypertension*. 2005;28:601-609

248. Takeda K, Nakata T, Takesako T, Itoh H, Hirata M, Kawasaki S, Hayashi J, Oguro M, Sasaki S, Nakagawa M. Sympathetic inhibition and attenuation of spontaneous hypertension by PVN lesions in rats. *Brain research*. 1991;543:296-300

249. Shanks J, Manou-Stathopoulou S, Lu CJ, Li D, Paterson DJ, Herring N. Cardiac sympathetic dysfunction in the prehypertensive spontaneously hypertensive rat. *American journal of physiology. Heart and circulatory physiology*. 2013;305:H980-986

250. van den Buuse M, Wegener N. Involvement of serotonin1a receptors in cardiovascular responses to stress: A radio-telemetry study in four rat strains. *European Journal of Pharmacology*. 2005;507:187-198

251. Julius S, Esler M. Autonomic nervous cardiovascular regulation in borderline hypertension. *The American Journal of Cardiology*. 1975;36:685-696

252. Oliveira-Sales EB, Colombari DS, Davisson RL, Kasparov S, Hirata AE, Campos RR, Paton JF. Kidney-induced hypertension depends on superoxide signaling in the rostral ventrolateral medulla. *Hypertension*. 2010;56:290-296

253. Davis G, Johns EJ. Baroreceptor and somatic sensory regulation of kidney function in two-kidney, one-clip goldblatt hypertensive rats. *The Journal of physiology*. 1994;476:167-176

254. Campese VM. Salt sensitivity in hypertension. Renal and cardiovascular implications. *Hypertension*. 1994;23:531-550

255. Cowley AW, Jr., Roman RJ. The role of the kidney in hypertension. *Jama*. 1996;275:1581-1589

256. Davrath LR, Goren Y, Pinhas I, Toledo E, Akselrod S. Early autonomic malfunction in normotensive individuals with a genetic predisposition to essential hypertension. *American Journal of Physiology. Heart and circulatory physiology*. 2003;285:H1697-1704

257. Han C, Wang XA, Fiscus RR, Gu J, McDonald JK. Changes in cardiac neuropeptide y after experimental myocardial infarction in rat. *Neuroscience Letters*. 1989;104:141-146

258. Erlinge D, Burnstock G. P2 receptors in cardiovascular regulation and disease. *Purinergic Signal*. 2008;4:1-20

259. Hano T, Rho J. Norepinephrine overflow in perfused mesenteric arteries of spontaneously hypertensive rats. *Hypertension*. 1989;14:44-53

260. Docherty JR. Age-related changes in adrenergic neuroeffector transmission. *Autonomic Neuroscience*. 2002;96:8-12